Title
Cochleotopic organization and connections of the anterior auditory field (AAF) of the cat

Author
Knight, Paul Louis

Publication Date
1977

Peer reviewed|Thesis/dissertation

COCHLEOTOPIC ORGANIZATION AND CONNECTIONS OF THE ANTERIOR AUDITORY FIELD (AAF) OF THE CAT: EVIDENCE FOR PARALLEL PROCESSING OF ACOUSTIC INFORMATION IN THE CEREBRAL CORTEX

by

Paul Louis Knight
B.A. Occidental College 1968
M.S. New York Medical College 1972

DISSERTATION

Submitted in partial satisfaction of the requirements for the degree of

DOCTOR OF PHILOSOPHY

in

PHYSIOLOGY

in the

GRADUATE DIVISION

(San Francisco)

of the

UNIVERSITY OF CALIFORNIA

PAUL LOUIS KNIGHT

CONTENTS

ABSTRACT

COCHLEOTOPIC ORGANIZATION AND CONNECTIONS OF THE ANTERIOR AUDITORY FIELD (AAF) OF THE CAT: EVIDENCE FOR PARALLEL PROCESSING OF ACOUSTIC INFORMATION IN THE CEREBRAL CORTEX

The anterior auditory field (AAF) is a large auditory representation in the cerebral cortex of the cat located on the middle and anterior ectosylvian gyri rostral to the so-called "primary" auditory cortex (AI). Fine-grained microelectrode maps of unit best frequencies were made in AAF of 16 ketamine anesthetized cats. Among the results were the following: (1) Most neurons in AAF that were driven by tonal stimuli had tuning curves with a single, sharply-definable minimum (the best frequency). Occasionally, units were found to have multiple tuning curve minima. (2) Penetrations made normal to the cortical surface of AAF isolated units that had remarkably similar tuning curves throughout the middle and deep cortical layers. (3) In most of AAF, a restricted sector of the cochlear partition is represented by a straight belt of cortex crossing the entire field. (4) There is a highly-organized representation of the cochlea within AAF. The cortical belt representing the most basal sector of the cochlea

(highest best frequencies) is oriented dorsoventrally along the border with the high frequency region of AI. Proceeding rostrally for some distance within AAF, lower frequency cortical belts are parallel to one another and maintain a highly-ordered representation of progressively more apical cochlear sectors. The orientation of the lowest frequency representation usually rotates following the ventral curvature of the anterior ectosylvian gyrus. (5) In the portion of the field caudal to the axis of rotation of the representation, best frequency (represented cochlear position) is a simple (and apparently relatively constant) function of distance from the mutual high frequency AI-AAF border. (6) There is a proportionately larger representation of the highest frequency octaves within AAF. (7). The results of penetrations down the banks of the suprasylvian sulcus indicate that there may be units of vertical organization within AAF similar to those in AI, and in somatosensory and visual cortical fields. (8) The boundaries of AAF as well as the frequency representation within it are highly variable when referenced to cortical surface landmarks. (9) The cytoarchitectonic boundaries of AAF approximately correspond with the physiologically-defined boundaries. (10) There were no cells driven to discharge by tonal stimuli in the fields dorsal and ventral to AAF.

Neuroanatomical tracing experiments were carried out on 12 cats to determine the relationship between the medial geniculate body (MGB) and physiologically-defined loci within AAF. Among the results were the following: (1) Any single site or multiple sites along any given isofrequency contour within AAF receive convergent projections from a long column of cells passing rostro-caudally through the deep dorsal division of the MGB and the posterior group nuclei (Po) and from a small group of cells within the ventral division of the MGB at its most lateral margin. (2) Cortical cells at any single site or multiple sites along any given isofrequency contour within AAF project divergently to terminals within the deep dorsal-posterior group column. (3) The thalamocortical and corticothalamic projections between the MGB and AAF are reciprocal within the deep dorsal-posterior group column.

Comparison of the properties of AAF and AI show that these two fields are remarkably similar in many important features including: unit response properties under ketamine anesthesia, short latency to earliest unit discharge, organization in depth, units of vertical organization, size, spatial representation of frequency and proportionately greater representation of higher frequency octaves. Loci of the same best frequency

within both AAF and AI receive thalamocortical projections from the same deep dorsal-posterior group column, and both fields project reciprocally upon that column. These similarities suggest that AAF is not a "secondary" cortical field, but, rather, that AAF and AI are virtually mirror images of one another and are co-participants in the earliest and fundamental processing of acoustic information at the cortical level.

ACKNOWLEDGEMENTS

I wish to express my deepest appreciation to my mentor, Michael M. Merzenich, for the direction and insight that he has given to me while I was his student. Some of the concepts I have presented in this work evolved from my collaboration with Michael Merzenich and G. Linn Roth in the mapping study of AI and with Richard Andersen in the neuroanatomical study presented here. The neuroanatomical techniques used in this project were demonstrated to me by my friend, Steven Colwell. Technical assistance for these projects was given by Patricia Clepper, Seymour Winston and Annette Lowe. To all of these people, I give my sincerest thanks.

To the members of my dissertation committee, Michael Merzenich, Henry J. Ralston, III, and Roy Steinberg, I express the thanks of a student who has been given the rights of passage by their approval of this work.

I would also like to extend my thanks to people who contributed to my life away from the laboratory during these years, particularly, Jeff, Doris, Bea and Leo Dwork, my oldest friends.

This work is dedicated to my family.

The work described herein was partially supported by NIH Grant NS-10414, the Coleman Fund, the Earl C. Anthony Fund, and Hearing Research, Inc.

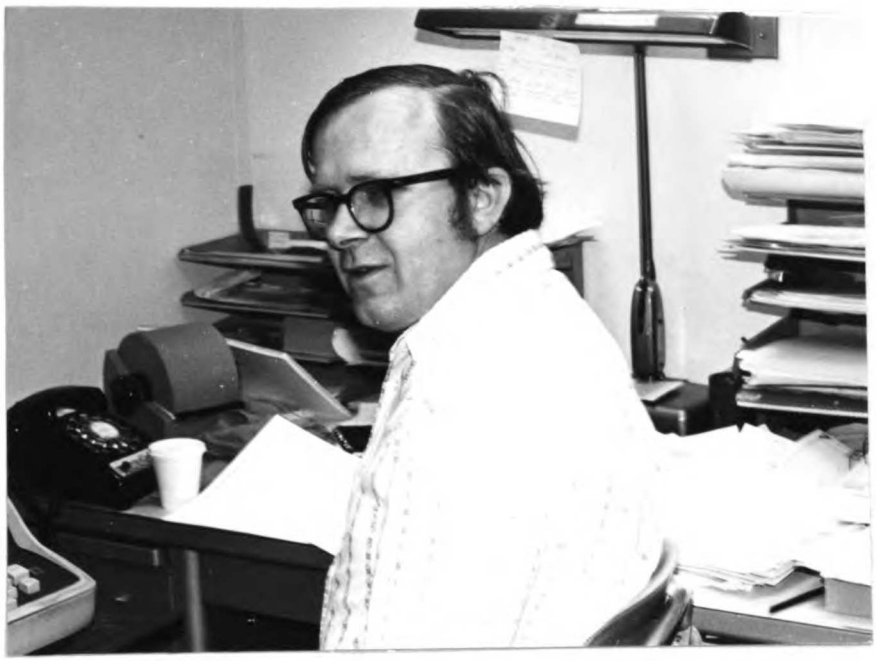

MICHAEL M. MERZENICH

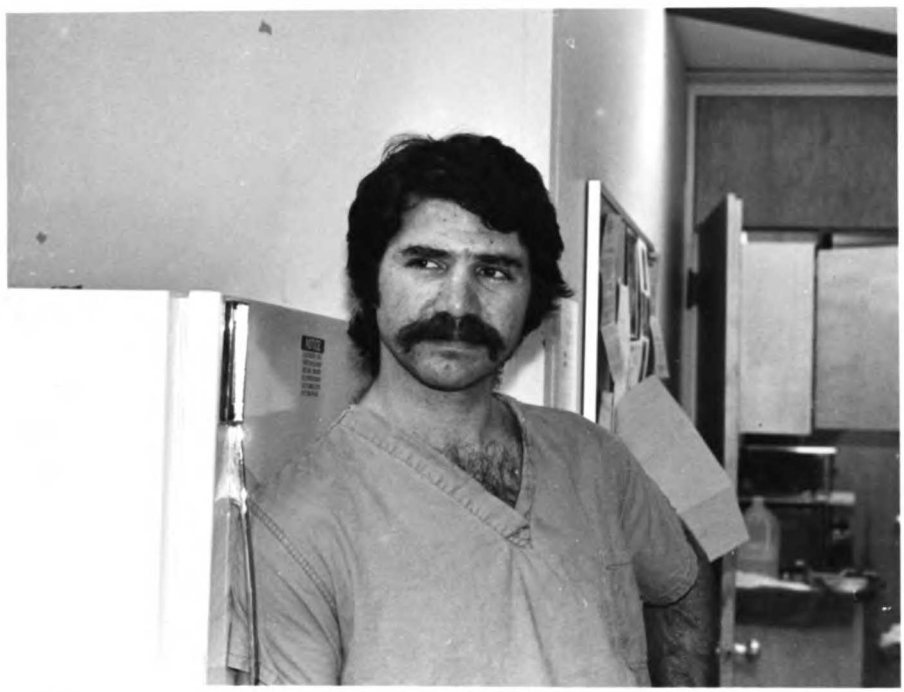

GEORGE LINN ROTH

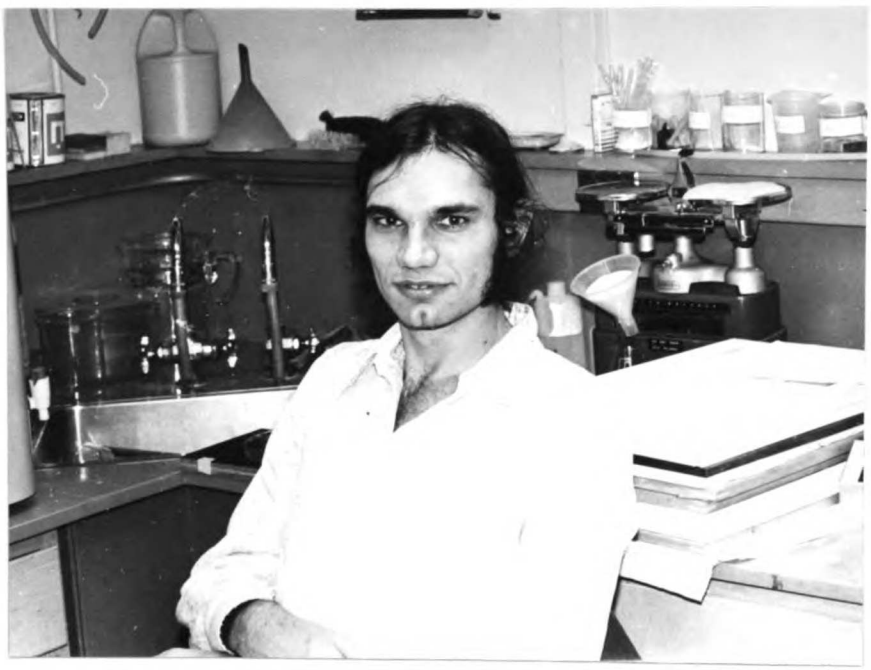

RICHARD ANDERSEN

NEUROANATOMICAL TERMINOLOGY

AAF	anterior auditory field
AEG	anterior ectosylvian gyrus
AES	anterior ectosylvian sulcus
AI	"primary auditory cortex"
AII	a "secondary" auditory field
AVCN	anterior ventral cochlear nucleus
ALS	anterior lateral sulcus
AS	ansate sulcus
AVCN	anterior ventral cochlear nucleus
CC	corpus callosum
CS	cruciate sulcus
D	deep dorsal division of the MGB
DCN	dorsal cochlear nucleus
Ep	posterior ectosylvian auditory field
LGD	dorsal lateral geniculate nucleus
LGV	ventral lateral geniculate nucleus
MGB	medial geniculate body
OR	optic radiation
PAG	periaquaductal gray
PES	posterior ectosylvian sulcus
PP	pes pedunculi
PS	pseudosylvian sulcus
SC	superior colliculus
SF	suprasylvian fringe

SS	suprasylvian sulcus
SSF	suprasylvian fringe
SSG	suprasylvian gyrus
V	ventral division of the MGB
VB	ventrobasal complex of the thalamus
ZM	marginal zone of the MGB

HISTORICAL FIGURE 1. Depiction of localization in the brain by Albertus Magnus (1206-1280) in Philosophia pauperum (the 1560 edition), a book dealing with the soul. At this time, the "cell doctrine of the brain" held that functions of behavior originated in the ventricles. Each ventricle was described as having dual function, hence their division in this figure. The association of the ventricles with behavior began in the second century A.D. with Galen. (This and following HISTORICAL FIGURES are from E. Clarke and K. Dewhurst, An Illustrated History of Brain Function. Berkeley: University of California Press, 1972.)

INTRODUCTION

INTRODUCTION

It is axiomatic that understanding the functions of the nervous system requires information concerning the functional and structural relationships between its component parts. As will be shown, a fundamental principle in the organization of the mammalian central auditory system is the orderly representation of the cochlea within most of its component nuclei and cortical fields. The experimental results reported in this work, in combination with earlier microelectrode mapping experiments by Merzenich, Knight and Roth (1973,1974,1975), show that there are at least two cochleotopic auditory fields within auditory cortex of the cat. The first is the so-called "primary auditory cortex", AI, and the other is the anterior auditory field, AAF. The spatial organizations of the cochlear representations in these fields are virtually mirror images of one another. Furthermore, physiological and anatomical evidence will be presented to show that these fields are processing some acoustic information in parallel, thus substantially modifying the concept of a single "primary" auditory cortex heirarchically

interacting with adjacent "secondary" auditory representations.

Before the application of fine-grained microelectrode mapping techniques to determine the representation of the cochlea within cat auditory cortex, there were three main lines of evidence suggesting cochleotopic organization in cat auditory cortex: (1) Within the cat auditory system, precortical nuclei, including the medial geniculate body (MGB), were shown to be cochleotopically organized, and an orderly projection from MGB to auditory cortex was described. (2) Cochleotopic organization has been clearly demonstrated within at least some auditory representations in the cerebral cortex of other mammalian species. And (3), studies based on recording of evoked potentials from cat auditory cortex gave preliminary evidence for cochleotopic organization of one or more auditory representations there.

Orderly Representation of the Cochlea Within Prethalamic Auditory Nuclei

Physiological and anatomical studies of the prethalamic auditory nuclei (the three divisions of the cochlear nuclear complex, the superior olivary nuclear complex, the nuclei of the lateral lemnisci and the central nucleus of the inferior colliculus) have shown that there are orderly representations of the cochlea within each of these nuclear groups. In each of the physiological studies, microelectrode recording revealed that at least some cells in these nuclei were sharply tuned with respect to stimulus frequency and intensity. The best frequency for an auditory neuron is defined as the tonal stimulus frequency that causes the neuron to discharge at the lowest stimulus intensity. A sharply tuned neuron may be said to represent that best frequency and also to represent the cochlear position corresponding to that best frequency.

Anatomical determinations of the pattern of first-order projections of the spiral ganglion are based on Golgi studies of the cochlear nuclei (Lorente de No, 1933a, 1933b) and studies of axonal degeneration within the cochlear nuclei following damage to the cochlea in the cat (Sando,1965) and other species (Noda and Pirsig,

1974; Moskowitz and Liu, 1972; Webster, 1971). These studies demonstrated that the cochlea projects to all three divisions of the cochlear nuclear complex: the anterior ventral cochlear nucleus (AVCN), the posterior ventral cochlear nucleus (PVCN), and the dorsal cochlear nucleus (DCN). In the degeneration studies, these investigators showed that a broad sector of the cochlea projects in an orderly manner to a three dimensional array of neurons crossing each major division of the cochlear nucleus from edge to edge.

Physiological evidence for orderly projections of the cochlea upon the cochlear nuclei of the cat is based on the finding of orderly changes of unit best frequency (or, equivalently, represented cochlear position) recorded in microelectrode penetrations through the subdivisions of the cochlear nuclear complex (Rose, Galambos and Hughes, 1959, 1960). Discontinuities in orderly sequences of best frequencies along electrode tracks were found at the cytoarchitectonic boundaries of the major divisions of the cochlear nucleus.

For several species, the subdivisions of the cochlear nuclei have been shown to project to the subdivisions of the superior olivary complex, the nuclei of the lateral lemnisci and the central nucleus of the inferior colliculus (Osen, 1972; Woollard and Harpman, 1940; Adams and Warr, 1976; Fernandez and Karapas, 1967;

Strominger and Strominger, 1971; Strominger, 1973; Strominger, Nelson and Dougherty,1977; van Noort, 1969; Harrison and Warr, 1962; Barnes, Magoun and Ranson, 1943; Adams, 1975; Aitkin and Moore, 1975; Aitkin, Roth and Merzenich, unpublished results). There are also projections from the nuclei of the lateral lemnisci and the superior olivary complex to the central nucleus of the inferior colliculus (Stotler, 1953; van Noort, 1969; Adams, 1975; Aitkin, Roth and Merzenich, unpublished results). While these projection systems are complex, they are structured to preserve the cochleotopic organization of these nuclei (Aitkin, Anderson and Brugge, 1970; Goldberg and Brown, 1968; Merzenich and Reid, 1974; Rose, Greenwood, Goldberg and Hind, 1963; Tsuchitani and Boudreau, 1966; Guinan, Norris and Guinan, 1972; Aitkin and Moore, 1975; Brownell, 1977; Tsuchitani, 1977) as shown schematically in Figure 1.

Medial Geniculate Body and Auditory Thalamocortical Projections

Microelectrode mapping of best frequencies of units encountered in penetrations into the MGB of the cat by Aitkin and Webster (1972) have shown that there is an orderly representation of the cochlea within the laminated portion (LP) of the ventral division (Morest,

1964, 1965) and possibly other divisions. Within the laminated portion, the cochlear apex was found to be represented laterally and the cochlear base was represented medially. Similar organization has been shown in microelectrode studies of the cochlear representation in the MGB of the squirrel monkey (Gross, Lifschitz and Anderson, 1974). Thus, the spatially-ordered ascending projection from the inferior colliculus (Moore and Goldberg, 1963; Morest, 1965b) preserves the cochleotopic organization of the laminated central nucleus of the inferior colliculus (Rockel and Jones, 1973) and may constitute point-to-point projections between these nuclei (Merzenich and Reid, 1974).

Physiological (Woolsey, 1964) and anatomical studies (Waller, 1940; Poliak, 1927; Mettler, 1932; Woollard and Harpman, 1939; Rose and Woolsey, 1949, 1958) of the projection of the medial geniculate body upon auditory cortex in the cat and other species (e.g., Poliak, 1932; Clark, 1936; Walker, 1937,1938; Pandya and Sanides, 1972; Mesulam and Pandya, 1973) have emphasized the orderly arrangement of the auditory geniculocortical pathways. These studies have suggested point-to-point connections between some subdivisions of the MGB and cytoarchitectonic divisions of the auditory cortex. More recently, Colwell and Merzenich (1975) have clarified the nature of these thalamocortical projections in the cat

using the retrograde transport of horseradish peroxidase from physiologically defined loci within AI. Their results have clearly shown that a two dimensional injection site in AI receives a convergent projection from three dimensional arrays of MGB neurons within four cochleotopically organized divisions of the MGB. Among other results, these studies have demonstrated that information derived from the initial transformation of stimulus frequency to cochlear postion is conserved through the precortical auditory nuclei and projectional pathways.

Functional Localization of Auditory Cortex: Early Behavioral, Anatomical and Physiological Observations

The first observations of the location of the cortical projections of the mammalian auditory system were made by David Ferrier (1876). He showed that electrical stimulation of restricted regions of the cortex of various species was followed by a behavioral response indicative of auditory activity. In the cat, stimulation of the middle and posterior ectosylvian gyri (as shown in Figure 2) was followed by retraction of the ears and turning of the head and eyes to the side of the body contralateral to the stimulated cortex. His pioneering work first demonstrated the general location

of auditory cortex in the cat and other species. All subsequent studies of auditory function in the cortex have been in general agreement with his observations.

Confirmation of Ferrier's observations of a possibly homologous auditory region in the ectosylvian cortex of the dog came from Munk in 1881. He showed that lesions involving part of the dog's ectosylvian cortex caused temporary behavioral deficits in understanding verbal commands.

Just before the turn of the century, Larionow (1899) stimulated the cochlea of the dog using sounds produced by tuning forks and crudely recorded (with a galvanometer) electrical responses from the cortical region identified by Ferrier. He suggested that an S-shaped belt of cortex on the middle and posterior ectosylvian gyri was the faithful representation of the unfurled cochlea (shown in Figure 3).

One of the early neuroanatomical observations by C. Vogt (1900) pointed out a discrete region of early myelinization in the middle ectosylvian gyrus that was interpreted as the location of primary auditory cortex in the cat. This area was anatomically similar to the area described as the primary auditory cortex in man (Vogt and Vogt, 1919, 1926) shown in Figure 4. Subsequently, Campbell (1905), Winkler and Potter (1914) and Kornmuller (1933) described temporal auditory regions in the cat on

the basis of cytoarchitecture. Each recognized a region (koniocortex) in which there was a conspicuous radial orientation of cells, particularly in laminae 2 and 3 (the "rainshower formation" of von Economo and Koskinas, 1925).

Campbell also introduced the concept of heriarchical processing in the cat auditory cortex. He described two auditory cortical regions, a central primary acoustic region (Ectosylvian A) (his "audito-sensory" cortex) receiving projections from the medial geniculate body and a secondary auditory region (Ectosylvian B) surrounding the primary region and subserving "higher" auditory function (his "audito-psychic" cortex), as shown in Figure 5. On the basis of cytoarchitecture, he also described a similar organization of auditory cortex in primates, including man (Figure 6). The central region of koniocortex bears a striking resemblance to the central region in primate auditory cortex (Campbell, 1905; von Economo, 1929; Beck, 1929; Sanides, 1972; Pandya and Sanides, 1973), which has been shown to be primate A1 (Merzenich and Brugge, 1973; Imig, Ruggero, Kitzes, Javel and Brugge, 1977).

Subdivision of cat auditory cortex similar to that of Campbell was indicated by Mettler's (1932) observation of retrograde degeneration in the medial geniculate body

from lesions in Ectosylvian A as well as strong intracortical connections within this region. He found intracortical projections to Ectosylvian B, but they were more sparse than those within Ectosylvian A. Furthermore, Mettler found no projections from MGB to Ectosylvian B. These studies supported the findings by Woollard and Harpman (1939) and Ades (1941) of anterograde degeneration in the middle ectosylvian gyrus following electrolytic lesions within the medial geniculate body.

Technical improvements in electrical recording allowed Kornmuller (1933) to produce a map of cat auditory cortex based on the cortical responses to sound stimulation (shown in Figure 7). He observed surface evoked potentials restricted to the middle ectosylvian gyrus. In their later study of surface evoked potentials, Bremer and Dow (1939) mapped strongly driven responses in the area described by Kornmuller, but also found weaker responses in surrounding areas. They argued that the auditory cortex may be physiologically divided as indicated by the cytoarchitectonic parcellation .

There have been many differences between the parcellation of auditory cortex by these authors. One reason for these differences was pointed out by Ades (1941). He cautioned that the variability of sulcal patterns in the auditory region of the cat could cause

considerable difficulty in generalizing maps of auditory cortex from one animal to another.

Topographic Representations of the Cochlea in Cat Auditory Cortex

Woolsey and Walzl (1942) were the first investigators to demonstrate a topographic representation of restricted sectors of the cochlear partition within auditory cortex of the cat. While electrically stimulating short sectors of eighth nerve fibers within the osseous spiral lamina in the dissected cochlea, they recorded the stimulus-locked evoked potential from a large number of points on the cortical surface of the anterior, middle and posterior ectosylvian gyri. Their results were as follows: (1) Responses to stimulation of apical fibers of both the contralateral and ipsilateral cochleas were centered dorsally on the posterior ectosylvian gyrus, ventrally on the middle ectosylvian gyrus, and rostrally on the anterior ectosylvian gyrus. (2) Responses to stimulation of more basal fibers of either ear were centered ventrally on the posterior ectosylvian gyrus and over a broad, apparently continuous, region of the middle and anterior ectosylvian gyri. A composite diagram of their results is shown in Figure 8. They interpreted their results as showing

double and bilateral representations of the cochlea within each hemisphere. The dorsal one, AI (Woolsey and Fairman, 1946), had a topographic map of the cochlea with the cochlear base represented rostrally near the dorsal tip of the anterior ectosylvian sulcus and the cochlear apex represented caudal to the dorsal tip of the posterior ectosylvian sulcus. They described a second region, AII, immediately ventral to AI, having a reversed cochlear map with the cochlear base represented caudally on the posterior ectosylvian gyrus and the cochlear apex represented rostrally on the ventral portion of the anterior ectosylvian gyrus.

Ades (1943) showed that the acoustically responsive area on the posterior ectosylvian gyrus was separate from the rest of Woolsey and Walzl's (1942) AII. He demonstrated projections to this area from strychnine-treated patches within AI physiologically identified by strong responses to click stimuli.

With this information, Rose (1949) was able to divide the auditory cortex of the cat into four regions on the basis of cytoarchitecture: the dorsal AI (koniocortex), a ventral AII, corresponding to the rostral two-thirds of the AII described by Woolsey and Walzl (1942) and Ades (1943), the posterior ectosylvian area (Ep), and the suprasylvian fringe (SF), a field partially exposed on the ventral anterior ectosylvian

gyrus but mostly buried on the ventral bank of the suprasylvian sulcus. In a companion retrograde degeneration study, Rose and Woolsey (1949) showed that AI received an orderly and essential (i.e., degenerating with lesions restricted to AI) projection from the principal division (Rioch, 1929) of the MGB. Auditory areas outside of AI were said to receive sustaining projections from the MGB (i.e., projections which do not degenerate with lesions restricted to one of these other fields, but which degenerate with lesions in both AI and surrounding fields).

The notion of a single primary acoustic area heirarchically connected to adjacent secondary fields received support from Bremer (1953), Mickle and Ades (1953) and Downman, Woolsey and Lende (1960). They showed that Woolsey's AII and Ep had different response characteristics than AI (e.g., higher thresholds, longer response latencies) and were dependent on an intact AI for activation.

Support for the parcellation of the anterior ectosylvian acoustic area came from experiments showing centers of evocable auditory responses on the ventral aspect of this region that were spatially separate from the AI region, but that responded with similar amplitude and latency to acoustic stimulation. In his later syntheses (shown in Figure 9) of the evoked potential

data, Woolsey (1960,1961) concluded that these studies showed a complete representation of the cochlea in the suprasylvian fringe.

Recording surface evoked potentials from small strychnine-treated patches of auditory cortex, Hind (1953) determined tuning curves for restricted loci in cat auditory cortex. In his most extensive map of a single animal (Figure 10) he showed a clear caudal-to-rostral progression of higher frequencies within AI and a clear reversal in the sequence of represented frequencies on the anterior ectosylvian gyrus. However, in his composite map (Figure 11), he combined data from several animals to give an overall summary that obscured this reversal.

Concurrent evoked potential studies of the cochlear representations within auditory cortex of the dog by Tunturi (1945, 1950a, 1950b,1952) showed that AI of the dog has a complete and orderly representation of the cochlea with the apical cochlea represented caudally and the basal cochlea represented rostrally. His maps showed that a sector of the cochlear partition was represented by a straight belt of cortex with a dorsoventral orientation crossing the entire representation. Furthermore, he defined another partial cochlear

representation, AIII, located ventrally on the anterior ectosylvian gyrus.

Woolsey (1960,1961) evaluated these and other studies in an effort to synthesize a complete map of auditory cortex in the cat. This map is shown in Figure 9. His map shows a central auditory region comprising four central fields plus five more peripheral regions. Within each of the central fields, AI, AII, SF, and Ep, he described a complete and orderly representation of the cochlea . In this figure, "A" denotes areas of representation of the cochlear apex, and "B" denotes areas of representation of the cochlear base. Long latency responses (under chloralose anesthesia) to click stimulation were recorded in all associational areas except AIII, which was inferred from Tunturi's work , but was never clearly demonstrated in the cat. Woolsey's belief in complete representations of the cochlea within each of the central fields led him to draw the low frequency region of SF on the ventral bank of the anterior ectosylvian sulcus as being part of a larger field, the "suprasylvian fringe" (SF), that was continuous with a high frequency area dorsocaudal to AI.

Until recently, this map has been considered to be the "standard" map of auditory cortex and has been used as a reference to determine the locations of electrode penetrations and ablations within the multiple

representations of the cochlea in cat auditory cortex. It will be shown that this map is incorrect in detail, and, furthermore, that it is impossible to create any map of auditory cortex that accurately depicts the cortical representation of the cochlea in more than one animal.

Advances in Mapping Technique: Fine-grained Microelectrode Mapping

The descriptions of cochlear representation in the cerebral cortex based on the recording of surface evoked potentials are limited by the resolution of the stimulation and recording techniques used in these earlier studies. Microelectrode mapping techniques have a finer spatial resolution than evoked potential recording methods and have been used to determine the representation of the sensory epithelium in visual (e.g., Kaas, Hall and Diamond, 1970) and somatosensory (e.g., Paul, Merzenich, and Goodman, 1972; Welker, Johnson and Pubols, 1964) cortices before being applied to the mapping of auditory cortex.

There are several reasons for the potentially greater resolution of microelectrode mapping techniques as compared with surface evoked potential mapping in studies of auditory cortex: (1) The response of the

cochlea at threshold intensities for detection of discharge of cortical neurons is more spatially restricted than the suprathreshold cochlear response to acoustic stimuli or direct electrical excitation used in the evoked potential studies. As a consequence of this more restricted cochlear stimulation, a more spatially restricted set of cortical neurons is brought to discharge if those cortical neurons are sharply tuned with respect to stimulus frequency. (2) Response properties of single cortical neurons (e.g. latency, tuning curves, response consistency) that may be used to differentiate units in different cortical fields are evident in single unit recording but may be obscured by recording the surface evoked potential that is due to the summed activity of many neurons. (3) The small distances between the large number of penetrations commonly used in microelectrode mapping studies give finer spatial resolution to maps of unit response properties than the larger distances typically used between cortical points in surface evoked potential studies. And (4), gliosis and electrolytic lesions produced by microelectrodes can be located in tissue sections to give accurate cyto- and myeloarchitectonic correlations with the representational boundaries determined physiologically.

Cochleotopic Organization of Auditory Cortex in Other Species Determined by Microelectrode Mapping

The technique of fine-grained microelectrode mapping has been used to determine the cochlear representations on the superior temporal plane of two species of macaques (Merzenich and Brugge, 1973). By mapping the best frequencies of neurons found in a large number of closely spaced penetrations into auditory cortex, they were able to demonstrate the presence of at least five distinct auditory representations on the superior temporal plane (see Figure 12) that were not appreciated in earlier evoked potential studies (Kennedy, 1955; Licklider and Kryter, 1942; Walzl, 1947; Walzl and Woolsey, 1943; Woolsey and Walzl, 1944; Bailey, von Bonin, Garol, and McCulloch, 1943; Woolsey, 1971; Pribram, Rosner and Rosenblith, 1954).

They found that the auditory cortex of the macaque includes the following fields: AI, a field of sharply tuned units having a complete and orderly representation of the cochlea (see Figure 13), the caudomedial field (CM), an incompletely mapped field with broadly-tuned units, the rostrolateral field (RL), an orderly but only partial representation of the apical cochlea, the lateral field (L), apparently containing a complete cochlear

representation, and one or two incompletely mapped adjacent fields.

Similar microelectrode mapping studies have been carried out on the auditory cortex of the owl monkey (Imig, Ruggero, Kitzes, Javel and Brugge, 1977). They demonstrated a complete and orderly representation of sharply tuned neurons within AI and the rostral field (R) as well as auditory responses in the surrounding fields, the caudomedial (CM), the anterolateral (AL) and the posterolateral (PL), as shown in Figure 14.

In the grey squirrel, Merzenich, Kaas and Roth (1976) found that there was a central AI field of sharply-tuned units with a complete and orderly representation of the cochlea. Surrounding AI they found an active belt of cortex in which neurons were sharply tuned as well as a more peripheral belt of less responsive neurons (shown in Figure 15).

Similarly, a strictly tonotopic (cochleotopic) organization has been shown within AI resulting from microelectrode mapping experiments seeking to determine the cochlear representation within that field of the tree shrew (Oliver, Merzenich, Roth, Hall and Kaas, 1976).

A notable exception to this pattern of cochlear representation in AI is found in the echo-locating mustache bat. While most of AI appears to be similar to that in other species, there are two disproportionately

large high frequency representations. One specialized region is thought to subserve processing of constant-frequency echo location information (61 to 63 kHz) and the other for processing frequency-modulated sounds (50 to 60 kHz) (Suga, 1977).

Initial Microelectrode Mapping of Cat AI

The first applications of microelectrode mapping in auditory cortex of the cat (Goldstein, Abeles, Daly and McIntosh, 1970; Evans and Whitfield, 1964; Evans, Ross and Whitfield, 1965; Hind *et al.*, 1960) did not show the highly-ordered cochlear representation suggested by the earlier evoked potential studies. While each of these studies showed a tendency for units of higher best frequency to be located more rostrally in AI, they suggested that units of any best frequency could be located in any portion of AI. On the basis of these and other experiments (see Figures 16 and 17) cochlear representation has been described as being progressively degraded in ascending auditory pathways (Clopton, Winfield and Flamino, 1973; Evans, 1968; Evans, 1974; Evans and Whitfield, 1964; Whitfield, 1971).

The particular method of data analysis used in these experiments could lead to serious distortion of the

picture of the orderly representation of the cochlea within auditory cortex. In each of these studies, partial maps with few penetrations were made in each animal. By assuming a consistent relationship between sulcal patterns and the position of AI on the cortical surface, each of these investigators combined data points from several animals to give composite maps of AI. However, it is clear that the sulcal patterns of the cortex are highly variable among animals (Ades, 1941, 1959; Kawamura, 1971; Rose, 1949) and, therefore, considerable error could result from trying to combine data from several animals using sulci as references. Thus, extensive maps of AI in individual cats were needed to confirm the complete and orderly representation of the cochlea in that field.

Confirmation of Cochleotopic Organization of Cat AI

Recognizing the variability of the cortical sulcal patterns, Merzenich, Knight and Roth (1973, 1974, 1975) re-examined the representation of the cochlea within AI of individual cats. For each animal in this study, extensive, fine-grained maps of single unit and unit cluster best frequencies were made in AI, and, to a limited extent, in adjoining fields. Several important conclusions were drawn from this study concerning the

pattern of the representation of the cochlea in AI of the cat.

Single units in AI were found to be sharply tuned near threshold allowing unequivocal assignment of a value for best frequency. When recording multiple neurons at a given cortical point, all units driven to discharge to the tonal stimuli had identical best frequencies. AI was found to be radially organized with units of similar best frequencies being found through the middle and deep cortical layers in penetrations normal to the cortical surface. Similar results had been noted previously by other workers (Abeles and Goldstein, 1970; Gerstein and Kiang, 1964; Hind et al., 1960; Parker, 1965; Oonishi and Katsuki, 1965).

In extensive maps of AI such as shown in Figures 18 and 19, it was demonstrated that there was a complete and orderly representation of the cochlea within AI. As can be seen in these figures, the lowest best frequencies recorded were found caudally in AI, and there was an orderly progression to higher best frequencies rostrally. Furthermore, penetrations of similar best frequency were arranged along a line of dorso-ventral orientation. Long penetrations directed down the banks of the posterior ectosylvian sulcus (shown in Figures 18 and 19) passed through discrete regions in which all units had similar

best frequencies followed by a step-like change to a region of lower best frequency. From these data it was concluded that AI had units of vertical organization similar to those found in visual (Hubel and Wiesel, 1962, 1963, 1974; LeVay, Hubel and Wiesel, 1975; Wiesel, Hubel and Lam 1974; Kaas, Lin and Casagrande, 1974) and somatosensory cortex (Mountcastle, 1957; Powell and Mountcastle, 1959).

Further analysis of the spatial distribution of best frequencies was carried out for 5 cats (Figure 20). For each cat, a series of parallel lines with rostro-caudal orientation was drawn perpendicular to the isofrequency contours. Best frequencies found on or near these lines were plotted as a function of distance from the most caudal isofrequency line on the exposed cortical surface with a different symbol used for each line. These functions showed that the relationship between best frequency and distance across AI is similar for all lines crossing AI. Thus, it was concluded that: (1) a given frequency band is represented by a nearly straight belt of cortex crossing AI with a predominantly dorso-ventral orientation; (2) a cortical belt representing a given frequency band must be nearly straight across AI; (3) such a sector must be of nearly constant width across AI; (4) the proportionality of representation of different frequencies must be maintained across AI; and, (5) from

the slope of these curves, it was evident that there was a proportionately larger representation of higher frequency octaves along the rostro-caudal dimension of AI.

To compare the representations of best frequency in AI of different cats, best fit curves (shown in Figure 21A) were drawn through these data points. In Figure 21A these curves were displaced on the ordinate to facilitate comparison. As can be seen, these curves closely parallel one another showing that the spatial organization is similar for most cats.

To show the cochleotopic organization of AI, two of these curves were replotted after conversion of best frequency to represented cochlear position (Figure 21B) using the function of Greenwood (1961, 1974). From these curves it was evident that: (1) a cochlear sector is represented in AI by a belt of cortex crossing this field with a dorso-ventral orientation; (2) such a belt of cortex must be of nearly constant width along the rostro-caudal dimension; and (3), the cortical belts representing the most basal sectors are wider along the rostro-caudal dimension of AI than the belts representing more apical cochlear sectors of constant width.

The total areas of representation of best frequency bands and cochlear sectors in AI are shown in Figure 22. From this figure, it can be appreciated that there is a proportionately larger total area devoted to the representation of progressively higher octaves, or, equivalently, more basal equal-length sectors. This relationship is a clear exception to the "rule" that cortical representatation is proportional to peripheral innervation density suggested as applying to the visual (Holmes, 1945; Talbot and Marshall, 1941) and somatosensory systems (Rose and Mountcastle, 1959; Welker, 1973; Woolsey, Marshall and Bard, 1942).

In addition to penetrations directed into AI, some penetrations were made into adjacent auditory fields including the field immediately rostral to AI (shown in Figure 19) across the high frequency border. On the basis of these few penetrations, it was suggested that there might be a second cochlear representation in this rostral field with low frequencies represented rostrally and high frequencies represented caudally along the high frequency border with AI.

If there were a complete representation of the cochlea rostral to AI with a reversed frequency representation, then it would help to explain the discrepancy in size between the large AI described by

Woolsey (1960; 1961) in his syntheses of evoked potential data (shown in Figure 9) and the smaller AI field described by Merzenich, Knight and Roth (1973, 1974 1975).

To determine the pattern of representation of the cochlea within this rostral field, fine-grained microelectrode maps of unit best frequencies were made within it. In order to avoid implying homology with the rostral field in primates , this field is renamed the anterior auditory field (AAF). The anterior auditory field has a complete and orderly cochlear representation. The cochlear apex is represented rostrally and the cochlear base is represented caudally along the rostral border of AI. Spatially, the cochlear representations in AI and AAF are virtually mirror images of one another reflected about their mutual border representing the extreme cochlear base. The finding of similar short response latencies (10-12 msec) suggested that these two fields are processing acoustic information in parallel.

Neuroanatomical experiments were undertaken to determine whether or not AAF and AI were receiving similar inputs from the medial geniculate body. These experiments have strengthened the concept of parallel processing by showing that AAF and AI (Colwell and

Merzenich, 1975) receive afferents in common from some of the same MGB divisions.

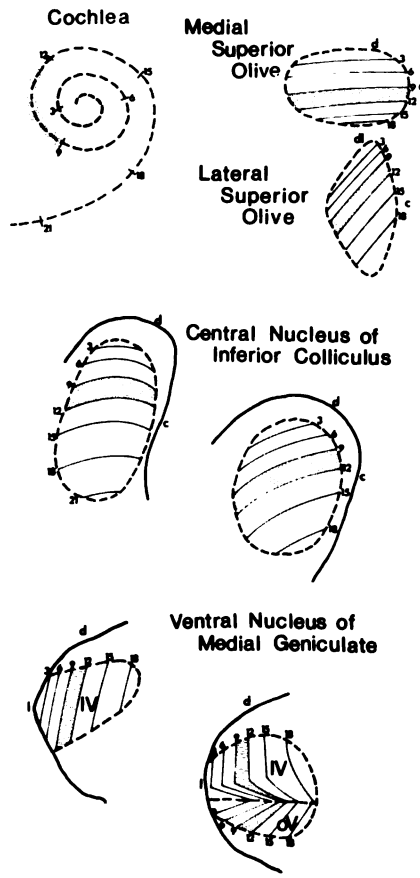

FIGURE 1. Representations of sectors of the cochlea within precortical auditory nuclei of the cat. Numbers indicate distance from cochlear apex. Outlines of the superior olivary complex are schematic. (From Merzenich, Roth, Andersen, Knight, and Colwell, 1977.)

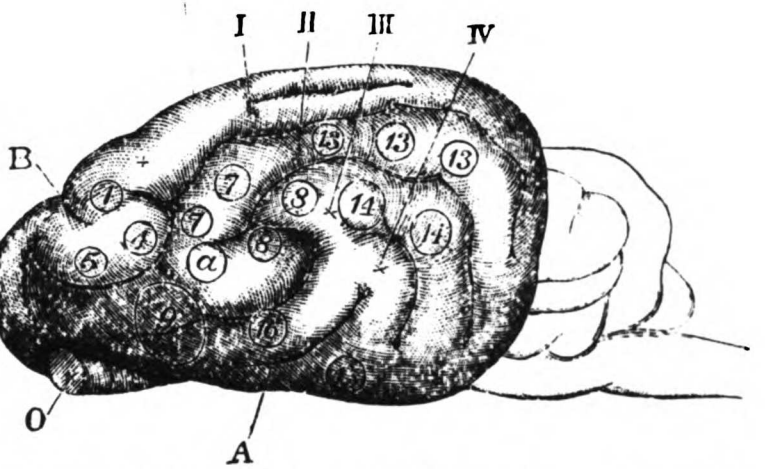

FIG. 35.—Left Hemisphere of the Brain of the Cat. A. The fissure of Sylvius. B. The crucial sulcus. O. The olfactory tract, cut. I. The superior external convolution. II. The second external convolution. III. The third external convolution. IV. The fourth external convolution.

FIGURE 2. Location of auditory cortex in the cat by Ferrier (1876). Behavioral responses indicative of auditory responses were observed for electrical stimulation of points labelled "14".

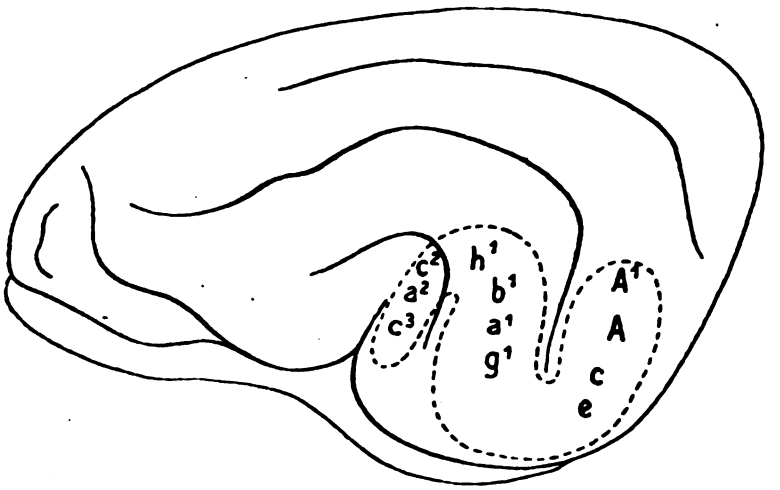

Fig. 1.

FIGURE 3. Representation of the unfurled cochlea within auditory cortex of the dog described by Larionow (1899) from galvanometric measurements of cortical responses to tonal stimuli. Letters indicate musical scales of tuning forks used for stimulation.

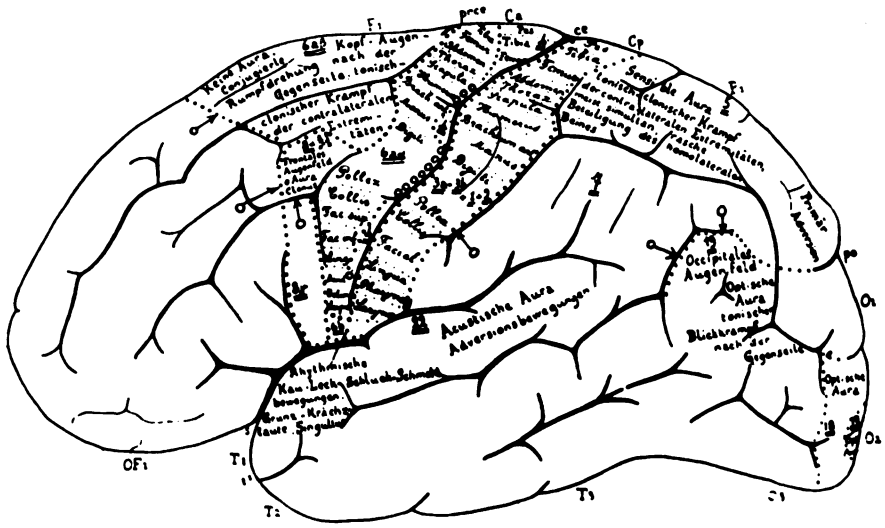

FIGURE 4. Human cortical localization based on the anatomical studies of Vogt and Vogt (1926). Auditory cortex ("Acustische Aura") is shown on the dorsal surface of the temporal lobe.

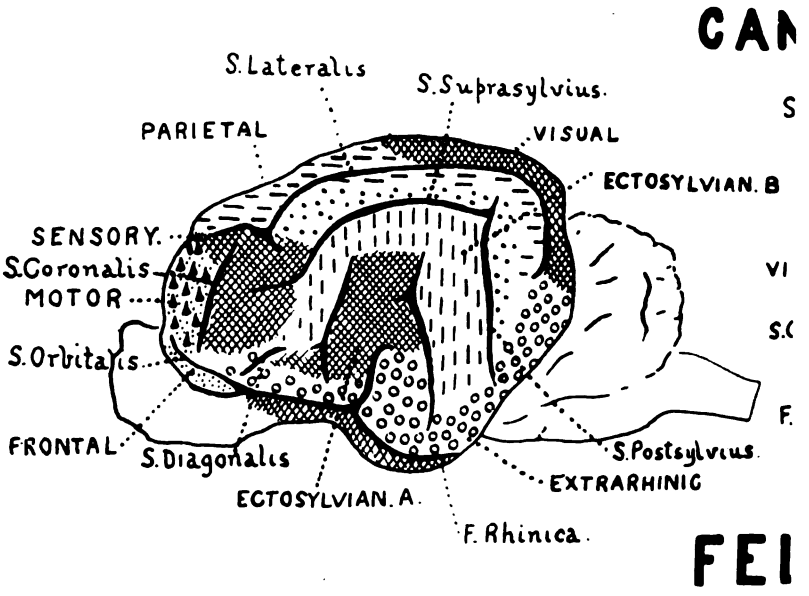

FIGURE 5. Auditory cortex in the cat described by Campbell (1905) on the basis of cytoarchitecture. Region Ectosylvian A was considered to be "audito-sensory", while the region Ectosylvian B was considered to be "audito-psychic".

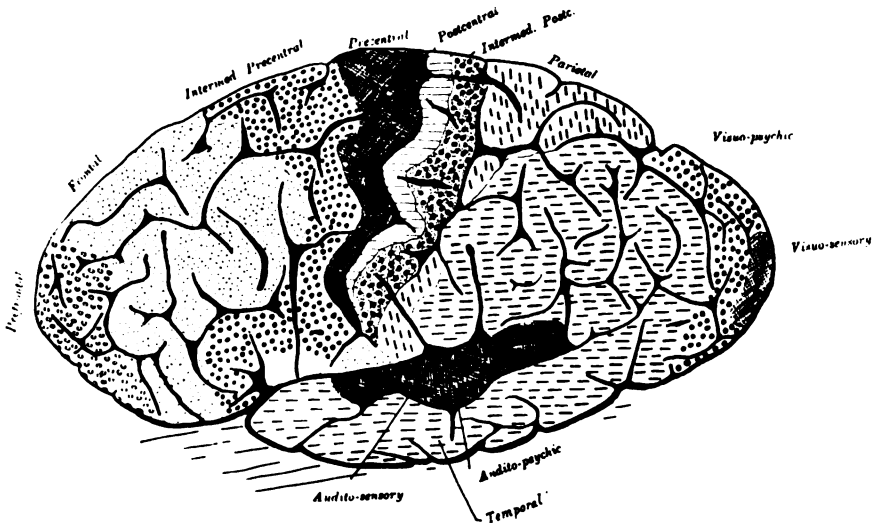

FIGURE 6. Parcellation of the human auditory cortex by Campbell (1905) into a central "audito-sensory" field and a more peripheral "audito-psychic" area.

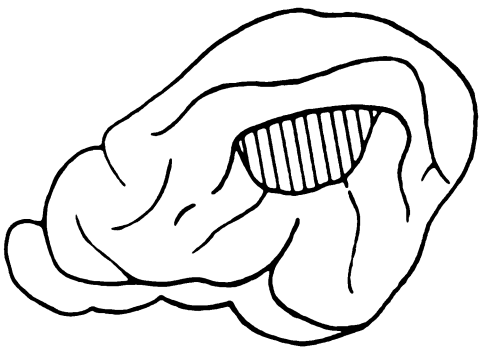

FIGURE 7. Areas of the cerebral cortex in the cat from which Kornmuller (1937) recorded surface evoked potentials following acoustic stimulation.

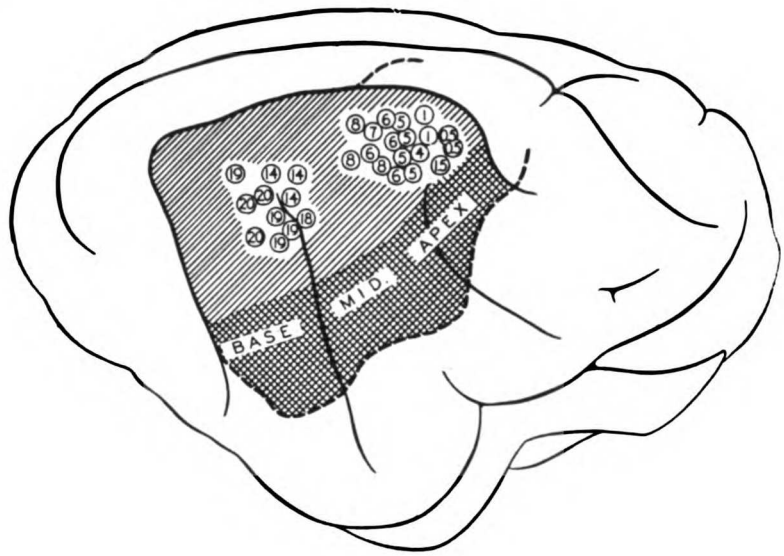

FIGURE 8. Two complete representations of the cochlea in cat auditory cortex as determined by Woolsey and Walzl (1942). In the dorsal representation, AI, numbers indicate stimulation positions along the cochlea as distance in millimeters from the cochlear base. Regions of cochlear representation are shown in the ventral AII. Note reversed order of the two representations crossing the cortical surface.

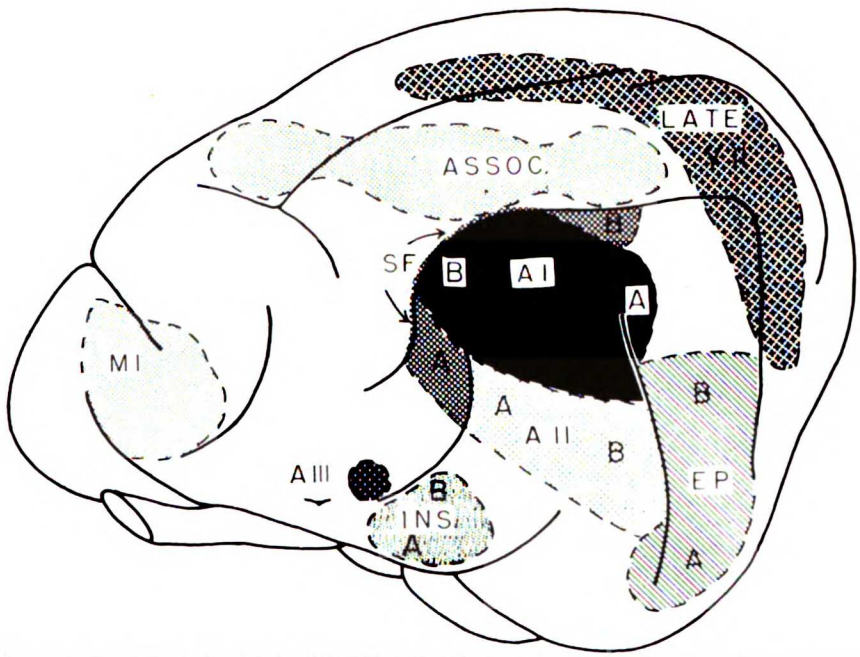

FIGURE 9. Woolsey's (1960) composite map of cat auditory cortex showing a central region with four highly-ordered cochlear representations (AI, AII, SF, Ep), as well as associational areas responding to sound stimulation. "A" denotes areas of representation of the cochlear apex; "B" denotes areas of representation of the cochlear base.

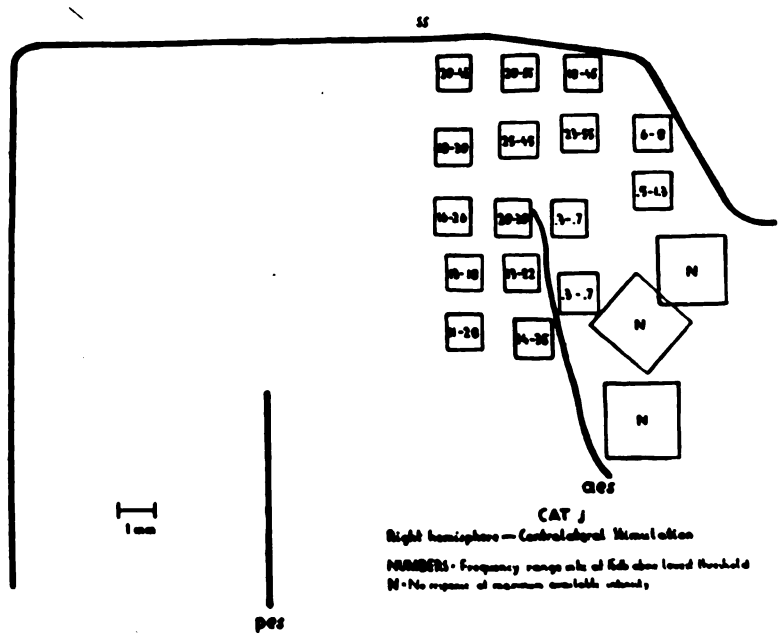

FIGURE 10. A map of auditory cortex in a single cat by Hind (1953) showing restricted loci responsive to tones of the frequencies shown (in kHz). Determinations were made by recording surface evoked potentials from patches of strychnine treated cortex. Note reversal in best frequency sequence moving rostrally.

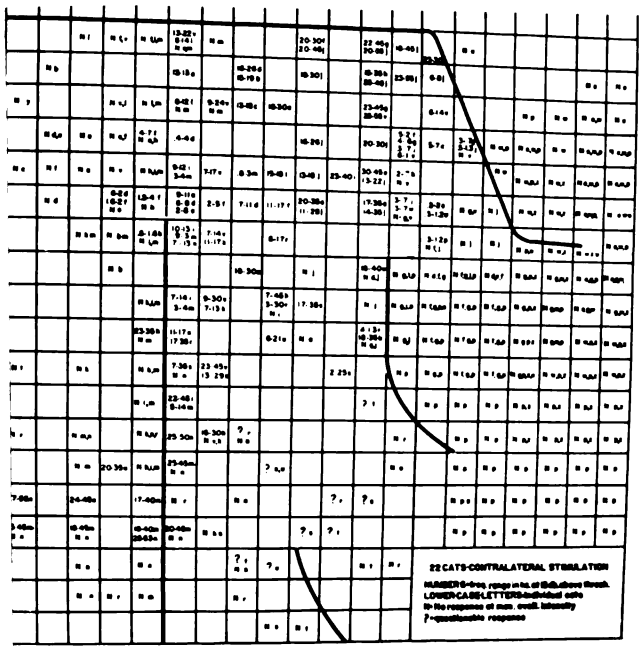

FIGURE 11. Composite map of auditory cortex in the cat by Hind (1953) showing the results of mapping auditory cortex in several cats and combining these results on a "standard" map of cortex referencing sulcal patterns.

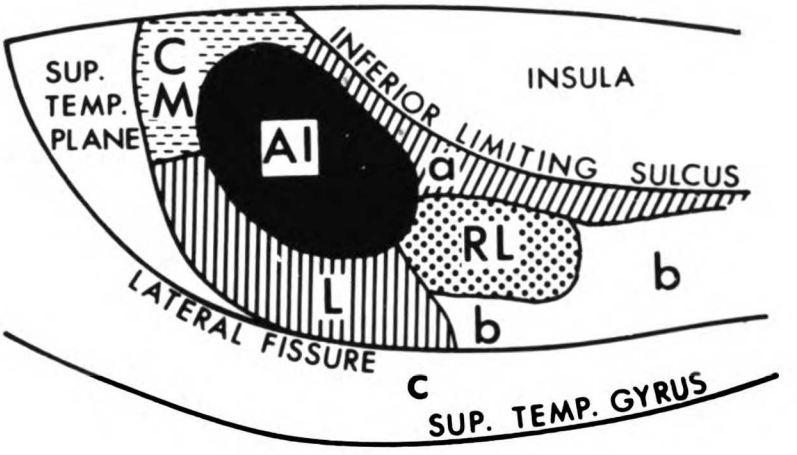

FIGURE 12. Schematic representations of multiple cochlear representations on the right superior temporal plane of the macaque monkey by Merzenich and Brugge (1973). RL, rostrolateral field; L, lateral field; CM, caudomedial field.

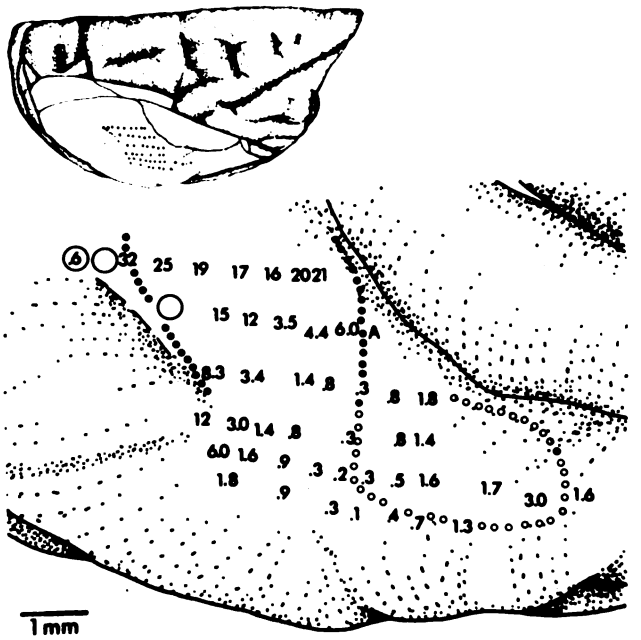

FIGURE 13. Map of best frequencies recorded in three cortical auditory fields (AI,RL and L) in a single Macaca arctoides by Merzenich and Brugge (1973). Closed circles denote boundary of AI; open circles denote boundary of the rostrolateral field (RL).

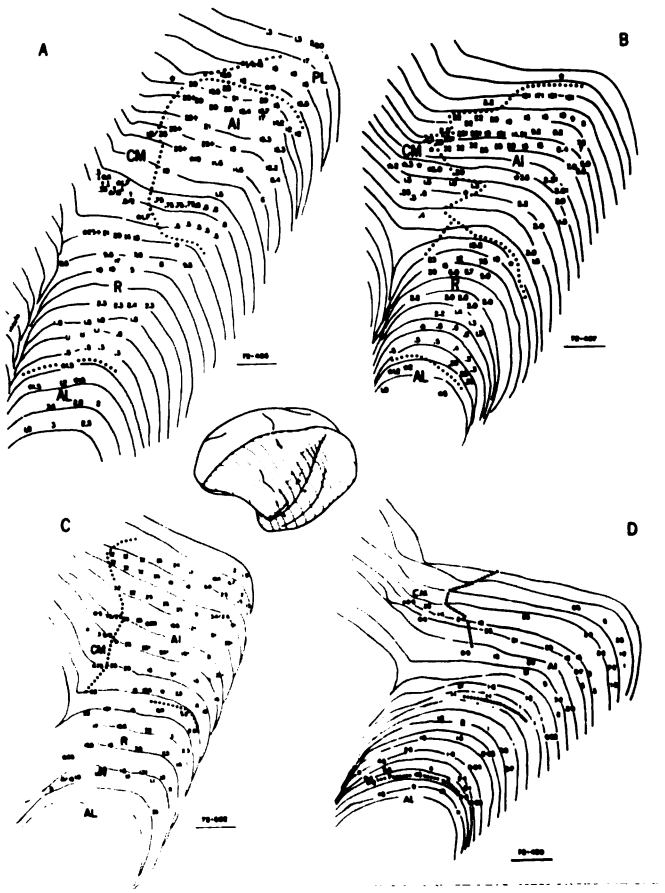

FIGURE 14. Representations of best frequency (in kHz) for penetrations into four auditory fields in the owl monkey by Imig, et al., (1977). CM, caudomedial field; R, rostral field; AL, anterolateral field; PL, posterior lateral field.

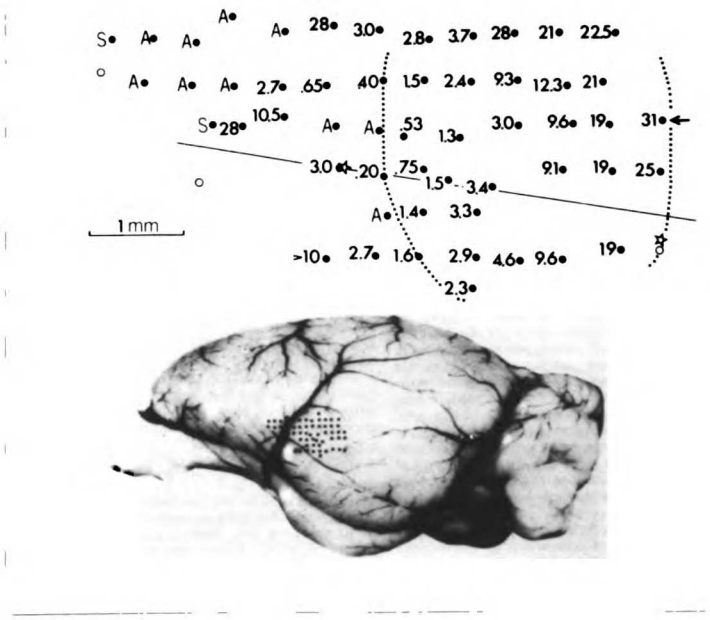

FIGURE 15. Tonotopic organization of AI in the grey squirrel determined by Merzenich, Kaas and Roth (1976). AI is outlined by solid circles. Tuned auditory responses as well as broadly-tuned auditory responses (A) and somatosensory responses (S) were recorded outside AI. Best frequencies are shown in kHz. Penetration sites are shown on inset photograph.

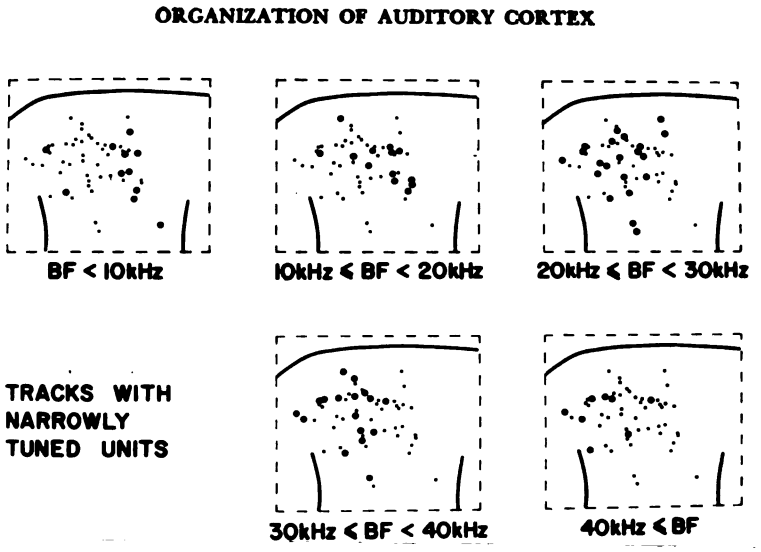

FIGURE 16. Composite maps of auditory cortex in the cat showing the distribution of best frequencies across the cortical surface. Note low frequency microelectrode penetrations on the anterior ectosylvian gyrus. (From Goldstein, Abeles, Daly and McIntosh, 1970.)

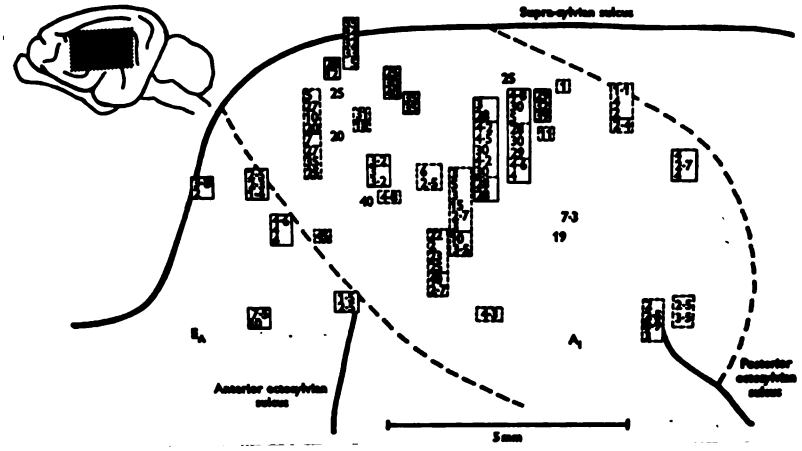

FIGURE 17. Composite map of AI and the anterior ectosylvian cortex (EA) in the cat showing distributions of best frequencies found in microelectrode penetrations into these fields in several cats. Note low frequency penetrations in area EA. From Evans and Whitfield (1964).

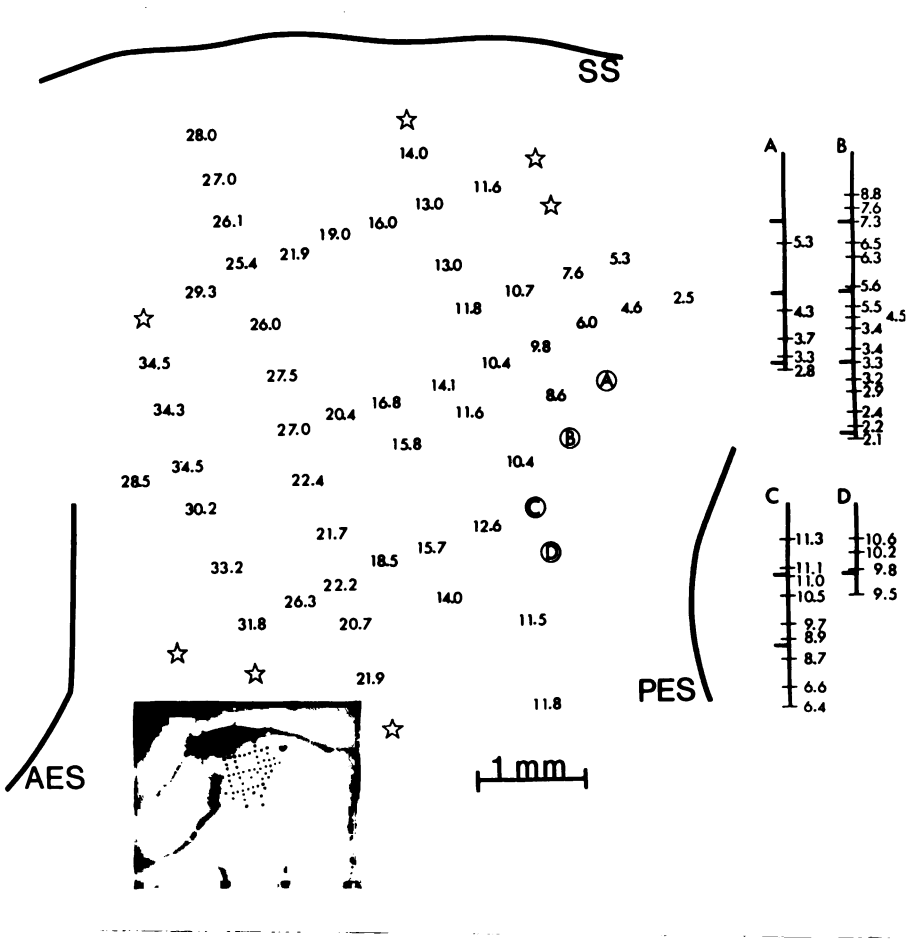

FIGURE 18. Map of best frequencies (kHz) within AI of the cat. Penetration sites also shown on inset photograph. Penetrations down the bank of the posterior ectosylvian sulcus (PES) are shown on the right. Broad bars indicate cortical depth in mm. Narrow bars indicate recording positions. Stars indicate penetrations outside AI. From Merzenich, Knight and Roth (1975).

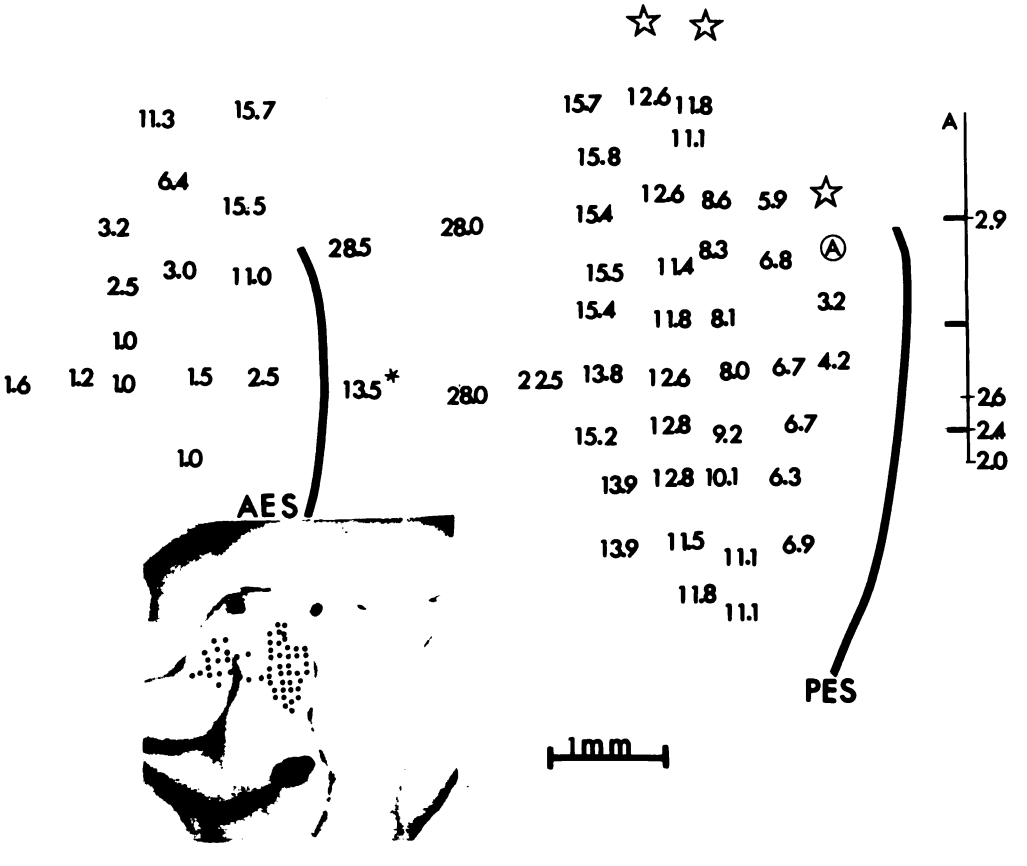

FIGURE 19. Map of best frequencies in AI and rostral field (in kHz). Asterisk indicates penetration down bank of the anterior ectosylvian sulcus (AES). See legend of Figure 18 for details. From Merzenich, Knight and Roth (1975).

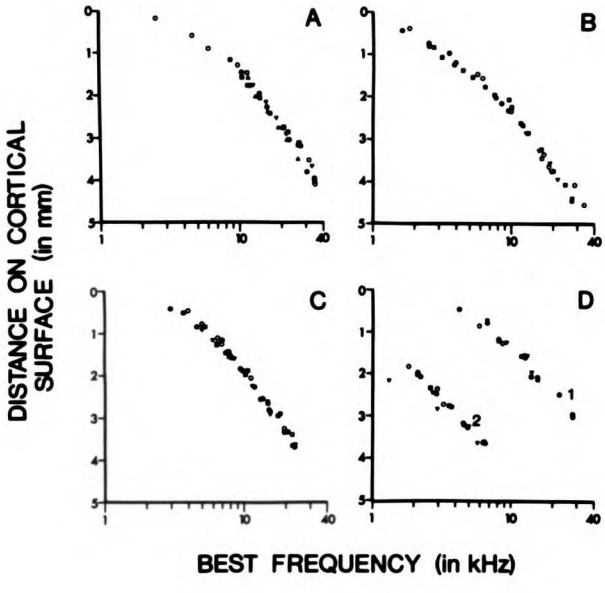

FIGURE 20. Best frequencies of units in AI as a function of distance crossing the cortical surface. Distance (mm) increases moving rostrally. See text for details. From Merzenich, Knight and Roth (1975).

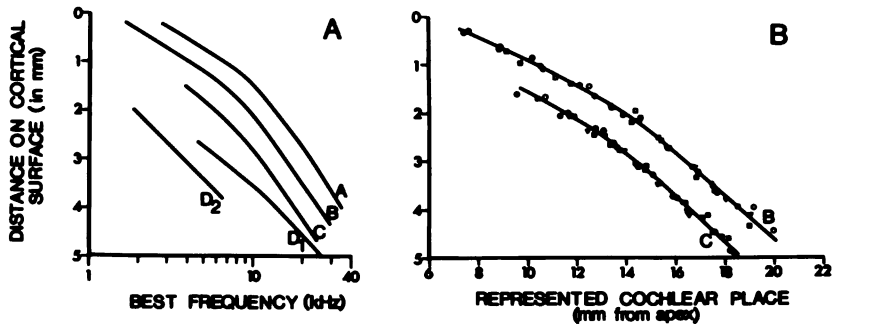

FIGURE 21. A. Tonotopic organization of AI in the cat. Best fit curves for data shown in Figure 20. Curves were displaced along ordinate to facilitate comparison. B. Cochleotopic organization of AI. The curves here were derived from 2 on the left. Best frequency has been converted to cochlear position using the function of Greenwood (1961,1974). From Merzenich, Knight and Roth (1975).

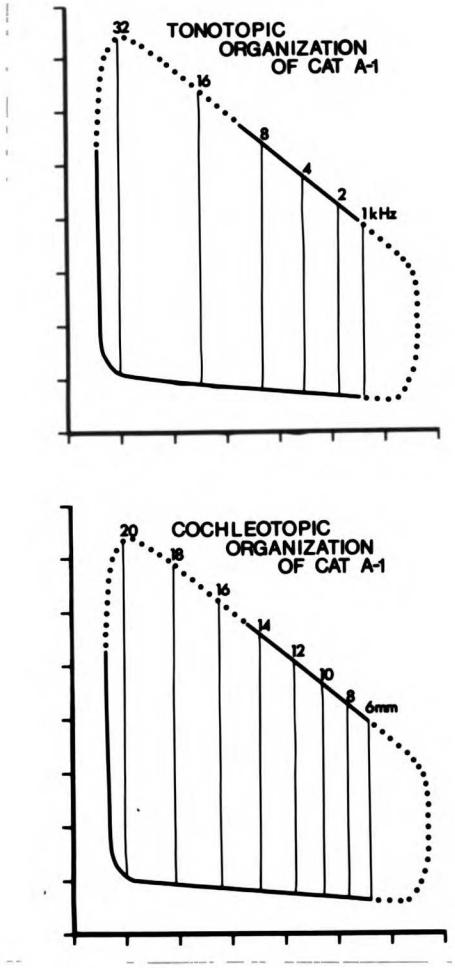

FIGURE 22. Tonotopic (upper graph) and cochleotopic (lower graph) organizations of AI in the cat. Upper graph shows the approximate area of representation of frequency bands (kHz) in AI. Lower graph shows the approximate area of representation of cochlear sectors (in mm from cochlear apex) in cat AI. Axes represent mm across the cortical surface. From Merzenich, Knight and Roth (1975).

METHODS

HISTORICAL FIGURE 2. A drawing by an unknown artist from about 1310. The "cell doctrine" is further illustrated here in which specific behavioral functions have been assigned to the ventricular spaces.

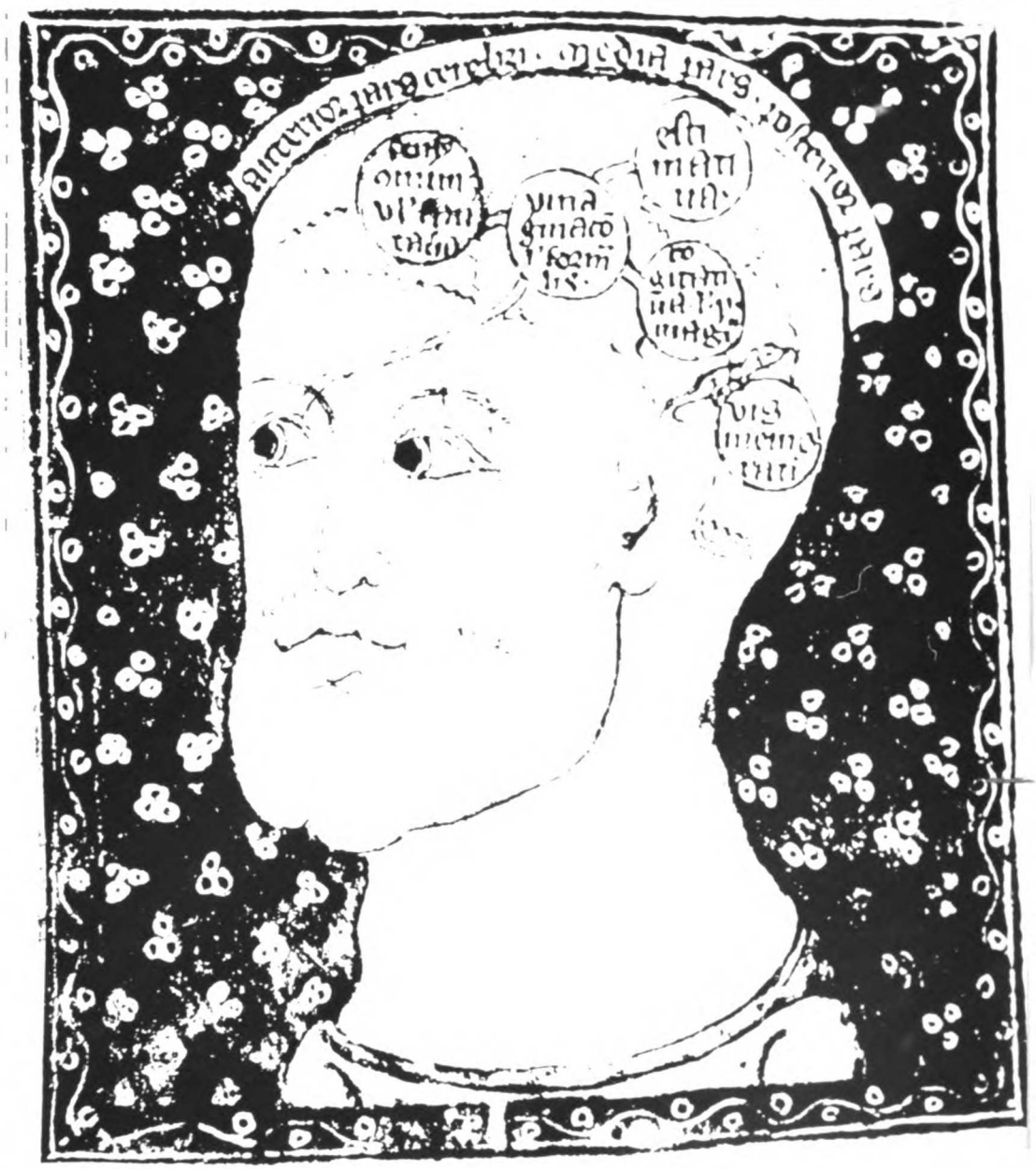

METHODS

Physiological Determination of Cochlear Representation within AAF

Animal Preparation

Experiments from 15 to 36 hours in duration were conducted on 16 cats initially anesthetized with ketamine hydrochloride (33 mg/kg, I.M.). Following the insertion of a venous cannula, a single small dose of sodium pentobarbital (6.0 mg/kg, I.V.) was administered. Surgical anesthesia was subsequently maintained by supplemental doses of ketamine. In order to reduce the possibility of cerebral edema, most animals were administered dexamethasone sodium phosphate (0.14 mg/kg, I.M.) prior to and during these long experiments. Animals were maintained at 37 degrees C.

Following the introduction of a tracheal cannula, the pinnae were removed to facilitate the sealing of hollow sound delivery tubes into the external auditory meati. A wide craniotomy was then performed to expose the left cortical surface in the region of the anterior and middle ectosylvian gyri. The dura was resected and a mineral oil well was constructed with methyl methacrylate. The cortical surface vasculature was then

photographed; a working print was made with an overlying grid corresponding to 0.5 mm squares on the cortical surface.

Glass-coated platinum-iridium recording electrodes (with impedances of 2.5 to 3.5 megaohms at 1.0 kHz) were introduced into the cortex normal to the cortical surface at the top of the middle ectosylvian gyrus with a hydraulic microdrive (Kopf) remotely controlled by a stepping motor (outside the sound room). All penetrations in a given experiment were parallel to one another. Each point of entry of a penetration was viewed through a dissecting microscope (Zeiss) and its location marked on the working photograph. In some penetrations, lesions were made by passing a DC current through the electrode (10 or 15 microamp, electrode positive, 10 seconds).

At the end of the experiment, reference marks were made on the cortical surface (and denoted on the photograph of the brain surface) with carbon black. The brain was fixed by immersion in formol saline or by intracardiac perfusion with normal saline followed by formol saline. Brains of several cases were sectioned frozen and stained with cresylviolet to provide cytoarchitectonic correlations with the physiological results.

Recording and Stimulation

Stimulation and recording techniques used in these experiments were similar to those described in earlier reports from this laboratory (Merzenich and Reid, 1974; Merzenich, Knight and Roth, 1975). Experiments were conducted in a sound room (IAC). The sound stimuli were delivered via hollow flexible tubes sealed into the external auditory meati. Each of these sound tubes was sealed into a separate chamber in which an audiometric driver (Telex model 61470) was mounted. Stimuli were tone pips with trapezoidal envelopes having rise and fall times of 5 msec delivered to one or both ears. The drivers were calibrated with the use of a probe microphone (Bruhl and Kjaer, 0.50 inch) and a waveform analyzer (General Radio model 1900). There was continuous reference to these calibration curves in these studies. With isolation of a unit or cluster of units, the best frequency for a response (i.e., that frequency at which the unit or cluster of units would respond with discharges at the lowest sound level) was determined by observation of the stimulus-synchronized sweep on the oscilloscope, and by listening to the amplified oscilloscope input on a loudspeaker. The dynamic range of the audiometric drivers was sufficient to define best frequency up to 35 kHz.

Neuroanatomical Tracing of Projections to and from AAF

Animal Preparation

Each of the 12 cats in this series was given an intramuscular injection of dexamethasone sodium phosphate (0.1 mg/kg) 12 to 16 hours prior to the experimental surgery, immediately before surgery, and at the end of the recording/injection session in order to prevent the possibility of cerebral edema. Each animal was initially anesthetized with ketamine hydrochloride (22 mg/kg, I.M.) and a small dose of sodium pentobarbital (6 mg/kg, I.P.); surgical anesthesia was maintained by supplemental doses of ketamine. Each animal was maintained at 37 degrees C.

Surgery was performed under clean conditions in order to minimize systemic infection during the two day postoperative survival period. A wide craniotomy was performed, and the dura was resected over one or both hemispheres to expose the middle and anterior ectosylvian gyri. A thin layer of mineral oil was applied to the cortical surface to prevent damage due to drying. The cortical surface was then photographed, and a working print was made with an overlying grid corresponding to 0.5 mm squares on the cortical surface.

Following the recording session and tracer injections (as described below), the cortical surface was washed with sterile saline solution, the temporal muscles

were sutured back in place, and the scalp incision was closed. The animal was then given an injection of bicillin (100,000 IU/kg, I.M.) to supress systemic infection. The animal was then transferred to an incubator until the following day when it was returned to its normal cage.

Stimulation and recording procedures were similar to those used in the previous mapping study, except that the flexible ear tube was inserted into the intact external auditory meatus contralateral to the hemisphere in which the recording was made. The microelectrode mapping experiment was designed to determine the frequency representation at given cortical loci in AAF and/or AI.

Tracer Techniques

Two tracer techniques were used in this series of experiments to determine the afferent and efferent subcortical projections to and from physiologically-defined tracer injection sites in AAF and AI (Colwell and Merzenich, 1975). The first tracer technique, horseradish peroxidase (HRP) histochemistry, was used to determine the location of subcortical neurons projecting to the tracer injection site by the histochemical staining of HRP which is selectively transported in a retrograde direction from at least some of the terminals near the injection site back to their cell bodies (LaVail

and LaVail, 1972, 1974 1975; LaVail, Winston and Tish, 1973; Nauta, Pritz and Lasek, 1974). While there is evidence for the anterograde transport of HRP (Sherlock and Raisman, 1975), only labelled cell bodies in this series of experiments were considered in the analysis of the thalamocortical projection pathways.

The second tracer technique, tritiated amino acid autoradiography, was used to identify the subcortical projections of neurons having cell bodies near the injection site by the autoradiographic demonstration of materials incorporating the labelled amino acid which are selectively transported in an orthograde direction from those cell bodies to their axon terminals (Cowan, Gottlieb, Hendrickson, Price and Woolsey, 1972).

The tritiated amino acid, 4,5 ^{3}H-leucine, was prepared by dessicating 0.1 ml of this tracer solution (61 C/mM; 0.5 mC/ml) and redissolving it in 6 microliters of sterile distilled water or normal saline to give a final concentration of 8.3 microC/microliter. For separate injections, the HRP solution was prepared by dissolving HRP (Sigma type VI) in 6 microliters of sterile distilled water or normal saline to the point of saturation (approximately 40%). For combined injections, the HRP was dissolved in the concentrated tritiated leucine solution (Colwell, 1975; Colwell and Merzenich, 1975; Trojanowski and Jacobson, 1975).

When an appropriate injection site was located physiologically on the cortical surface in AAF or AI, a few microliters of tracer solution were drawn into a 10 microliter microsyringe (Hamilton, 27 or 31 gauge needle). The syringe was held by a clamp to the micrometer drive of the stereotaxic apparatus, and the needle was advanced into the cortex carefully so as to avoid injury to the surface vasculature and to the underlying white matter and thus minimizing the possibility of uptake of HRP by damaged axons projecting to and from regions of the cortex some distance from the injection site (Halperin and LaVail, 1975; Ralston and Sharp, 1973). Injection volumes were between 0.1 and 0.5 microliters. The needle was left in place 15 to 40 minutes following the injection, and, in most cases, sound stimulation was applied to the contralateral ear at the best frequency for the injection site at 20 to 30 db above unit threshold at that site to increase HRP uptake into afferent terminals (Heuser and Reese, 1973; Holtzman, Freeman and Kashner, 1971).

Histological Procedures

Following the postoperative survival period, the animal was given a large I.P. dose of sodium pentobarbital and was perfused intracardially with cold, heparinized, normal saline solution followed by phosphate-buffered (pH 7.6) 2.5% paraformaldehyde

solution. The brain was then removed and placed in cold fixative for 5 to 24 hours for further hardening. The brain was then passed through a graded series of phosphate-buffered (pH 7.6) sucrose solutions (5%, 15%, 30%) over the next 24 hours.

The specimen (midbrain through cortex) was sectioned serially in the frontal plane on a freezing microtome according to the following schedule: 90 microns, 30 microns, and 30 microns. The 90 micron sections were incubated for 10 to 15 minutes in a solution of 3,3' diaminobenzidine (0.07%) in Trizma buffer (pH 7.6) to which a few drops of 3% hydrogen peroxide were added (a modification of the method of Graham and Karnovsky, 1969). This histochemical treatment demonstrated the presence of HRP-containing granules in the MGB cell bodies. These sections were then mounted on gelatinized slides and coverslipped for subsequent examination. The second set of serial sections were also processed to demonstrate the presence of HRP and were also mounted on gelatinized slides. These slides were subsequently dipped in Kodak NTB-2 nuclear track emulsion to simultaneously demonstrate the presence of tritiated products. The third series of sections were processed for autoradiography alone (Cowan, Gottlieb, Hendrickson, Price and Woolsey, 1972). Autoradiograms were developed after approximately 90 days according to the following

schedule: development in Kodak D-19 developer, 2 minutes (at 16 degrees C.), rinse in distilled water, fixation in Kodak Rapid Fix, 2 minutes, and wash in running distilled water, 2 hours. Slides processed for HRP and autoradiography were coverslipped after drying; slides processed for autoradiography alone were counterstained with cresyl violet or neutral red and coverslipped.

Reconstruction of Projections

Outlines of sections having HRP-labelled cells or autoradiographically-labelled terminals were traced using a low power projecting microscope (Bausch and Lomb). Cells containing HRP were examined under brightfield illumination with a Zeiss Photomicroscope III. In order to avoid false identification of cells with endogenous peroxidase activity (Wong-Riley, 1976), cells were considered to contain HRP reaction product only if darkly-stained granules were visible within the cells seen under 40X dry objective or 100X oil-immersion objective (each with 10X eye pieces). Such cells were marked on the tracing of the section. Autoradiographic sections were examined with both dark and brightfield illumination, and areas having grain density greater than background were marked on section tracings. Some of these sections were photographed at low power in dark field with a Nikon Multiphot.

RESULTS

HISTORICAL FIGURE 3. A more complex scheme of brain localization based on the "cell doctrine of the brain" by Fludd (1619).

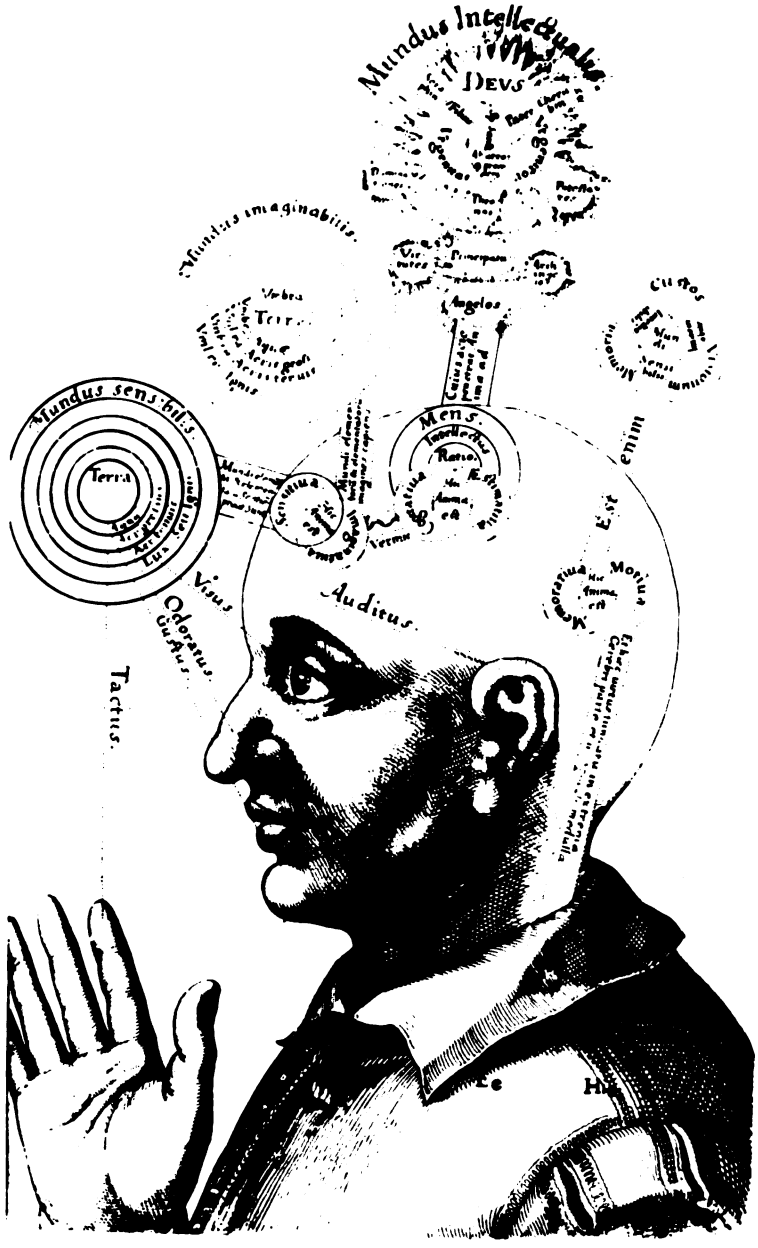
Mundus Intellectualis
DEVS
Mundus imaginabilis
Angelos
Mundus sensibilis
Terra
Mens
Visus
Auditus
Odoratus
Gustus
Tactus
Motus

RESULTS

Response Characteristics of Neurons within AAF

In electrode penetrations into AAF, a characteristic, broadly-tuned intracortical evoked potential of negative polarity could be recorded with a latency of 10 to 12 msec. Typically, this evoked potential could be detected at about a 5 dB lower stimulus intensity than single unit discharge thresholds in the same penetration. At tone intensities only about 10 dB above the threshold for unit excitation, the evoked potential commonly spanned several octaves in low frequency regions of the field; it was somewhat sharper in regions of the field where units had higher best frequencies. At stimulus intensities near threshold for unit discharge, this evoked response was commonly prominent from approximately 400 microns below the cortical surface down through the deepest cortical layers. The intracortical evoked potential recorded in AI is of significantly lower amplitude at 10 dB above threshold for unit discharge and is more sharply tuned than in AAF (Merzenich, Knight and Roth, 1975). This striking difference in appearance of the intracortical evoked potential was a major physiological criterion in assigning units to one field or the other, particularly in the region of the border between the two fields.

A second difference between penetrations into the two fields was the presence of a greater number of "spontaneously" active cells in AAF as compared to AI. This difference was particularly evident when rows of penetrations crossed the border between AAF and AI, and direct comparisons between the responses and "spontaneous" activity in the two fields could be made between successive penetrations crossing this border in both directions. The level of this "spontaneous" activity in AAF was a marked function of the depth of anesthesia and was often depressed during periods of deepest anesthesia.

However, frequency response characteristics of isolated neurons driven by sound stimuli in AAF and AI were strikingly similar. In both fields, neurons recorded in the superficial cortical layers were poorly driven (if driven at all) by tonal stimuli. Strongly driven responses were encountered in the middle and deep cortical layers from about 600 microns to 1200 microns in depth in penetrations normal to the cortical surface. Under ketamine, the typical recorded response in both fields was a short burst of spikes from one or more units locked to the stimulus onset and coincident with the evoked potential.

Single units in AAF and AI were usually found to have sharply-definable threshold best frequencies. Once a single unit or cluster of units responding to the tonal stimuli was isolated, an approximate frequency response range was determined. Stimulus intensity was then systematically reduced, and approximate frequency response ranges were found to narrow. Best frequency was defined when a single frequency or a small frequency range (usually less than 0.1 octave) could be found at threshold intensity. This determination was verified by making broad sweeps of frequency covering the entire audible range using stimulus intensities equal to that found for the best frequency threshold using the calibration curves for the drivers as a reference. In multiunit clusters, all recorded neurons had virtually identical tuning properties. In such clusters, units with exceptional best frequency would be found with the broad frequency sweeps used for the verification of best frequency. Such units with exceptional best frequency were constantly sought, but none were found. Furthermore, for each recorded unit or cluster, the best frequency found was always within the frequency range of the associated intracortical evoked potential.

Occasionally, units with unequivocal multipeaked tuning curves were found with similar threshold intensities at each peak. These were observed for

neurons isolated throughout the depths of active cortex in several penetrations into AAF in this series. Because of the relative infrequency of such responses in this experimental series, it is not possible to determine if there was a systematic relationship between the peaks in the tuning curves of such units. Units with multipeaked tuning curves were not found in penetrations located in AI (Merzenich, Knight and Roth, 1975), but have been described for units in penetrations into incompletely mapped auditory cortex in the cat by other investigators (Hind, et al., 1960; Oonishi and Katsuki, 1965).

Responses in Depth

Best frequencies were determined at two or more depths through the cortex in 149 of the more than 450 penetrations into AAF in this series. In these penetrations, if the range of best frequencies in a given penetration was expressed as a fractional bandwidth ((highest BF - lowest BF)/ lowest BF), then that fractional bandwidth was less than 0.1 in 89% of all studied penetrations not near the sulci; it exceeded 0.5 in only 2 such penetrations (both in the lowest frequency sector of the field). Common best frequency through cortical depth is a property that has been found for mapped AI (Merzenich, Knight and Roth, 1973, 1974, 1975)

and in incompletely mapped auditory cortex in the cat (Abeles and Goldstein, 1970; Gerstein and Kiang, 1964; Hind, et al. , 1960; Parker, 1965) as well as for AI of other species (Brugge, 1975; Imig, Ruggero, Kitzes, Javel and Brugge, 1977; Merzenich and Brugge, 1973; Merzenich, Kaas and Roth, 1976; Oliver, Merzenich, Roth, Hall and Kaas, 1976). In the few penetrations in which multipeaked tuning curves were defined for neurons or clusters in AAF, the complex tuning curve was observed for neurons all through the active cortical depth.

On the basis of these observations, maps in later experiments in this series (including most of those illustrated) were constructed with a single determination of best frequency in most penetrations normal to the cortical surface. In penetrations in which multiple best frequency determinations were made at different depths, the best frequency assigned to a penetration was the mean of the best frequencies found at all depths, provided that the penetration was normal to the cortical surface. Responses of neurons in penetrations that were not normal to the overlying cortical surface (most of which passed down sulci) will be described separately.

Representation of Frequency in AAF

There is an orderly representation of sound frequency within AAF in the cat. Maps illustrating some common features of the frequency representation within this field are shown in Figures 23-26 and 28. The drawings in these illustrations represent the magnified views of the cortical surface in these studied cats. Each number is the best frequency (in kHz) defined for neurons studied in a penetration deep to that site. These penetration sites are shown again as dots on the inset photographs of each brain. In most experiments, mapping was initiated in AI. Rows of penetrations were then extended across the border between the two fields (represented approximately by the dashed line crossing Figures 23-26 and 28C).

The highest best frequencies are represented along the caudal or dorsocaudal aspect of AAF, along its boundary with AI. In the region of AAF near the border with AI, any given high frequency is represented along a line crossing AAF on a dorso-ventral axis. The line of representation of a given frequency in this region is straight, and parallel to the "isofrequency contours" of AI (Merzenich, Knight and Roth, 1975). Moving rostrally in AAF away from the AI-AAF border, there is an orderly progression to lower frequency contours for a variable distance.

Further rostrally isofrequency contours (in most cases) rotate progressively counterclockwise (for the left hemisphere), roughly following the surface of the anterior ectosylvian gyrus. The point of rotation varies among animals. For example, in cat 75-68 (Fig. 25), rotation of the field begins rostral to the line of representation of 7 kHz, while in cat 75-79 (Fig. 26) rotation occurs rostral to the 19 kHz line.

In most cases, the lowest frequencies are represented ventrally on the anterior ectosylvian gyrus. Isofrequency contours in this low frequency sector of the field appear to be straight in some cases (e.g., the 0.9 kHz line of cat 75-73, Fig. 28D), but more commonly appear to be sinuous or are ill-defined.

By comparison, isofrequency contours in AI are also straight and parallel to one another (in that portion of the AI field rostral to the posterior ectosylvian gyrus). Furthermore, the progression to lower isofrequency contours moves rostrally in AAF and caudally in AI (Merzenich, Knight and Roth, 1973, 1974, 1975).

In several animals, long penetrations were made through the active cortical layers of the ventral and caudal banks of the anterior descending limb of the

suprasylvian sulcus (Figs. 25, pen. A-D; 26, pen. A,B; and 28B, pen. A), roughly parallel to the surface of AAF. As is evident in the electrode track reconstructions in these figures, an orderly progression to higher best frequencies with increasing depth was recorded in all such penetrations. Furthermore, as in AI (Merzenich, Knight and Roth, 1975), there appeared to be stepwise changes in best frequency in these long penetrations. That is, at a given locus, all units had very similar best frequencies; with the advance of the electrode all units encountered suddenly responded to another higher best frequency for some variable distance until a region of even higher best frequency was encountered.

As is evident in these cases, AAF extends over the crest of the anterior ectosylvian gyrus and continues into the depths of the suprasylvian sulcus in some cats. The best frequency sequences encountered in the sulcus indicate that the parallel isofrequency contours on the lateral surface of the cortex bend rostrally within the depths of the dorsal limb of the sulcus (Figs. 25 and 28B); they bend somewhat ventrally in the anterior limb of the sulcus with reference to their surface representation (Fig. 26).

Tonotopic and Cochleotopic Organization of AAF

The highly-ordered mapping of represented best frequency on the cortex of AAF has been represented graphically in Figure 27 (upper graph) for two cats in this series. These curves represent the relationship between best frequencies of penetrations and location of penetration sites on the cortical surface expressed as their distance (in mm) rostral to the AI-AAF border. Such figures were possible to draw for these particular cats, as most of the field was represented by parallel isofrequency contours on the exposed surface of the cortex. The graph for cat 75-68 was constructed in the following manner: (a) on the cortical map of this animal (Fig. 25), a series of parallel lines was drawn perpendicular to the border with AI and separated by 0.5 mm (actual cortical distance); (b) best frequencies encountered within 0.25 mm (actual cortical distance) of these lines were plotted as a function of the distance rostral to the AI-AAF border (one symbol is used for each of the parallel lines). The only points included were those in the region of AAF where isofrequency contour lines were parallel. The function of best frequency vs. cortical distance for cat 75-67 was plotted in a similar manner from the map shown in Figure 24, except that in Figure 27 it was displaced upward 4 mm on the ordinate to facilitate comparison. A similar function for a typical

AI representation was redrawn from the study of Merzenich, Knight and Roth (1975) on the same graph. It was also displaced on the ordinate for comparison. In the function for AI, the cortical distance is measured moving caudal to the AI-AAF border.

These curves reveal that the relationship between best frequency and cortical distance is similar for each parallel line crossing the region in which isofrequency contours are parallel. One may then conclude that, as in AI (Merzenich, Knight and Roth, 1975), a given frequency band is represented by a nearly straight belt of cortex crossing the field dorso-ventrally; the belts must be of nearly constant width across the mapped portion of the field; and the proportionality in the representation of different frequencies must be maintained across the field. The slopes of the curves indicate that there is a somewhat greater proportional representation of the highest frequency octaves. It must be borne in mind that these curves were drawn through those regions of the field in which the isofrequency contours were parallel to the AI-AAF border. The rotation of the field made it difficult to continue these graphs to the lowest octaves represented on the lateral surface of the cortex. Similarly, it was not possible to draw such graphs for

the portion of the field buried within the suprasylvian sulcus.

In the lower graph of Figure 27, best frequency values were replotted as represented cochlear loci using the function of Greenwood (1961, 1974). It is evident that in AAF, as in AI (Merzenich, Knight and Roth, 1975), a sector of the basilar partition of a given length is represented across a nearly straight belt of cortex of nearly constant width that crosses the mapped portions of the fields on a dorso-ventral axis; and that the belts representing the more basal equal-length sectors are wider that the belts representing the more apical sectors.

The similarity between the curves for the two cats is noteworthy. For most of the other animals in this series, the portion of the field where isofrequency contours were parallel was too small to provide a complete comparison with cats 75-67 and 75-68. Cat 74-66 (Fig. 28C) is an anomolous case with the 22 kHz and 27 kHz isofrequency contours apparently not parallel to the AI-AAF border.

Variability of AAF Location on the Cortical Surface

The location of AAF with respect to surface anatomical landmarks varies significantly. Surface landmarks provide only a gross indication as to the location of the field, but provide no information as to the boundaries or frequency organization within the representation. This variability will be illustrated.

The location of the dorsal boundary of the field can be seen to vary considerably. In Figures 24, 26 and 28D the open stars indicate penetrations in which there was no driven cell response with tonal stimulation, indicating that the penetration sites were outside the boundaries of both AI and AAF. In these three maps the dorsal boundary of the field was clearly on the lateral surface of the ectosylvian gyrus. By contrast, the maps shown in Figure 25 and 28B have a dorsal border which must extend down into the suprasylvian sulcus, as indicated by the long penetrations down the ventral bank of the sulcus.

The location of the low frequency ventral border is similarly variable. In cat 75-79 (Fig. 26), an identified ventral border is less than 0.5 mm below the dorsal tip of the anterior ectosylvian sulcus; in cat 75-67 (Fig. 24) and cat 75-73 (Fig. 28D) the identified

borders are approximately 2.5 mm below the tip of the anterior ectosylvian sulcus.

The border of AAF with A1 shows a high degree of variability. In cats 74-49 (Fig. 23) and 75-73 (Fig. 28D) the border nearly intersects the tip of the anterior ectosylvian sulcus; in cats 75-67 (Fig. 24) and 74-66 (Fig. 28C), the border is over 2 mm caudal to the tip of the anterior ectosylvian sulcus.

Close comparison of the variability of the frequency representation in the field with respect to surface landmarks can be made by examining Figures 28A-D. In these drawings, it can be seen that the best frequency recorded nearest the tip of the anterior ectosylvian sulcus varies considerably: 0.90 kHz for cat 73-14; 0.92 kHz for cat 74-63; 10.9 kHz for cat 74-66; and 28 kHz for cat 75-73.

In Figure 29 is shown a diagrammatic representation of the location of the fields on drawings of the brains of six cats in this series. Superimposed on the drawings are arrows indicating the approximate location and orientation of the 3 kHz and 22 kHz isofrequency contours. It can be appreciated that the fields vary widely in their location on the brain surface when

referenced to cortical landmarks. Furthermore, as noted by others (Ades, 1939, 1959; Kawamura, 1971; Merzenich, Knight and Roth, 1975; Rose, 1949), there is a high degree of variability in the configuration of the sulcal patterns among cats in the area of AAF and for the entire hemisphere in general.

Adjacent Cortical Regions Other Than AI

In the cortical regions other than AI bordering AAF into which penetrations were directed, neurons could not be excited by tonal stimuli. Several penetrations were directed into the field dorsal to AAF (penetrations marked with open stars in Figs. 24, 26 and 28D) in those animals in which AAF did not extend over the dorsal crest of the ectosylvian gyrus. The units found in these penetrations could not be driven by tonal stimuli at any stimulus intensity. Furthermore, no intracortical evoked potentials could be seen in any of these penetrations. This suggests that this field is non-auditory or requires more complex auditory stimuli than the monaural or binaural tone pips used in these experiments with ketamine anesthetized cats. Similarly, penetrations into the cortical regions ventral and rostral to the low frequency sector of the field (Figs. 24, 26, 28D) did not record any intracortical evoked potential or driven unit activity with tonal stimulation. Due to the dense

vascular pattern near the anterior ectosylvian sulcus, only a small number of penetrations were directed into the region of the anterior bank of this sulcus, and, therefore, the ventromedial boundary of AAF was always somewhat uncertain.

Cytoarchitecture and the Boundaries of AAF

The cytoarchitecture of AAF and AI are similar in most respects. The proximity of the caudal boundary of AAF to the anterior ectosylvian sulcus causes distortion of the cytoarchitecture of both AAF and AI near their mutual boundary due to the infolding of the cortical surface in this sulcus. Furthermore, the rostral and dorsal boundaries of AAF are found within or near the suprasylvian sulcus and suffer from similar distortion. Thus, it is far more reliable to define the boundaries of AAF on the basis of physiological criteria rather than on cytoarchitectonic criteria alone.

Projection of the MGB to AAF

Having defined the complete representation of the cochlea within AAF and the remarkable similarity between the cochlear representations in AAF and AI, neuroanatomical tracing experiments using the retrograde transport of horseradish peroxidase (HRP) were performed

to compare the thalamocortical projections to AAF with the thalamocortical projections to AI (Colwell and Merzenich, 1975). In order to accurately locate injection sites within AAF or AI, partial microelectrode maps of represented frequency were made in 14 hemispheres of 12 cats. The criteria used to define penetrations into AAF were similar to those used in the previous mapping experiments: (a) sharply-tuned units with a radial organization through the middle and deep cortical layers and (b) an orderly progression of represented frequency with lower frequencies represented rostrally in AAF and higher frequencies represented caudally. Penetrations into AI were differentiated from those into AAF by the reversed direction of frequency progression crossing the cortex on a rostro-caudal axis. Small injections (0.1-0.5 microliters) of HRP solution (or tritiated leucine or a mixture of these two tracers) were made at physiologically-defined cortical loci in AAF and AI. In all cases, except 76-91 (Fig. 31), these tracers did not spread laterally beyond the boundaries of the injected field.

Retrograde transport of HRP (LaVail and LaVail, 1972, 1975; LaVail, Winston and Tish, 1973; Nauta, Pritz and Lasek, 1974) from AAF injection sites to the MGB was determined by the finding of darkly stained granules of HRP reaction product in the MGB cells projecting to the

injection loci as shown in Figure 30. As can be seen in this figure, labelled cells in the ventral division of the MGB (Morest 1964, 1965a) often had HRP granules filling their major dendritic branches. Most labelled dendritic branches of cells on the most lateral aspect of the MGB were oriented parallel to the laminae of the ventral division as was described by Morest (1965a) in Golgi-stained material. Such HRP labelling of dendrites was rarely seen in cells of Morest's deep dorsal division.

Neurons in the MGB projecting to a single injection site or to multiple injection sites along an isofrequency contour were located within a long (approximately 3 mm) column with a rostro-caudal orientation passing through the deep dorsal division (D) of the MGB into the posterior nuclear group (Po) (the boundary between the MGB and the posterior group was not evident in these reconstructions) and in a sheet or slab of cells in the ventral (V) division of the MGB ipsilateral to the injection site. Reconstructions of 6 HRP cases can be seen in Figures 31, 32, 33, 34, 36 and 37. In each of these figures, HRP labelled neurons are represented as dots on the tracings of the 90 micron sections developed for HRP alone. In these reconstructions, the deep dorsal

division is designated by "D", the posterior group by "Po", and the ventral division by "V".

In the largest injection case, shown in Figure 31, in which a small amount of HRP spread beyond the boundaries of AAF, HRP labelled neurons were located in a long (approximately 3 mm) column of cells with a rostro-caudal orientation passing continuously through the deep dorsal division into the more rostral posterior group. In this case, a number of cells in each section can be seen in transition groups between this column and the cell group on the lateral aspect of the ventral division of the MGB. In this case alone, some cells were also located in Morest's (1964) medial division and superficial dorsal division. Unequivocal cell labeling in the medial division was not seen in cases with more discrete injections and could have been the result of spread of HRP into AI which receives a projection from the medial division (Colwell and Merzenich, 1975).

In all other cases with more restricted injections, as shown in Figures 32, 33, 34, 36, 37, HRP-labelled neurons were found primarily within the deep dorsal column and in lesser numbers near the lateral margin of the ventral division, possibly in Morest's (1964, 1965a) and Cajal's (1909) marginal zone or in the low frequency

region of the laminated ventral division (Aitkin and Webster, 1972; Colwell and Merzenich, 1975). Occasional neurons were also labelled in regions that could be interpreted as being in the transition regions between the deep dorsal column and the ventral division seen most clearly in Figure 31.

The major difference in cell labeling between the cases of single injections and the cases of multiple injections along an isofrequency contour was primarily in the density of labelled cells within these projection groups and in the cross sectional area of the deep dorsal column seen in frontal section, i.e., multiple injections along an isofrequency contour caused more dense labelling and somewhat broader cross sections in the deep dorsal column than did single injections of the same volume.

Similar differences were apparent in comparisons among cases with single large and small injections, i.e., larger injections caused more dense labeling in a larger projecting cell column in the deep dorsal group than did small injections. The length of the deep dorsal-posterior group column was not well correlated with the total amount of HRP tracer injected. In the smallest injection case (cat 76-133 right, 0.2 microliters, as shown in Figure 34), this column was seen to be

continuous for 2.7 mm; in the largest single injection case (cat 76-62, 0.5 microliters, as shown in Figure 32), this column was seen to be continuous for 3.6 mm. in length.

In all cases (with injections at points representing frequencies between 1.7 and 30 kHz), except one, the cells in the ventral division were seen on the lateral margin of the ventral division of the MGB. In a similar previous study of the MGB projections to AI, low frequency injections were seen to label cells out to the lateral margin of the MGB. However, Cajal (1909) and Morest (1964, 1965a) both described a distinct marginal zone on the most lateral aspect of the MGB. It is possible that the neurons projecting to AAF from the lateral margin of the ventral division were located in this marginal zone. On the other hand, they may have come from the low frequency lateral region of the MGB (Aitkin and Webster, 1972; Colwell and Merzenich, 1975). The second possibility is attractive since it correlates with the physiological finding of broadly-tuned intracortical evoked potentials, especially in the low frequency portion of AAF. However, the present experiments cannot resolve this issue.

These results indicate that, within the level of resolution of this tracer technique, the array of MGB neurons projecting to any point in AAF representing a given frequency (or, equivalently, representing a given point on the cochlear partition) receives a convergence of input from cells along an entire deep dorsal-posterior group column and, to a lesser extent, from a sheet of cells within the ventral division near its lateral margin.

Corticothalamic Projections from AAF

The projections from physiologically-defined loci within AAF onto the MGB were examined using the autoradiographic demonstration of transport of protein incorporating tritiated leucine from cell bodies in AAF to their terminals in the MGB (Cowan, Gottlieb, Hendrickson, Price and Woolsey, 1972). In most cases, the tritiated leucine was mixed with the HRP injection solution to provide information concerning the degree of reciprocity between the thalamocortical and corticothalamic projection arrays (Colwell, 1975; Colwell ndaMerzenich, 1975).

The autoradiographic demonstration of labelled terminals showed a dense corticothalamic projection

ipsilateral to the injection site along a column of terminals passing through the deep dorsal division of the MGB rostrally into the posterior group (the boundary between these adjacent nuclei was not evident in this material). Reconstructions of two of these projections can be seen in Figures 35 and 36. In each of these figures, the ventral division of the MGB is designated by "V" and the deep dorsal-posterior group is designated by "D".

The results of a small (1.7 microCurie) injection is shown in the darkfield photographs of Figure 35 for cat 76-98. The most distinct labeling of terminals is apparent within a long (approximately 3mm) column passing rostrally through the deep dorsal division of the MGB into the posterior group. The presence of labelled terminals in the ventral division was seen in only two sections (11 and 12) in this case.

In cases with larger single injections or multiple injections along an isofrequency contour (Figure 36), the cross sectional area of the deep dorsal column was found to be larger, but the length of this column had only a small positive correlation with injection volume similar to that found with HRP uptake in combined injections. Labelling of terminals in the ventral division in cases with larger injections or multiple injections restricted

to AAF was always questionable. There are two possible reasons for this observation. Either there was no corticothalamic projection to this region, or, more likely, the density of these projections was too small to be unequivocally defined by this technique.

AAF Thalamocortical and Corticothalamic Reciprocity

The reciprocity between the corticothalamic and thalamocortical projections (at least in the deep dorsal-posterior group array) can be seen directly in Figure 36. In Figure 36, sections reacted for the presence of HRP and adjacent sections treated for the autoradiographic demonstration of tritiated leucine in axon terminals can be compared. As can be seen in this figure, there is a high degree of overlap in the two projection arrays within the deep dorsal-posterior group.

The relatively small number of thalamocortical projection neurons in the ventral division suggests that, if the lateral margin of the ventral division were reciprocally related with a locus in AAF, the corticothalamic projections might possibly not be seen due to the small number of labelled terminals projecting to the small number of neurons in the ventral division.

Comparison between AAF and AI Projections

Since AI and AAF are remarkably similar in organization, it is important to directly compare the thalamocortical projections to these two fields in the same animal. Such a comparison can be seen in Figure 37 for cat 76-119. In this case, Figure 37A shows the array of neurons projecting to an 11 kHz injection site in AAF of the left hemisphere; Figure 37B shows the array of neurons projecting to an 11 kHz injection site in AI of the right hemisphere in an adjacent section; and Figure 37C shows the array of terminals projecting to the MGB in an adjacent section from an 11 kHz injection site in AI of the left hemisphere. Comparison of Figures 37A and 37B shows that both AAF and AI (Colwell and Merzenich, 1975) receive projections from the deep dorsal-posterior group column, but that AI receives projections from a much larger number of cells in the laminated portion of the ventral division while there is only a small projection from the ventral division to AAF (and, possibly, from a different region of the ventral division).

The dorsal column projecting to loci in AAF and AI representing the same frequency can be seen to be nearly identical by comparison of Figures 37A and 37C. Since

the thalamocortical projection neurons from the MGB to AI receive a precisely reciprocal projection from the same locus in AI (Colwell and Merzenich, 1975), the corticothalamic projection from the 11 kHz injection site in AI (Figure 37C) must precisely overlap the thalamocortical projection to that same AI locus. Comparison of Figure 37C with the thalamocortical projection array to an 11 kHz injection site in AAF in the same hemisphere (Figure 37A) shows that the overlap within the dorsal column is nearly identical.

Thus, this case presents strong evidence that loci representing the same frequency (or, equivalently, the same position on the cochlear partition) in both AAF and AI must receive identical projections from the deep dorsal -posterior group column. Conversely, since AAF is similarly reciprocally related to the deep dorsal-posterior group column, loci within AAF and AI representing the same frequency (or, equivalently, representing the same position on the cochlear partition) must project to the same deep dorsal-posterior group column.

Additional Projections of AAF

Sections through the inferior colliculus were processed for HRP labelled cells and labelled cortico-tectal projection terminals for injections of tracers in both AAF and AI. No HRP cells were seen in the inferior colliculus with injections in either field. While bilateral projections to the central and pericentral nuclei of the inferior colliculus were seen with AI injections, no such projections were seen with AAF injections.

There was clear autoradiographic evidence for the projection of AAF to the contralateral hemisphere. This can be seen in Figure 38 in which is shown autoradiographic grains from tritiated leucine from a combined tracer injection at a 2.4 kHz site in AAF of cat 76-66. The grains can be clearly seen in fibers entering the corpus callosum projecting to the opposite hemisphere. The exact destination of these fibers is uncertain.

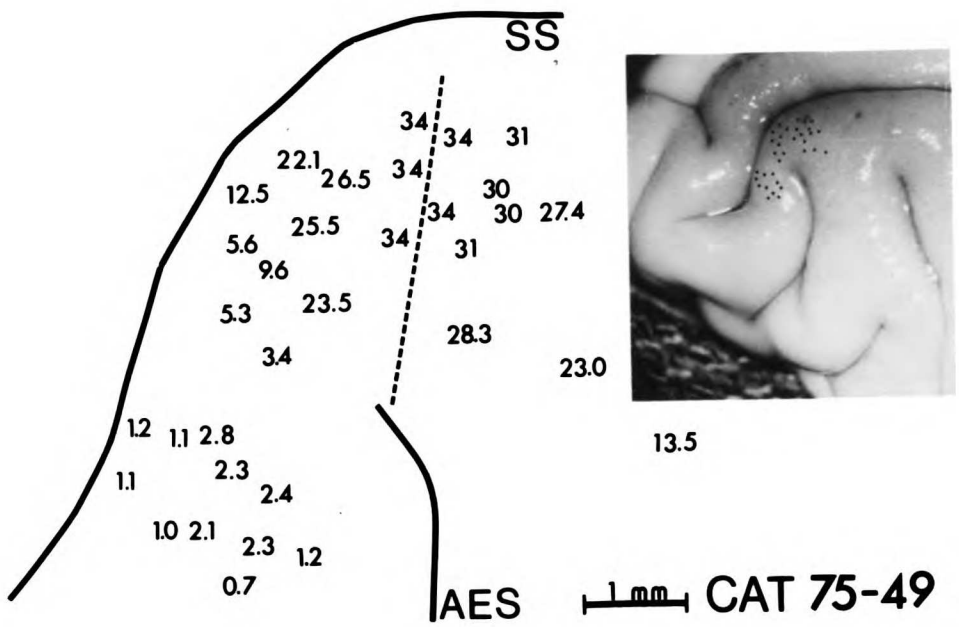

FIGURE 23. Map of best frequencies (kHz) of 33 penetrations into AAF and AI of the left hemisphere of cat 75-49. Dashed line in this and following figures represents the approximate boundary between AAF (left side of boundary) and AI (right side of boundary). Penetration site are shown on the inset photograph. SS: suprasylvian sulcus; AES, anterior ectosylvian sulcus.

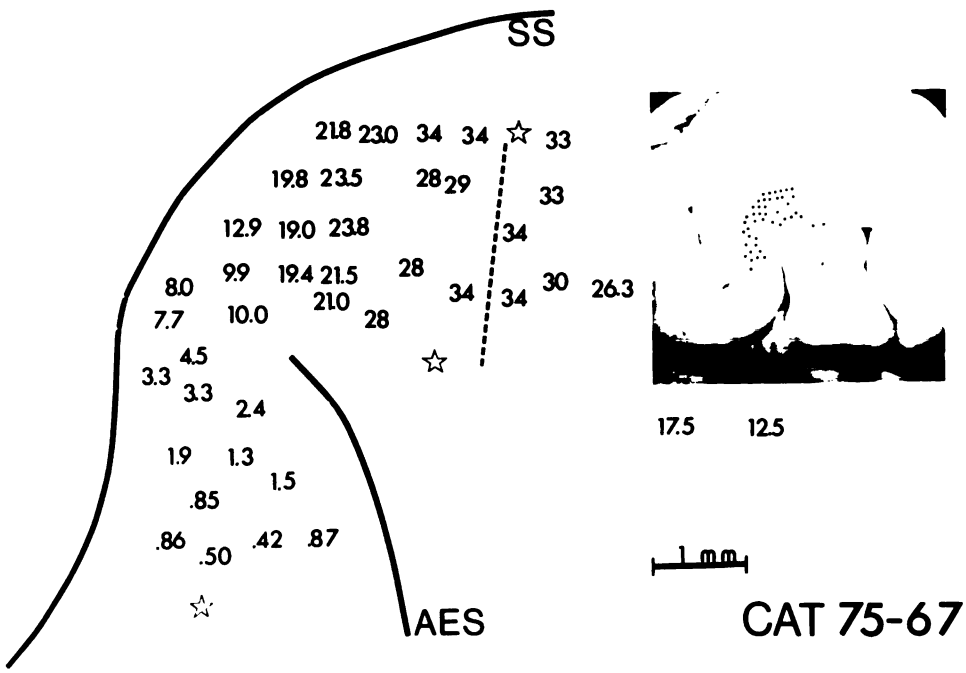

FIGURE 24. Map of best frequencies (kHz) of 44 penetrations into AAF and AI of the left hemisphere of cat 75-67. Stars indicate penetrations in which no cells responded to tones. Penetration sites are shown on inset photograph. SS, suprasylvian sulcus; AES, anterior ectosylvian sulcus.

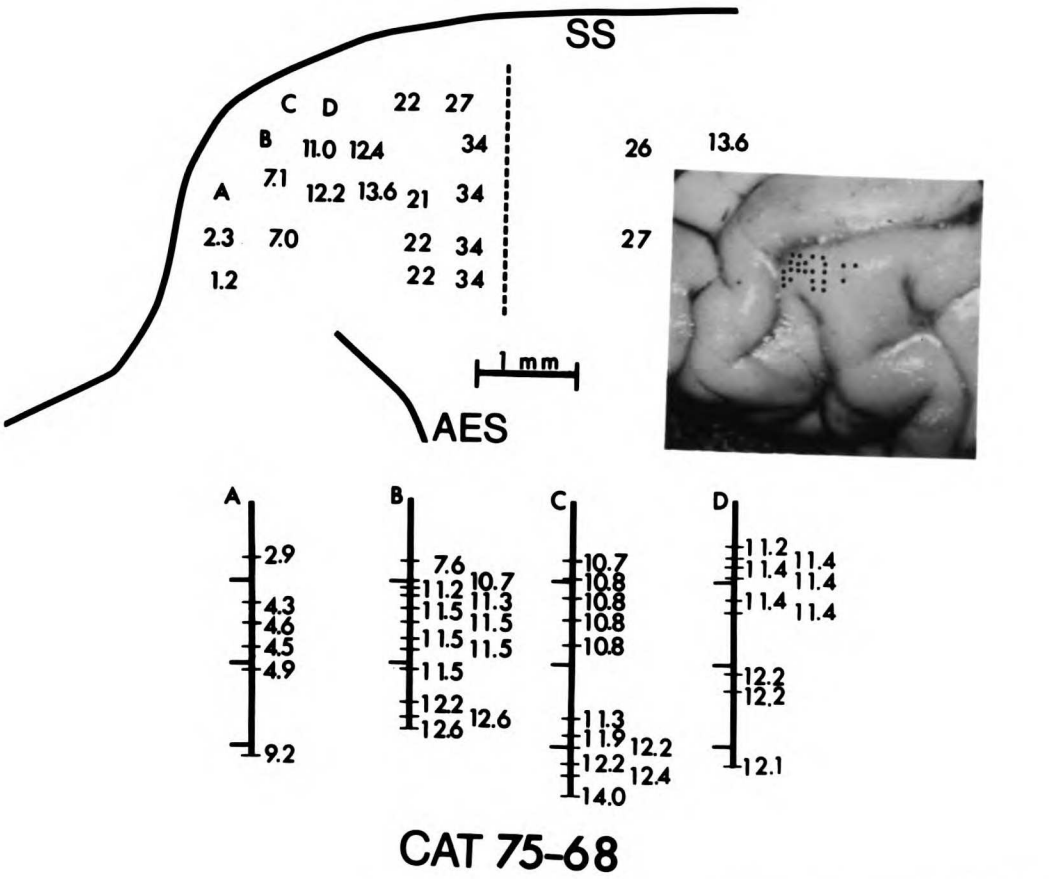

FIGURE 25. Map of best frequencies (kHz) of 24 penetrations into AAF and AI of cat 75-68. Penetrations A-D ran down through the middle cortical layers of the ventrocaudal bank of the suprasylvian sulcus and are reconstructed below. Broad dashes indicate 1 mm steps along track; narrow dashes indicate recording positions for which best frequencies (adjacent numbers, in kHz) are shown. Penetration sites are shown on inset photograph. SS: suprasylvian sulcus; AES, anterior ectosylvian sulcus.

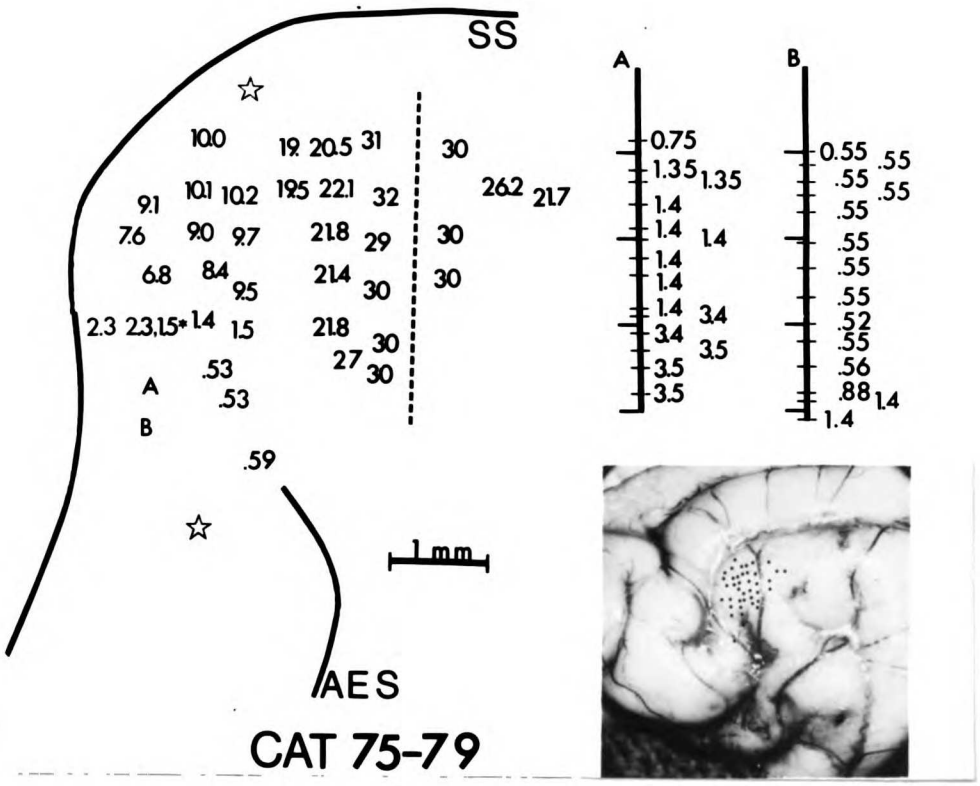

FIGURE 26. Map of best frequencies (kHz) of 40 penetrations into AAF of cat 75-79. Stars indicate penetrations in which no cells responded to tones. Asterisk indicates a penetration in which two threshold minima, 2.3 kHz and 1.5 kHz, were found at the same sound intensity. Penetrations A and B ran down through the middle cortical layers of the bank of the suprasylvian sulcus. See previous figure legend for details.

FIGURE 27. TOP GRAPH: Tonotopic organization of AAF in cats 75-67 and 75-68. Lower curve for cat 75-68 was derived in the following manner: (a) 6 parallel lines were drawn perpendicular to the boundary between AAF and AI on the map of best frequencies for this cat (Fig. 25); (b) best frequencies (kHz) of penetrations within 0.25 mm (actual cortical distance) of these lines were plotted as a function of distance (mm) on the cortical surface rostral to the AI-AAF border for that portion of the field in which isofrequency contours remained parallel to this border. Upper curve for cat 75-67 (shown in Fig. 24) was derived in a similar manner for 5 parallel lines crossing AAF, but the curve was displaced on the ordinate 4 mm for comparison. The middle curve is a similar function for a typical AI field (from Merzenich, Knight and Roth, 1975), and is displaced upward on the ordinate for comparison. BOTTOM GRAPH: Cochleotopic organization of AAF for the same cats as above. Curves are derived from the upper graph after conversion of best frequency to represented cochlear position using the function of Greenwood (1961,1974).

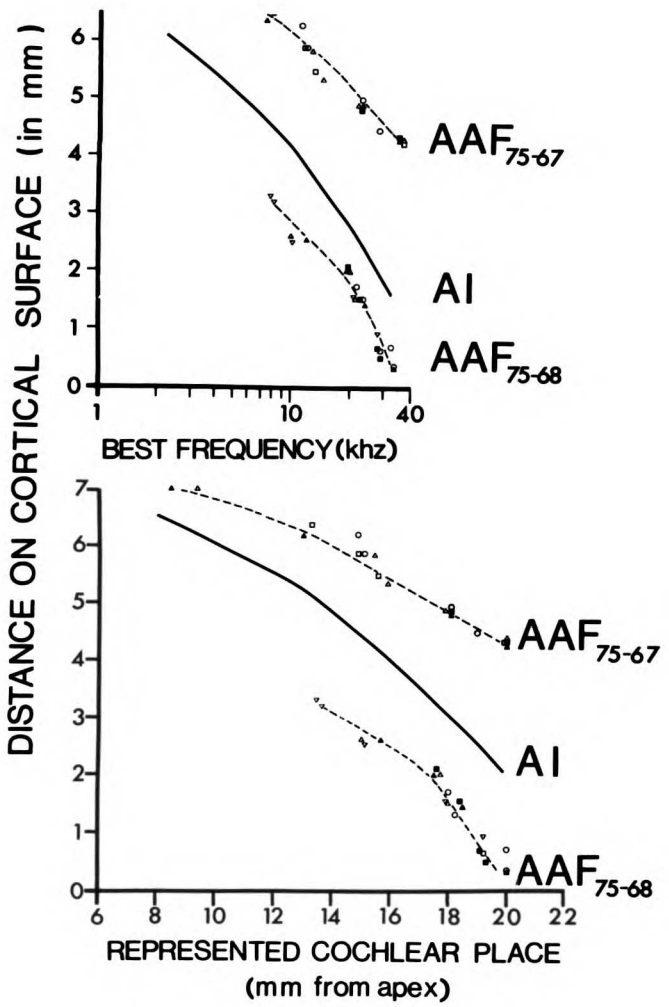
DISTANCE ON CORTICAL SURFACE (in mm)
AAF75-67
AI
AAF75-68
BEST FREQUENCY (khz)
AAF75-67
AI
AAF75-68
REPRESENTED COCHLEAR PLACE
(mm from apex)

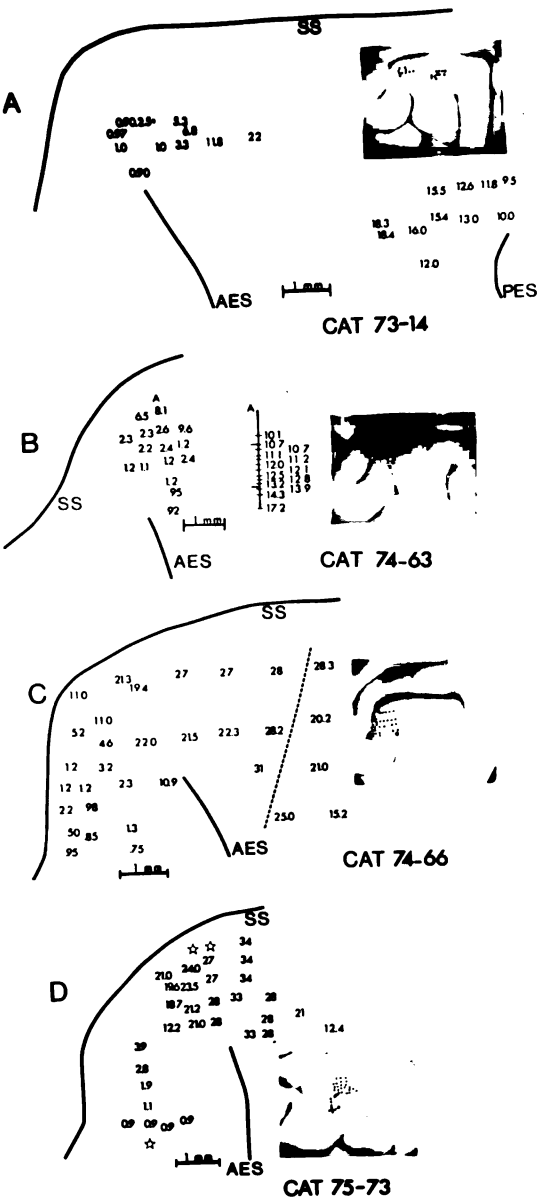

FIGURE 28. Best frequencies (kHz) for penetrations into AAF and AI of cats 73-14 (A), 74-63 (B), 74-66 (C), and 75-73 (D) Asterisk indicates penetration with two threshold minima at the same stimulus intensity. Stars indicate penetrations in which no cells were driven to discharge by tonal stimuli. See legends of Figures 25 and 26 for details.

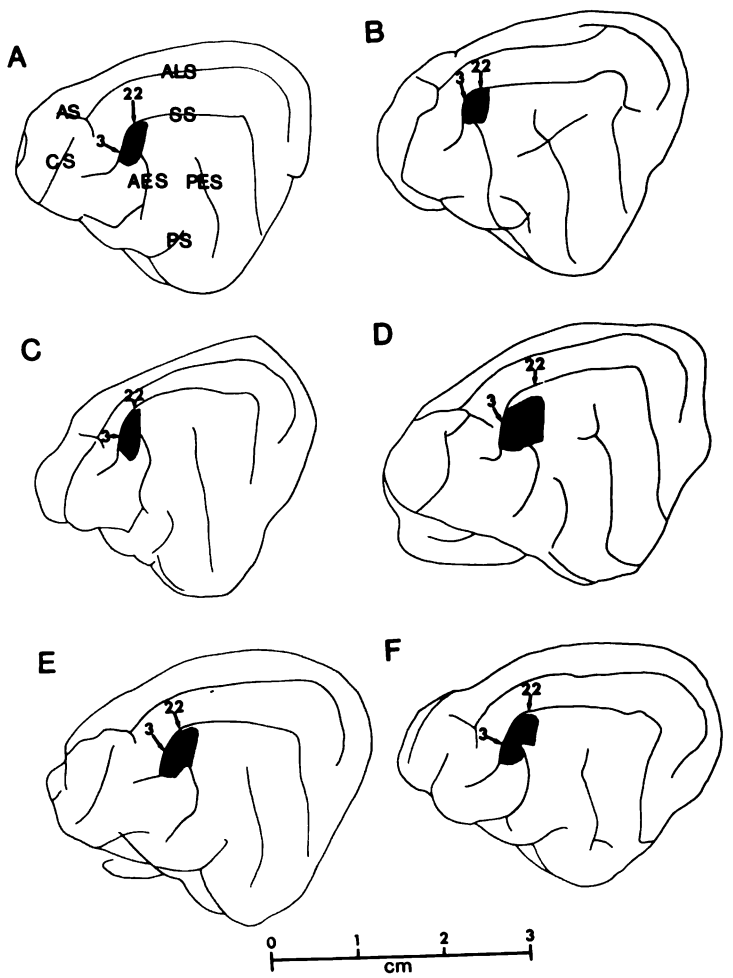

FIGURE 29. Variability in location of AAF with respect to cortical surface landmarks. Shaded areas indicate extent of AAF in 6 cats in this series. The field is probably of the same size in all cats, i.e., the portion of the field on the exposed surface is inversely related to the portion buried in the sulci. On each is shown the approximate position of the 3 kHz and 22 kHz isofrequency contours. For list of abreviations of sulcal terminology, see NEUROANATOMICAL TERMINOLOGY.

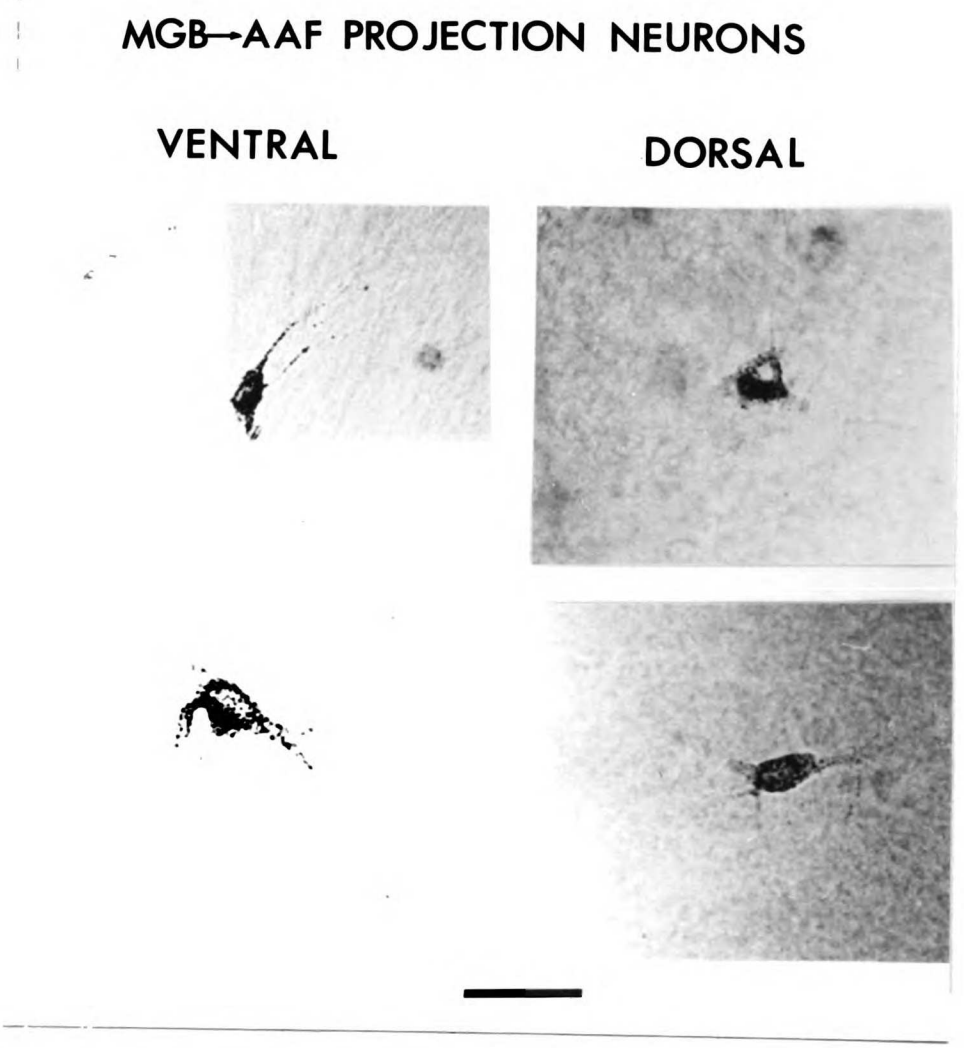

FIGURE 30. MGB neurons projecting to AAF from the deep dorsal and ventral divisions. Note darkly stained granules of HRP reaction product. Granules can be seen in the dendrites of the cells in the ventral division. Calibration bar is 50 microns.

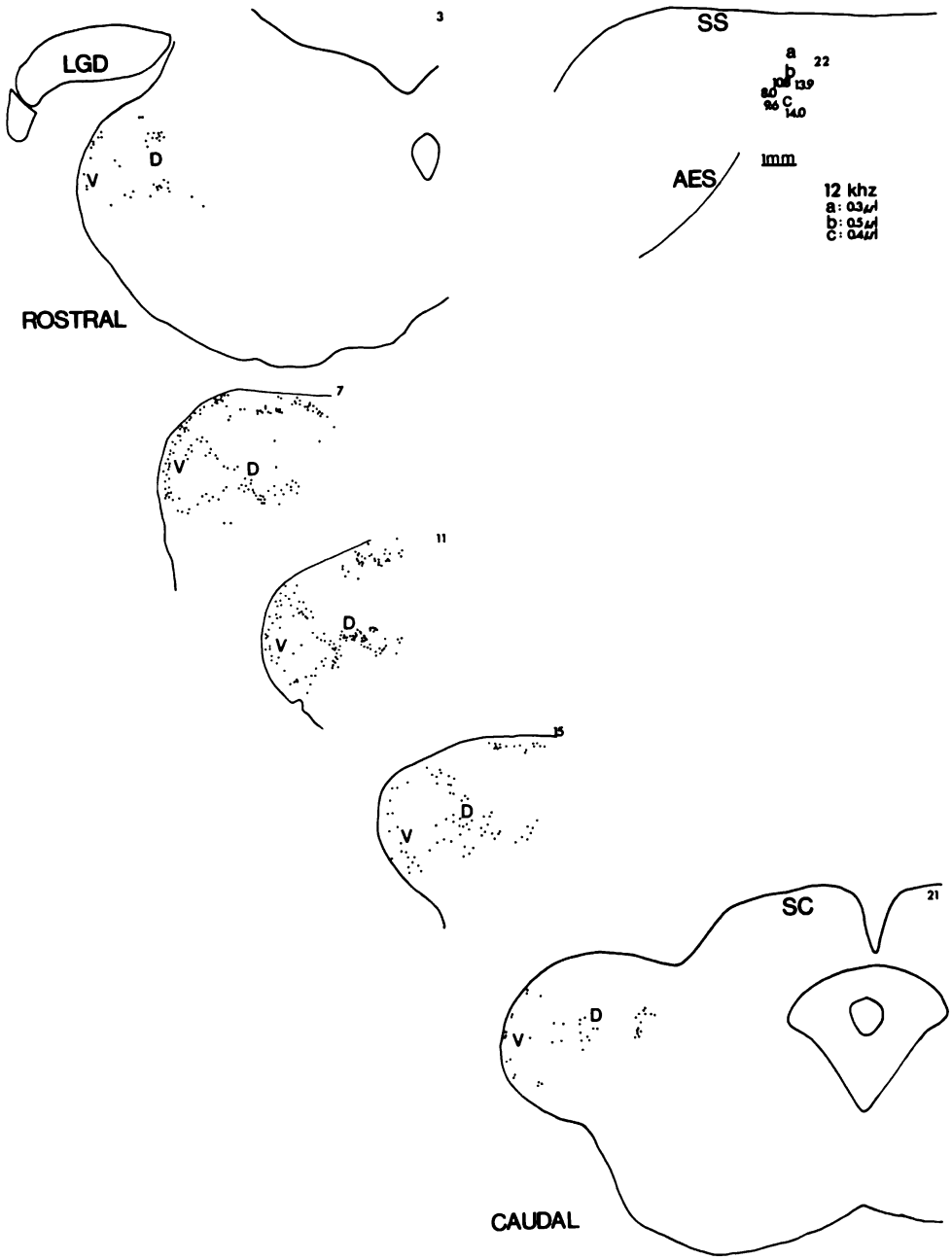

FIGURE 31. MGB neurons projecting to AAF of cat 76-91. Injection sites and frequency shown on cortical map. HRP was seen to spread beyond boundaries of AAF. For list of abreviations, see NEUROANATOMICAL TERMINOLOGY. Section numbers of 90 micron sections are shown.

FIGURE 32. MGB neurons projecting to AAF of cat 76-62. Injection site and frequency shown on cortical map. For list of abreviations, see NEUROANATOMICAL TERMINOLOGY.

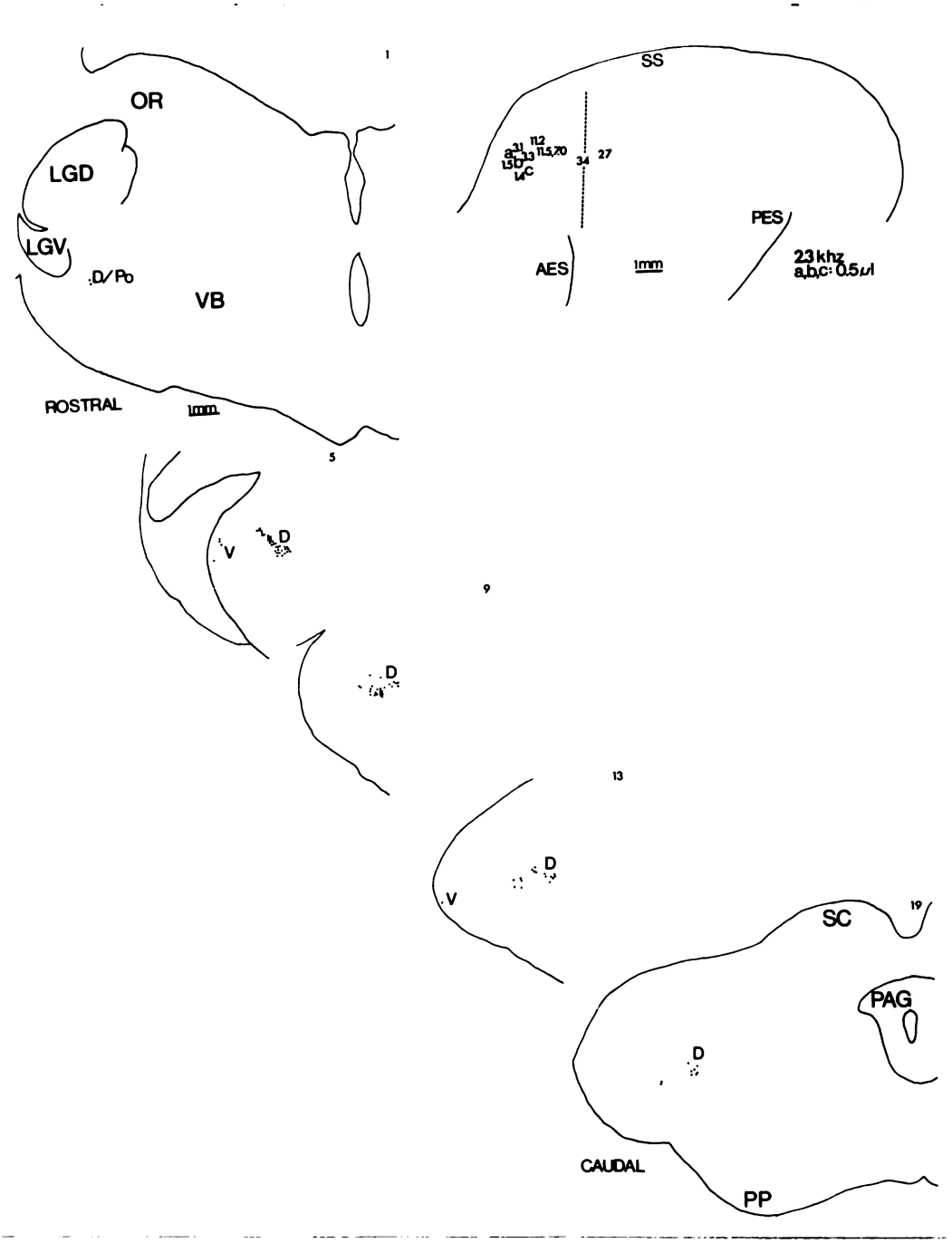

FIGURE 33. MGB neurons projecting to AAF. Injection sites and frequencies shown on cortical map of cat 76-66. For a list of abreviations, see NEUROANATOMICAL TERMINOLOGY.

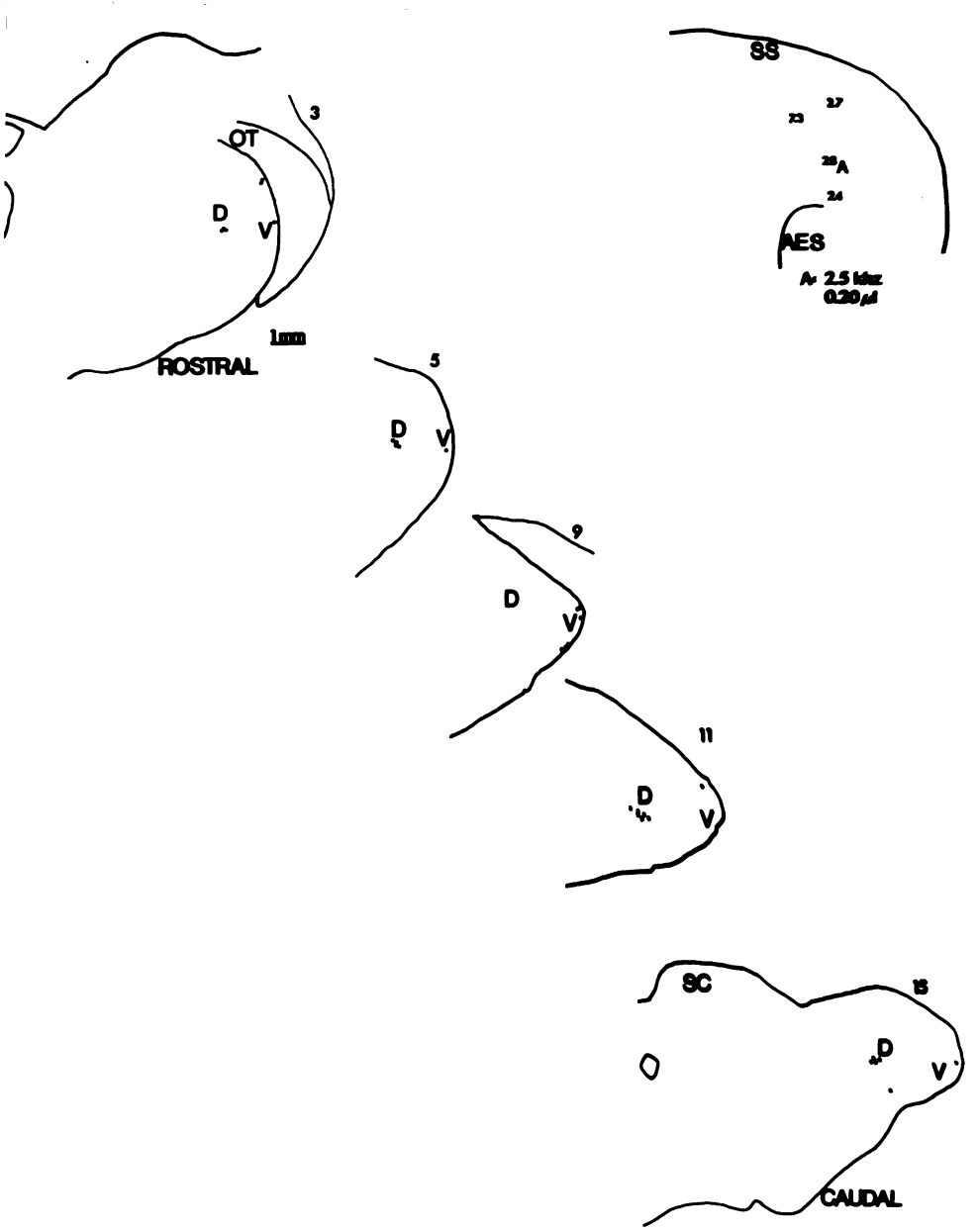

FIGURE 34. MGB neurons projecting to AAF. Injection site and frequency shown on cortical map of cat 76-133. For a list of abreviations, see NEUROANATOMICAL TERMINOLOGY.

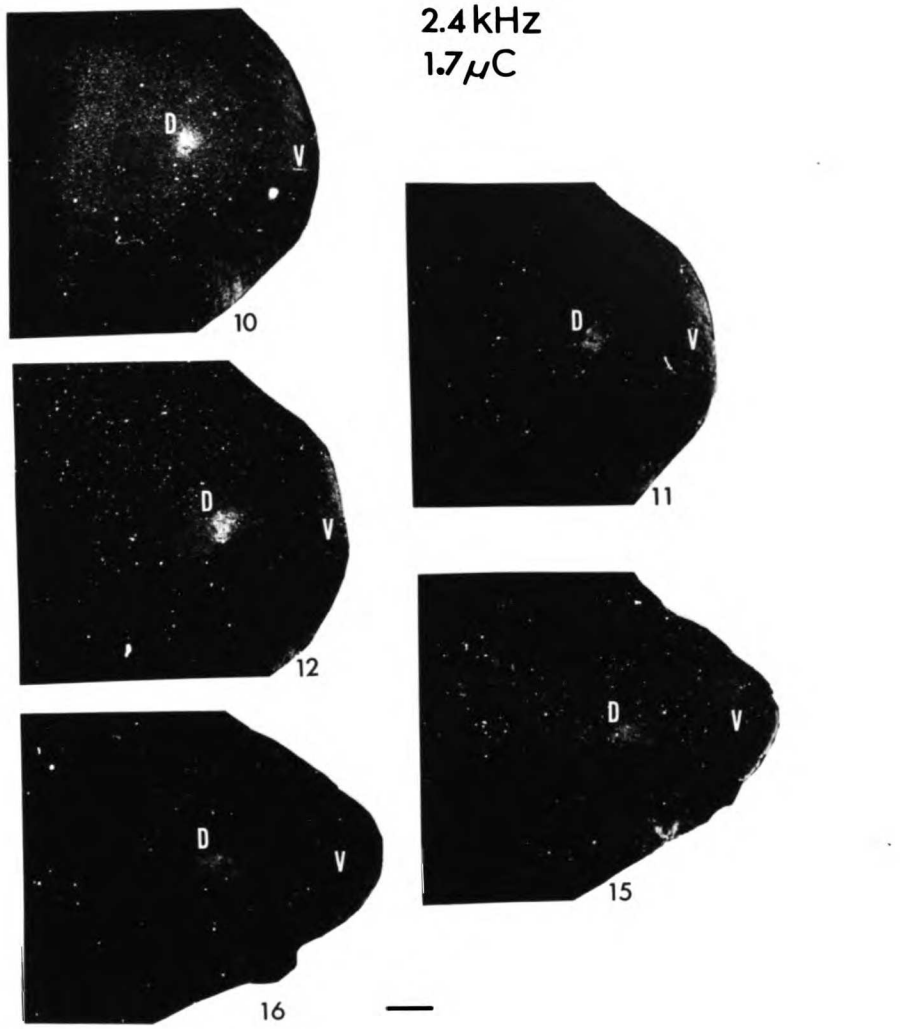

FIGURE 35. Autoradiographically-labelled terminals through the deep dorsal division (D) of the MGB in cat 76-98 from a tritiated leucine injection into a 2.4 kHz site in AAF. Labelling in the ventral division, usually uncertain, can be seen in sections 11 and 12 in this case. Calibration bar is 1 mm. Section numbers are adjacent to sections.

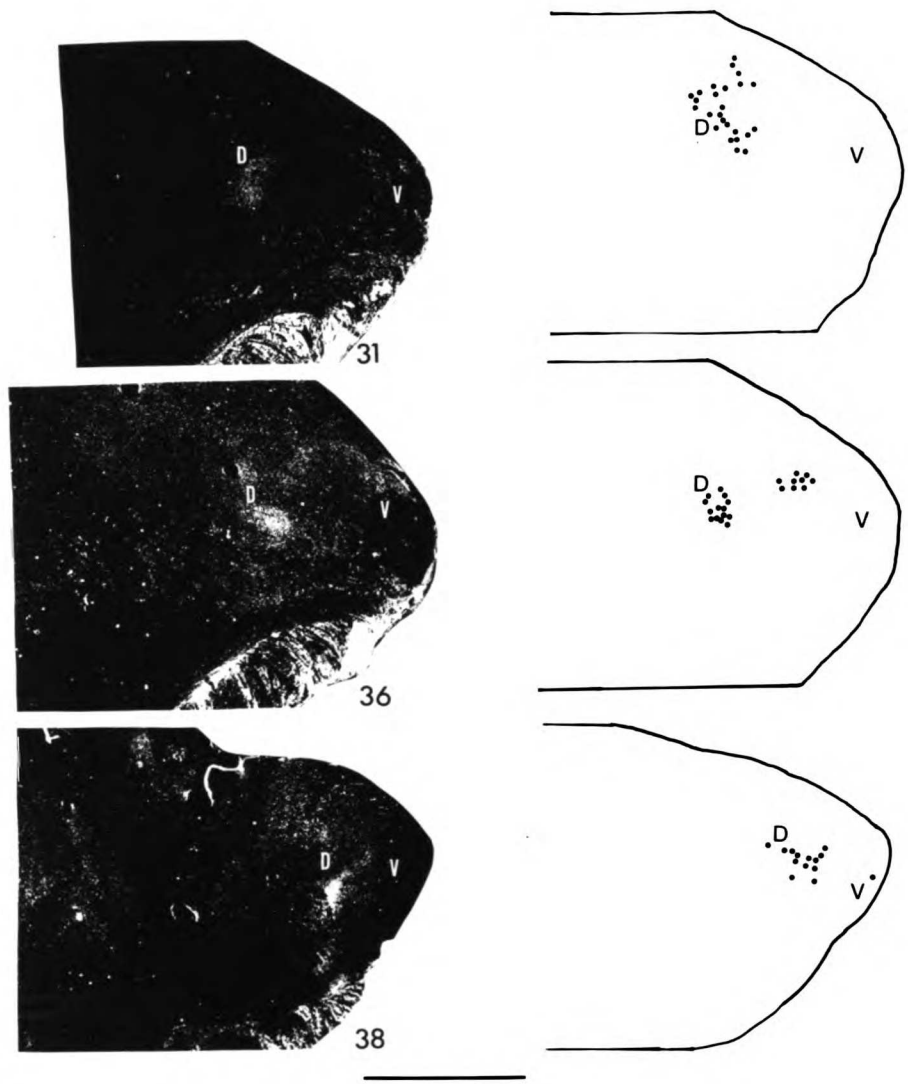

FIGURE 36. AAF thalamocortical and corticothalamic reciprocity. Left: 3 autoradiograms of labelled terminals through the MGB from a single injection of combined tracers into a 6.2 kHz site in AAF of cat 76-62. Right: Adjacent sections showing the array of HRP-labelled neurons projecting to the same injection site. Calibration bar is 5 mm.

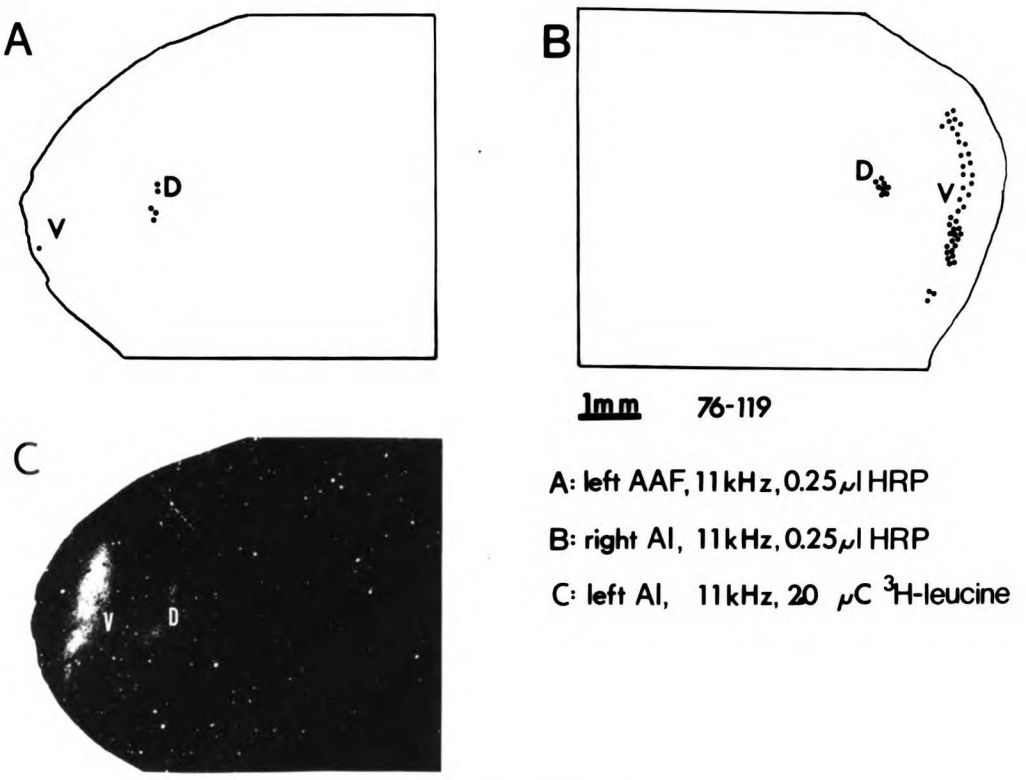

FIGURE 37. Comparison of AAF and Al thalamocortical and corticothalamic projections in cat 76-119. A: Array of MGB neurons projecting to an 11 kHz injection site in AAF of the left hemisphere. B: Array of MGB neurons projecting to an 11 kHz injection site in Al of the right hemisphere. C: Array of terminals projecting to the MGB from an 11 kHz injection site in Al of the left hemisphere. See text for details. Sections are adjacent.

AAF INTERCORTICAL PROJECTION

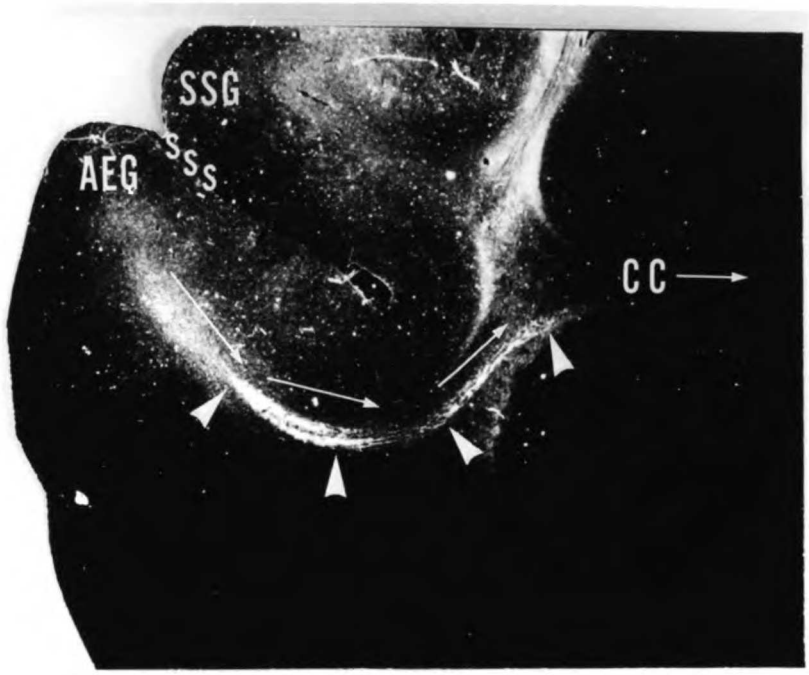

FIGURE 38. Intercortical projection from AAF of cat 76-66. Arrows show path and direction of autoradiographically-labelled fibers passing through the corpus callosum (CC). AEG, anterior ectosylvian gyrus; SSG, suprasylvian gyrus; SSS, suprasylvian sulcus. Frontal section.

DISCUSSION

HISTORICAL FIGURE 4. An illustration of the ventral aspect of the brain from De homine (1662) by Rene Descartes. He believed that the pineal gland (H) was the center of the soul and controlled the flow of spirits in the ventricles (A). Nerve tubes (BC) connected the ventricles with the cortex.

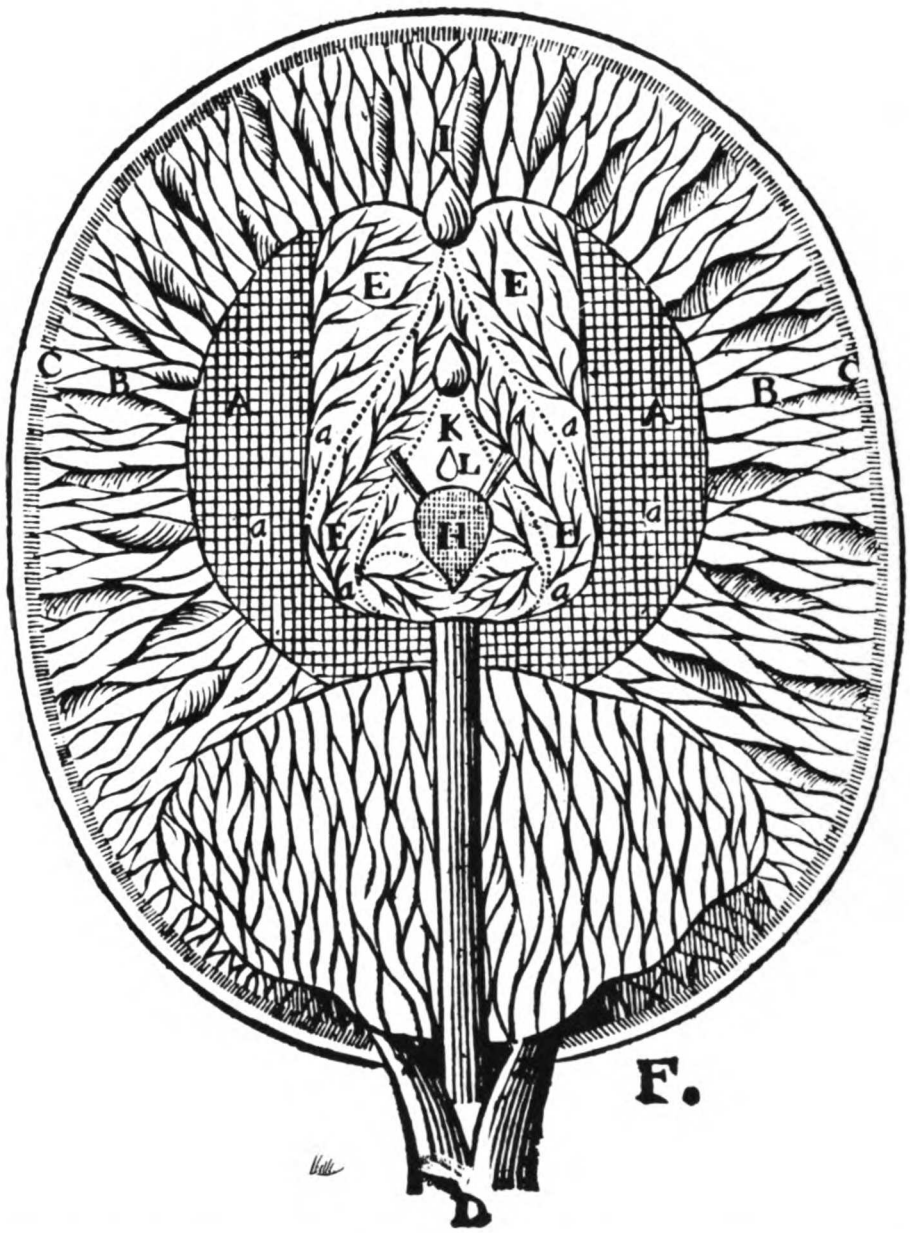

F.

DISCUSSION

Organization of AAF in the Cat

This study constitutes the first detailed microelectrode mapping of a "secondary" auditory cortical field in the cat. The results of this study show that there is a highly-ordered representation of the cochlea in the anterior auditory field of the cat.

Results of penetrations made radially through the depths of the middle and deep cortical layers below a given point on the surface of AAF reveal that all units responding with discharges have sharply-tuned response profiles with nearly identical best frequencies. This radial organization is also characteristic of the few penetrations encountering units with tuning curves having multiple peaks at similar thresholds. Thus, acoustic information (near threshold) representing a single point or multiple points along the cochlear partition (i.e., having a single or multipeaked tuning curve, respectively) is processed along a radial column of cells in the middle and deep cortical layers of AAF.

A given frequency band (or, equivalently, cochlear sector) is represented on much of the exposed cortical surface of AAF by a nearly straight belt of neurons in the active cortical layers (under ketamine anesthesia) crossing the entire field. Frequency bands are systematically represented across the cortical surface. There is an orderly progression from parallel high frequency bands (representing the more basal cochlear sectors) near the caudal AI-AAF border to lower frequency bands (representing more apical cochlear sectors) rostrally. In most cases, there is a rotation of the lower frequency sectors following the curvature of the anterior ectosylvian gyrus. AAF may also continue down the bank of the suprasylvian sulcus. These features are shown diagrammatically for a hypothetical cat (Figures 40B and 40C).

Penetrations down the bank of the suprasylvian sulcus cross discrete regions of similar best frequency. This suggests that there may be units of "vertical organization" in AAF similar to the "columns" of somatosensory (Mountcastle, 1957; Powell and Mountcastle, 1959) and visual cortex (Hubel and Wiesel, 1962, 1963, 1974; LeVay, Hubel and Wiesel, 1975; Kaas, Lin and Casagrande, 1976; Wiesel, Hubel and Lam, 1974).

Relationship between AAF and the Auditory Thalamus

Neuroanatomical experiments, using the retrograde transport of horseradish peroxidase from physiologically-defined injection sites within AAF, were undertaken to determine the arrays of neurons within the medial geniculate body that project to sites within AAF. These experiments revealed that a restricted locus within AAF receives a major convergent projection from a continuous three dimensional column of cells passing through the deep dorsal subdivision of the MGB (Morest, 1964) rostrally into the posterior group nuclei as shown diagrammatically in Figure 39. There is also a smaller convergent projection to AAF from a sparse array of neurons within the ventral division of the MGB, usually seen at the lateral margin of this division. These cells are possibly within the marginal zone of Cajal (1909) and Morest (1964, 1965a) or within the low frequency region of the ventral division (Aitkin and Webster, 1972) that projects to AI (Colwell and Merzenich, 1975). Multiple injections along an isofrequency contour have also shown convergent projections from a single deep dorsal-posterior group column as well as projections from the ventral division. These data suggest that, taken at its limit, a point in AAF receives a convergent projection from a one dimensional line of cells in the deep dorsal-

posterior group column as well as from a few cells in the ventral division. Similarly, as shown by the orthograde transport of labelled amino acid from the cell bodies near the injection site to their axon terminals in the MGB, single two dimensional injection sites and multiple injection sites along an isofrequency contour project divergently to a three dimensional column within the deep dorsalposterior group column.

Furthermore, comparisons of the thalamocortical and corticothalamic projections to and from injection sites within AAF have revealed that these two projection systems are reciprocal, i.e., the array of thalamocortical neurons within the deep dorsal-posterior group column projecting to a given point in AAF receives an at least approximately coincident projection from that same point. There was no unequivocal evidence in this material that the sparse projection from the ventral division to AAF received a reciprocal corticothalamic projection.

Organizations of AAF and AI; Similarities and Differences

The organizations of AAF and AI are remarkably similar in many respects. Both AI (Merzenich, Knight and Roth, 1975) and AAF have similar radial organization with units of similar best frequency found through the active depths of cortex. This feature of organization has also been noted in other studies of incompletely mapped auditory cortex of the cat (Abeles and Goldstein, 1970; Gerstein and Kiang, 1964; Hind, et al. , 1960; Parker, 1965) and in mapped AI of other species (Brugge, 1975; Imig, Ruggero, Kitzes, Javel and Brugge, 1977; Merzenich and Brugge, 1973; Merzenich, Kaas and Roth, 1976; Oliver, Merzenich, Roth, Hall and Kaas, 1976). Similar evidence for AAF and AI suggests that both fields have units of "vertical organization" akin to cortical columns defined in other sensory modalities (Mountcastle, 1957; Powell and Mountcastle, 1959; Hubel and Wiesel, 1962, 1963, 1974; LeVay, Hubel and Wiesel, 1975; Wiesel, Hubel and Lam, 1974; Kaas, Lin and Casagrande, 1976). Furthermore, in most of the exposed region of each field, a given frequency band is represented by a nearly straight belt of cortex crossing the entire field.

The similarity in the spatial representation of frequency within AAF and AI (Merzenich, Knight and Roth, 1975) is remarkable. For the portions of both fields

where axes of representation of frequency are parallel, the graphs of Figure 27 show that both fields have similar, though reversed, functions of frequency (represented cochlear place) vs. distance across the cortical surface from their mutual boundary. Thus, in this respect, the two fields appear to be mirror images of one another reflected from their mutual high frequency boundary. Furthermore, in these regions of both AAF and AI, there is a proportionately larger representation of high frequency octaves (or, equivalently, more basal equal-length sectors of the cochlea) along the dimension of the field perpendicular to the line of frequency representation. These features of AI and AAF are illustrated schematically for a hypothetical cat in Figure 40B and C.

There were, however, also some notable physiological differences between the two fields in the mapping experiments. First, there are more "spontaneously" active units in AAF than in AI under ketamine anesthesia. Second, in individual penetrations into AAF, a broadly-tuned intracortical evoked potential was recorded near threshold for unit discharges; the intracortical evoked potential recorded in AI was much more sharply tuned (Merzenich, Knight and Roth, 1975). Third, in a few penetrations into AAF, units were found to have

multipeaked tuning curves at similar threshold intensities. Such units were not found under the same conditions of anesthesia in extensively mapped AI of the cat (Merzenich, Knight and Roth, 1975).

Comparison of AAF and AI Projections to and from the MGB

Comparison of these neuroanatomical data with those from similar experiments conducted to determine the thalamocortical and corticothalamic projections to and from physiologically-defined loci within AI (Colwell and Merzenich, 1975) has revealed that loci within both of these fields receive convergent projections from and project divergently and reciprocally to a column of neurons passing rostrally through the deep dorsal division of the MGB into the posterior group nuclei without obvious discontinuity, as shown in Figure 39.

The present experiments also show that the same deep dorsal-posterior group column projects to loci with the same best frequency (representing the same position on the basilar partition) within both fields and receives a reciprocal projection from points of similar best frequency in both fields.

However, the projection to AAF from the ventral division of the MGB comes from a small number of cells near the lateral margin of this division while AI receives a large projection from a continuous array of neurons within the laminated portion of the ventral division and the pars ovoidea (Colwell and Merzenich, 1975). It remains uncertain as to whether the cells in the ventral division of the MGB projecting to AAF are within the array of neurons projecting to a point of similar best frequency in AI. Thus, if the deep dorsal-posterior group column is directing similar information to both AAF and AI, AAF is analyzing a subset of the acoustic information analyzed by AI.

Implications of the Variability in Location of AAF with Respect to Cortical Surface Landmarks

The variability in the location of the boundaries of AAF and the frequency representation within it with respect to cortical surface landmarks has several important implications: (1) There is a large degree of uncertainty inherent in ascribing a particular cortical location to AAF, AI, or any surrounding field by comparing cortical landmarks in any individual animal with "standard" cortical maps (e.g., Woolsey's (1960, 1961) maps, Figure 40A, or the schematic representations

in Figures 40B and 40C and 40C) or with any of the individual maps in this series. (2) A penetration recording sharply-tuned units with a middle or high best frequency may be incorrectly ascribed to AAF or AI when referenced to cortical landmarks since the boundary between the two fields is highly variable in location on the cortical surface. And (3), it is impossible to reference cortical landmarks in combining data from several animals to create an accurate map of best frequencies for AAF or AI (Merzenich, Knight and Roth, 1975).

Relationship to Earlier Mapping Studies

The anterior auditory field has only recently been recognized as a distinct representation in the cat. In the microelectrode mapping study of AI in the cat by Merzenich, Knight and Roth (1975), this cochlear representation was recognized by the physiological criteria mentioned earlier, i.e., the presence of a broadly-tuned intracortical evoked potential and the reversal in the frequency progression crossing the border with AI. In this previous paper, this field was designated the "rostral field", but in the present study, this field is renamed the "anterior auditory field" to avoid implying homology with the "rostral field" in the

auditory cortex of the monkey (Brugge, 1975; Imig, Ruggero, Kitzes, Javel and Brugge, 1977; Merzenich and Brugge, 1973).

Although Tunturi (1945, 1950) described a cochlear representation on the anterior ectosylvian gyrus of the dog (his field "AIII") that corresponds to AAF (though it was far smaller than AI and was without a distinct frequency reversal across a border with AI). it was not appropriately defined in the cat. In the evoked potential studies of the auditory cortex of the cat by Woolsey and Walzl (1942) and Downman, Woolsey and Lende (1960), the high frequency region of AAF was included in the rostral portion of AI presumably because the direct electrical stimulation of the cochlear base in these studies caused widespread excitation of the high frequency regions of both fields simultaneously. Similarly, Hind (1953) did not distinguish the high frequency boundary between AAF and AI in his evoked potential study of auditory cortex in the cat using tonal stimuli. Although he showed a reversal in frequency progression crossing the cortex for one cat (Figure 10), he combined data from several animals on a standard cortical map (Figure 11), a procedure which would obscure the orderly representation of the cochlea in AAF and the boundary of AI with AAF. In his syntheses of earlier data on the auditory cortex, Woolsey (1960, 1961)

described the "suprasylvian fringe", a cochlear representation with a low frequency region on the exposed lateral surface of the anterior ectosylvian gyrus and a higher frequency representation within the depths of the suprasylvian sulcus (shown in Figures 9 and 40A). By comparing this figure with the schematic maps of AI and AAF (Figs. 40A and 40C), it can be seen that his description of auditory cortex exaggerated the size of AI by including in it the high frequency portion of AAF.

Earlier microelectrode mapping studies of auditory cortex in the cat (Evans, Ross and Whitfield, 1965; Evans and Whitfield, 1964; Goldstein, Abeles, Daly and McIntosh, 1970; Hind, et al., 1960) also failed to recognize a complete and orderly representation of the cochlea within AAF. In each of these studies, data was combined from several animals to give composite representations of AI (shown in Figures 16 and 17). It is clear, however, that in each of these studies penetrations were likely to have been directed into AAF of some animals. As has been discussed for AAF as well as for AI (Merzenich, Knight and Roth, 1975), this combination of data from several animals using cortical landmarks as a reference would tend to obscure rather than clarify the boundary between the two fields as well as the frequency representation within each field.

The classical description of the cytoarchitecture of the auditory region of the cat by Rose (1949) is somewhat different than that found in this study. His division of the auditory cortex on cytoarchitectonic criteria is not consistent with the physiological results in the present study. He probably included the dorsal region of AAF within AI and the ventral region of AAF within his "AII". The overall similarity between the cytoarchitecture of AI and AAF and, especially, difficulty in defining a cytoarchitectonic boundary between the two fields near the anterior ectosylvian sulcus could account for the differences between his results and those in the present study.

Relationship to Earlier Neuroanatomical Studies

This study constitutes, in part, the first determination of the projections to and from physiologically-defined points within a cortical auditory representation other than AI (Colwell and Merzenich, 1975). Since this work has shown AAF to be a complete auditory representation that was previously unappreciated, it is problematical to compare this work with previous neuroanatomical studies that used different descriptions of cortical fields without direct

physiological determination of the organization of auditory cortex in individual animals.

The early studies of the auditory geniculocortical pathways in the cat were based on mapping of orthograde degeneration of MGB axons in the cortex following lesions within the MGB (Woollard and Harpman, 1939; Ades, 1941). In both of these studies, lesions within the MGB produced degeneration across large regions of auditory cortex. Thus, these authors considered the entire auditory cortex to be homogenous with respect to these projections. Woollard and Harpman (1939) further described the thalamocortical projection to be point-to-point from the MGB to auditory cortex.

Waller (1939) recognized a degree of localization in the auditory geniculocortical projections in his studies of retrograde neuronal degeneration within the MGB following localized cortical lesions. In one of his cases (124R, shown on p. 531, Waller, 1939), a large lesion covering the dorsal aspect of the middle ectosylvian gyrus (probably including some of AI) caused a band of degeneration within the ventral division of the MGB dimensionally similar in frontal section to the array of neurons projecting to AI as shown by Colwell and Merzenich (1975). In another case (case 123, p. 530,

Waller, 1939), a small lesion rostral to the dorsal tip of the anterior ectosylvian sulcus caused a circular patch of degeneration (seen in frontal section) in the most rostral aspect of the MGB, dimensionally similar to that seen for neurons projecting to AAF from the deep dorsal-posterior group column. However, the sizes of the lesions and the uncertainty of the boundaries between cortical fields with respect to cortical surface landmarks in these cases precludes further comparison with this study.

In their classical retrograde degeneration study of the projection of the MGB onto auditory cortex, Rose and Woolsey (1949) put lesions in four auditory fields that they defined on the basis of cytoarchitecture (Rose, 1949) and correlations with the earlier evoked potential maps of Woolsey and Walzl (1942). Although their description of the boundaries of the lesioned fields differs from that found in the present study, they made small lesions that were likely to have been within AI (e.g. their case 12b, Fig. 7, p. 448, Rose and Woolsey, 1949) and (at least to some extent) in AAF (e.g. their case 10a, Fig. 27, p. 455, Rose and Woolsey, 1949). Lesions in their AI fields caused dramatic degeneration within the ventral (principal) division of the MGB. Although the lesion in their case 10a (which probably

included part of AAF) produced "possible cell rarefaction in the medial portion of the dorsoanterior segment of the principal division" (deep dorsal division), they questioned degeneration within the MGB following lesions outside AI. Lesions involving more than one field caused more widespread degeneration than lesions confined to any one field alone. They used the term "essential" projections to describe those projections to AI, from the ventral division of the MGB, which degenerated with AI lesions only; they used the term "sustaining" projections to describe those projections from regions deep to the ventral division, which survive lesions in areas outside AI, but that degenerate following lesions within both AI and adjacent auditory fields. They hypothesized that MGB cells giving rise to sustaining projections might send axon collaterals to more than one field.

The results of the present study show that points of similar best frequency in both AAF and AI receive projections from the same deep dorsal- posterior group column. Their interpretation of sustaining projections suggests that at least some of the cells within this column send axon collaterals to both AAF and AI. Another possible interpretation of sustaining projections is that corticothalamic projections may exert a trophic effect on the thalamocortical projection neurons, and removal of

these projections might enhance degeneration in the MGB. If this is the case, then the effects on the MGB of removal of one set of corticothalamic projections to the deep dorsal-posterior group column from either AAF or AI might not be apparent if the corticothalamic projection from the other field remains intact.

In their later study of auditory thalamocortical projections, Rose and Woolsey (1958) suggested that cortical fields receiving sustaining projections may be "equipotential" in processing information from the same array of projecting neurons, i.e., multiple cortical fields may similarly process information projected to each via sustaining projections from the same MGB locus. Such "equipotential" processing of some acoustic information appears to be the case with AAF and AI in which both fields represent information concerning the frequency of the sound information in a similarly organized manner.

Later retrograde degeneration (Neff and Diamond, 1958) and orthograde degeneration studies (Wilson and Cragg, 1969; Sousa-Pinto, 1974; Niimi and Naito, 1974; Heath and Jones, 1971; Graybiel, 1973) of the auditory thalamocortical projections used the maps of Rose and Woolsey (1949) and those of Woolsey (1960, 1961) as

guides to determine the sites of cortical lesions and the destinations of thalamocortical projections. In the study by Neff and Diamond (1958), cortical lesions were too broad to determine accurately projections to presently understood cortical fields. While diffuse projections from the MGB (Wilson and Cragg, 1969) and from the posterior group nuclei (Graybiel, 1973) to cortex have been described, relatively restricted areas of intense axonal degeneration on the anterior ectosylvian gyrus were illustrated for lesions in the region of the MGB deep to the ventral division by Niimi and Naito (1974) (cat 9 in their figure 1). In their orthograde degeneration study of the posterior group nuclei, Heath and Jones (1971) stated that the posterior group does project to the anterior ectosylvian gyrus, as confirmed in the present experiment.

In his extensive orthograde degeneration study of the cat auditory system, Sousa-Pinto (1974) suggested that AI receives a modality-specific projection from the ventral division of the MGB while surrounding areas (as described by Woolsey, 1960, 1961) receive non-specific multimodal input from regions deep to the laminated portion of the ventral division (Morest, 1964, 1965a). These contentions are clearly contradicted by the results of the present study and by companion studies of AI

(Merzenich, Knight and Roth, 1973, 1974, 1975; Colwell and Merzenich, 1975) which show that two highly organized cortical representations of the cochlea receive projections from the deep dorsal- posterior group column.

In their study of corticothalamic projections from Woolsey's (1960, 1961) cortical fields, Pontes, Reis and Sousa-Pinto (1975) stated that the area of the anterior ectosylvian gyrus did not have any projections to any divisions of the MGB while the suprasylvian fringe projected heavily upon the dorsal division. Since redefinition of the cochlear representation in AAF in the present study has shown that AAF is often located on the anterior ectosylvian gyrus and within the depths of the suprasylvian sulcus (in some cases), it is difficult to correlate their findings with the results of the present study.

This study, in part, along with a similar study of the projections to and from AI by Colwell and Merzenich (1975), resolves some of the ambiguities in these earlier descriptions of the relationships between the MGB and cortical representations of the cochlea. The combination of physiological description of the tracer injection sites with the modern tracer methods has provided a better understanding of the auditory thalamocortical

relationships for the following reasons: (a) Physiological definition of injection sites in AAF and AI took into account the new description of AAF and AI (Merzenich, Knight and Roth, 1973, 1974, 1975) and the variability in location of these representations on the cortical surface when referenced to cortical surface landmarks that were not appreciated in earlier studies. (b) Cortical injections of tracers were usually more discrete and controlled than the cortical lesions used in degeneration studies, and, therefore, labelled more discrete arrays of neurons and terminals in the MGB. (c) HRP histochemistry and tritiated amino acid autoradiography used in this study are more sensitive and more accurate than degeneration techniques for determining projectional pathways. And (d), lesions placed within the MGB were often large in orthograde degeneration studies, often interrupted fibers of passage, and often crossed the boundaries of the divisions of the MGB. This makes interpretation of orthograde degeneration difficult, especially from the present point of view, which recognizes the convergent projections from divisions of the MGB to cortex.

Hypothesis Concerning the Development of AAF

The arrangement of parallel isofrequency contours near the AAF-AI border and the rotation of lower frequency contours rostrally in some animals may be the result of the rotation of the cortical surface during development. A possible model for the development of the adult configuration of this field is as follows: Initially, the field consists of parallel isofrequency contours on a relatively flat cortical surface. As the cortex matures, the infolding of the cortical surface into the late-developing anterior ectosylvian sulcus (not present or poorly developed at birth) may cause the rotation of the parallel isofrequency contours on this surface. The variability among animals of cortical sulcal patterns and configurations of AAF on the cortex suggests that there is a degree of independence between factors specifying the development of the sulcal patterns and the factors localizing this field on the cortical surface. By extension, it is likely that a degree of independence exists between the development of all other sulcal patterns and locations of other cortical fields.

Parallel Processing of Acoustic Information

Comparisons between AI and AAF have revealed that they are remarkably similar in the following characteristics: short latency (10 to 12 msec) to the earliest unit discharge, sharp tuning of units responsive to sound stimulation, radial alignment of units with similar tuning curves through the middle and deep cortical layers, and a nearly identical spatial representation (with the same proportionality of representation) of the cochlea across a similarly sized cortical area. They also share common input from at least one subdivision of the medial geniculate body (the deep dorsal-posterior group column) and project reciprocally upon it. Given these considerations, particularly the identical short first-spike latency and common excitatory thalamic input, it is likely that AAF and AI are processing acoustic information in a temporally parallel manner rather than in a heirarchical manner. However, the fact that these two divisions of cortex receive input from and project to some different and some similar thalamic divisions indicates that the information being processed in parallel by both fields is not identical. Therefore, it does not seem appropriate to consider AAF as a "secondary" auditory field, a term which implies that AAF operates primarily on information

previously processed by AI. For the same reason, it is clearly inappropriate to consider AI to be the "primary " auditory cortex. Thus, AAF, which has not been clearly differentiated from AI in most earlier work, should be recognized as a co-participant in the earliest and fundamental cortical processing of acoustic information.

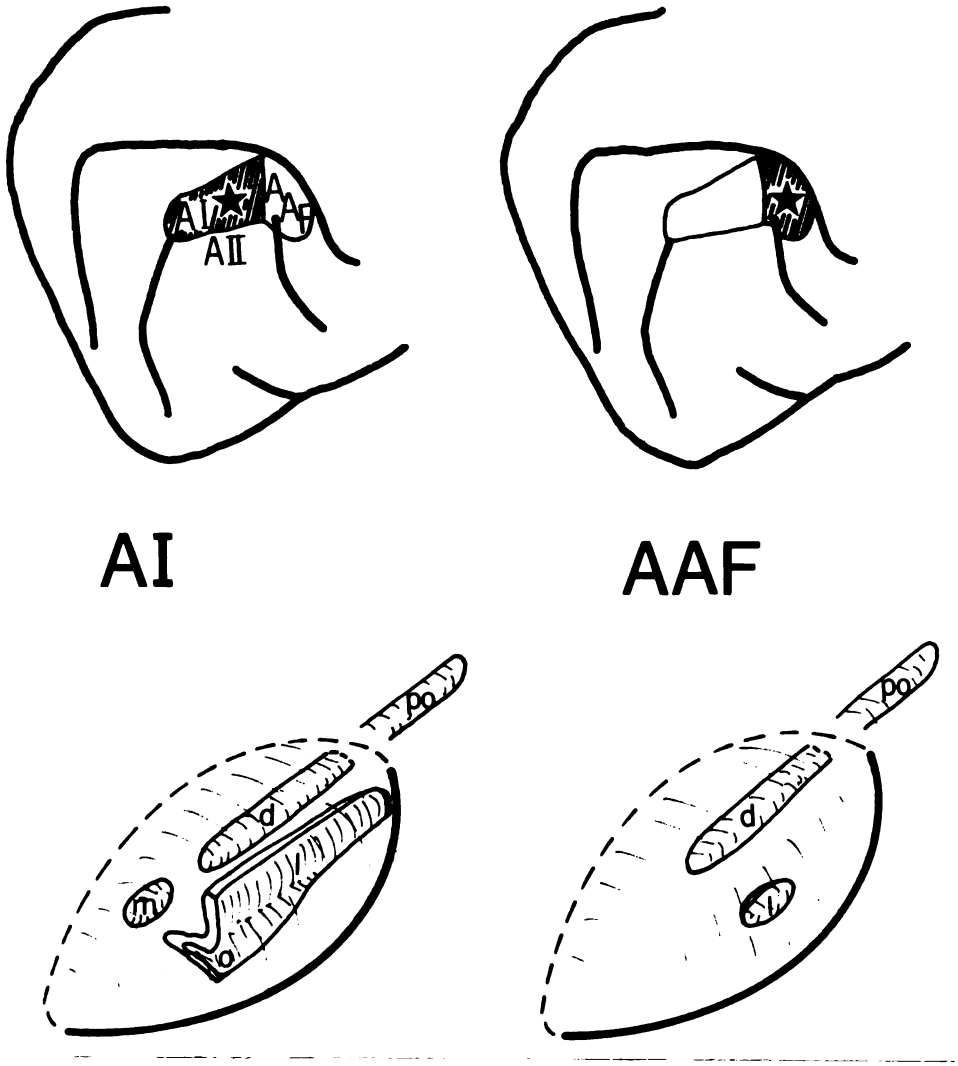

FIGURE 39. Comparison of projections to loci within AI (left) and AAF (right) from the MGB and Po. Stars indicate points of the same best frequency in AAF and AI. d, deep dorsal division; m, medial division; l, laminated portion of the ventral division; o, pars ovoidea; po, posterior nuclear group. Modified from Merzenich, Roth, Andersen, Knight and Colwell, (1977).

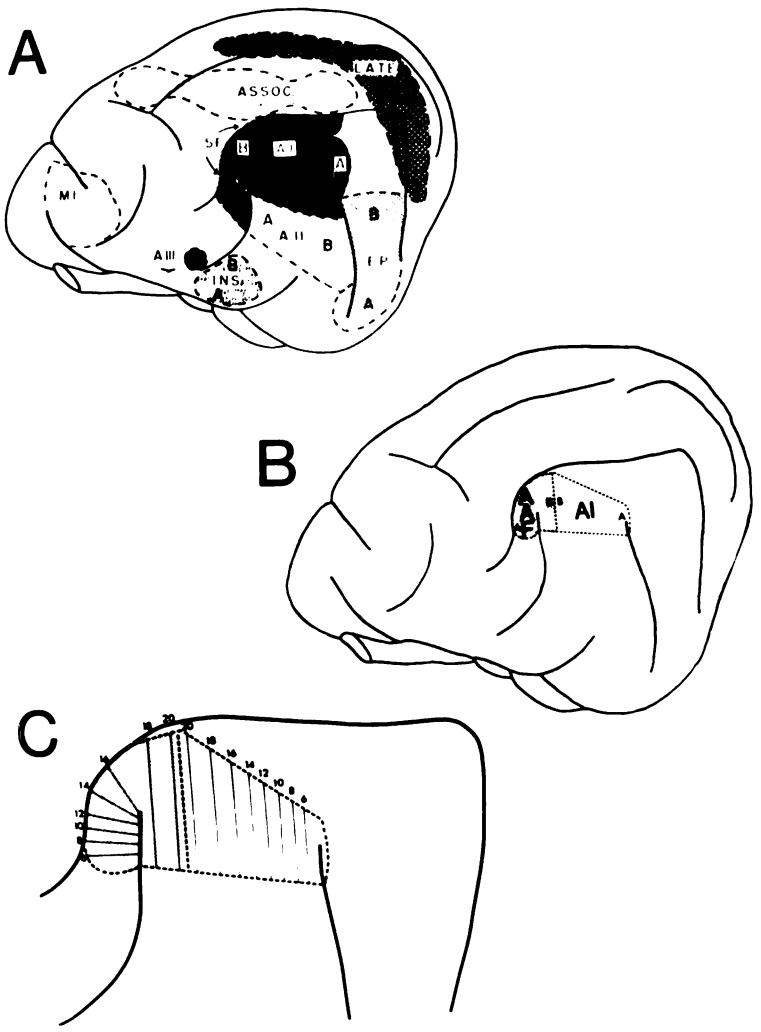

FIGURE 40. A. Woolsey's (1960) map of auditory regions in the cortex of the cat. B. Diagrammatic representation of AAF and AI drawn on the same sulcal pattern as in A. Small "A" indicates regions representing the cochlear apex; small "B" indicates regions representing the cochlear base. C. A magnified view of AAF and AI. Solid lines indicate the approximate length and orientation of the lines of representation of cochlear position indicated by numbers representing mm from the cochlear apex.

BIBLIOGRAPHY

HISTORICAL FIGURE 5. Phrenological map of the human head from a periodical published in the early part of the 20th century. This doctrine, introduced by Franz Joseph Gall (1758-1828), postulated that behavioral functions were discretely localized on the brain and could be deduced by examination of the surface topography of the head.


A
B
C
D
1
2
3
4
5
6
7
8
9
10
11
12
13
14
15
16
17
18
19
20
21
22
23
24
25
26
27
28
29
30
31
32
33
34
35
36

BIBLIOGRAPHY

Abeles, M. and Goldstein, M.H. (1970). Functional architecture in cat auditory cortex: columnar organization and organization according to depth. J. Neurophysiol. 33: 172-187.

Adams, J.C. (1975). Ascending and descending projections to the inferior colliculus. Neuroscience Abst. 5: 37.

Adams, J.C. and Warr, W.B. (1976). Origins of axons in the cat's acoustic striae determined by injection of horseradish peroxidase into severed tracts. J. Comp. Neurol. 170: 107-122.

Ades, H.W. (1941). Connections of the medial geniculate body in the cat. Arch. Neurol. Psychiat. 45: 138-144.

Ades, H.W. (1943). A secondary acoustic area in the cerebral cortex of the cat. J. Neurophysiol. 6: 59-63.

Ades, H.W. (1959). Central auditory mechanisms. In: J. Field, H.W. Magoun and V.E. Hall (eds.), Handbook of

Physiology. Section 1, Volume 1, Neurophysiology. Washington: American Physiological Society. pp. 585-613.

Ades, H.W. and Felder, R. (1942). The acoustic area of the monkey (Macaca mulatta). J. Neurophysiol. 5: 49-54.

Aitkin, L.M., Anderson, D.J., and Brugge, J.F. (1970). Tonotopic organization and discharge characteristics of single neurons in nuclei of the lateral lemniscus of the cat. J. Neurophysiol. 33: 421-440.

Aitkin, L.M. and Moore, D.R. (1975). Inferior colliculus. II. Development of tuning characteristics and tonotopic organization in central nucleus of neonatal cat. J. Neurophysiol. 38: 1208-1216.

Aitkin, L.M. and Webster, W.R. (1972). Medial geniculate body of the cat: organization and responses to tonal stimuli of neurons in ventral division. J. Neurophysiol. 35: 365-380.

Bailey, P., von Bonin, G., Garol, H.W. and McCulloch, W.S. (1943). Functional organization of temporal lobe of monkey (Macaca mulatta) and chimpanzee (Pan satyrus). J. Neurophysiol. 6: 121-128.

Barnes, W.T., Magoun, H.W. and Ranson, S.W. (1943). The ascending auditory pathway in the brainstem of the monkey. J. Comp. Neurol. 79: 129-152.

Beck, E. (1929). Die myeloarchitektonische Bau des in der Sylvischen Furche gelegen Teiles des Schlafenlappens beim Schimpansen (Troglodytes niger). J. Psychol. Neurol. (Leipzig). 38: 309-420.

Bremer, F. (1953). Some Problems in Neurophysiology. London: Athlone Press.

Bremer, F. and Dow, R.S. (1939). The cerebral acoustic area of the cat. A combined oscillographic and cytoarchitectonic study. J. Neurophysiol. 2: 308-318.

Brodmann, K. (1909). Vergleichende Lokalisationslehre der Grosshirnrinde. Leipzig: J.A. Barth. 324 pp.

Brownell, W.E. (1975). Organization of the cat trapezoid body and the discharge characteristics of its fibers. Brain Res. 94: 413-433.

Brugge, J.F. (1975). Progress in neuroanatomy and neurophysiology of auditory cortex. In: D.B. Tower (ed.), The Nervous System. New York: Raven Press. pp. 97-111.

Bunt, A.H., Haschke, R.H., Lund, R.D. and Calkins, D.F. (1976). Factors affecting retrograde axonal transport of horseradish peroxidase in the visual system. Brain Res. 102: 152-155.

Cajal, S. Ramon y. (1909). Histologie du systeme nerveux. Paris: Maloine. pp. 619.

Campbell, A.W. (1905). Histological Studies on the Localization of Cerebral Function. Cambridge: Cambridge University Press, 360 pp.

Clark, W.E. LeGros (1936). The thalamic connections of the temporal lobe of the brain in the monkey. J. Comp. Neurol. 70: 447-464.

Clopton, B.M., Winfield, J.A. and Flammino, F.J. (1973). Tonotopic organization over levels of the auditory system. J. Acoust. Soc. Amer. 54: 284.

Colwell, S.A. (1975). Thalamocortical-corticothalamic reciprocity: a combined anterograde-retrograde tracer study. Brain Res. 92: 443-449.

Colwell, S.A. and Merzenich, M.M. (1975). Organization of thalamocortical and corticothalamic projections to and

from physiologically defined loci within primary auditory cortex in the cat. Anat. Rec. 181: 336.

Cowan, W.M., Gottlieb, D.I., Hendrickson, A.E., Price, J.L. and Woolsey, T.A. (1972). The autoradiographic demonstration of axonal connections in the central nervous system. Brain Res. 37: 21-51.

Diamond, I.T., Jones, E.G. and Powell, T.P.S. (1968a). Interhemispheric fiber connections of the auditory cortex of the cat. Brain Res. 11: 177-193.

Diamond, I.T., Jones, E.G. and Powell, T.P.S. (1968b). The association connections of the auditory cortex of the cat. Brain Res. 11: 560-579.

Downman, C.B.B., Woolsey, C.N. and Lende, R.A. (1960). Auditory areas I, II, and Ep: cochlear representation, afferent paths and interactions. Bull. Johns Hopkins Hosp. 106: 127-142.

Economo, C. von (1929). The Cytoarchitectonics of the Human Cerebral Cortex. Oxford Medical Publications. London: Oxford University Press.

Economo, C. von and Koskinas, G.N. (1925). Die cytoarchitektonic der Hirnrinde der erwachsenen Menschen. Berlin: J. Springer. pp. 810.

Evans, E.F. (1968) Cortical representation. In: A.V.S. deReuck and J. Knight (eds.), Ciba Foundation Symposium on Hearing Mechanisms in Vertebrates. London: Churchill.

Evans, E.F. (1974). Neural processes for the detection of acoustic patterns and for sound localization. In: F.O. Schmidt and F.G. Worden (eds.), The Neurosciences. Third Study Program. Cambridge, Mass.: The MIT Press.

Evans, E.F., Ross, H.F. and Whitfield, I.C. (1965). The spatial distribution of unit characteristic frequency in the primary auditory cortex of the cat. J. Physiol. (Lond.) 179: 238-247.

Evans, E.F. and Whitfield, I.C. (1964). Classification of unit responses in the auditory cortex of the unanesthetized and unrestrained cat. J. Physiol. (Lond.) 171: 476-493.

Fernandez, C. and Karapas, F. (1967). The course and termination of the striae of Monakow and Held in the cat. J. Comp. Neurol. 131: 371-386.

Ferrier, D. (1876). The Functions of the Brain. London: Smith, Elder and Co. pp. 138-171.

Gerstein, G.L. and Kiang, N. Y-S. (1964). Responses of single units in the auditory cortex. Exp. Neurol. 10: 1-18.

Goldberg, J.M. and Brown, P.B. (1968). Functional organization of the dog superior olivary complex: an anatomical and electrophysiological study. J. Neurophysiol. 31: 639-656.

Goldstein, M.H., Abeles, M., Daly, R.L., and McIntosh, J. (1970). Functional architecture in cat primary auditory cortex: tonotopic organization. J. Neurophysiol. 33: 188-197.

Graham, R.C. and Karnovsky, M.J. (1966). The early stages of absorbtion of injected horseradish peroxidase in the proximal tubules of mouse kidney: Ultrastructural cytochemistry by a new technique. J. Histochem. Cytochem. 14: 291-302.

Graybiel, A.M. (1973). The thalamo-cortical projection of the so-called posterior nuclear group: a study with

anterograde degeneration methods in the cat. Brain Res. 49: 229-244.

Greenwood, D.D. (1961). Critical bandwidth and the frequency coordinates of the basilar membrane. J. Acoust. Soc. Amer. 33: 1344-1356.

Greenwood, D.D. (1974). Critical bandwidth in man and in some other species in relation to the travelling wave envelope. In: H.R. Moskowitz, B. Scharf and J.C. Stevens (eds.), Sensation and Measurement. Dordrecht: D. Reidel, pp. 231-239.

Gross, N.B., Lifschitz, W.S. and Anderson, D.J. (1974). Tonotopic organization of the auditory thalamus of the squirrel monkey (Saimiri sciureus). Brain Res. 65:323-332.

Guinan, J.J., Norris, B.E. and Guinan, S.S. (1972). Single units in the superior olivary complex. II: Location of unit catagories and tonotopic organization. Intern. J. Neuroscience 4: 147-166.

Halperin, J.J. and LaVail, J.H. (1975). A study of the dynamics of retrograde transport and accumulation of

horseradish peroxidase in injured neurons. Brain Res. 100: 253-269.

Harrison, J.M. and Warr, W.B. (1962). A study of the cochlear nuclei and ascending auditory pathways of the medulla. J. Comp. Neurol. 119: 341-380.

Heath, C.J. and Jones, E.G. (1971). An experimental study of ascending connections from the posterior group of thalamic nuclei in the cat. J. Comp. Neurol. 141: 397-426.

Heuser, J.E. and Reese, T.S. (1973). Evidence for recycling of synaptic vesicle membrane during transmitter release at the frog neuromuscular junction. J. Cell Biol. 57: 315-344.

Hind, J.E. (1953). An electrophysiological determination of tonotopic organization in auditory cortex of the cat. J. Neurophysiol. : 475-489.

Hind, J.E., Rose, J.E., Davies, P.W., Woolsey, C.N., Benjamin, R.M., Welker, W., and Thompson, R.F. (1960). Unit activity in the auditory cortex. In: G. Rasmussen and W. Windle (Eds.), Neural Mechanisms of the Auditory

and Vestibular Systems. Springfield, Ill.: Charles C. Thomas, pp. 201-210.

Holmes, G. (1945). The organization of the visual cortex in man. Proc. Roy. Soc. Lond. Ser. B. 132:348-361.

Holtzman, E., Freeman, A.R. and Kashner, A. (1971). Stimulation-dependent alteration in peroxidase uptake at lobster neuromuscular junctions. Science 173: 733-735.

Hubel, D.H. and Wiesel, T.N. (1962). Receptive fields, binocular interaction and functional architecture in cat's visual cortex. J. Physiol. (Lond.) 160: 106-154.

Hubel, D.H. and Wiesel, T.N. (1963). Shape and arrangement of columns in cat's striate cortex. J. Physiol. (Lond.) 165: 559-568.

Hubel, D.H. and Wiesel, T.N. (1974). Sequence regularity and geometry of orientations columns in monkey striate cortex. J. Comp. Neurol. 158: 267-294.

Imig, T.J., Ruggero, M.A., Kitzes, L.M., Javel, E. and Brugge, J.F. (1977) Organization of auditory cortex in the owl monkey (Aotus trivirgatus). J. Comp. Neurol. 171: 111-128.

Kaas, J.H., Hall, W.C. and Diamond, I.T. (1970). Cortical visual areas I and II in the hedgehog: relation between evoked potential maps and cytoarchitectonic subdivisions. J. Neurophysiol. 33: 595-615.

Kaas, J.H., Lin, C-S. and Casagrande, V.A. (1976). The relay of ipsilateral and contralateral input from the lateral geniculate nucleus to the striate cortex in owl monkey: a transneuronal transport study. Brain Res. 106: 371-378.

Kawamura, K. (1971). Variations of the cerebral sulci in the cat. Acta Anat. 80: 204-221.

Kawamura, K. (1973). Corticocortical fiber connections of the cat cerebrum. I. The temporal region. Brain Res. 51: 1-21.

Kennedy, T.T.K. (1955). An Electrophysiological Study of the Auditory Projection on Areas of the Cortex in Monkey (Macaca mulatta). (Thesis) Chicago: University of Chicago.

Kornmuller, A.E. (1937). Die Bioelektrischen Erscheinungen der Hirnrindfelder. Leipzig: G. Thieme, 118 pp.

Larionow, W. (1899). Ueber die Musicalischen Centren des Gehirns. Arch. ges. Physiol. 76: 608-625.

LaVail, J.H. and LaVail, M.M. (1972). Retrograde axonal transport in the central nervous system. Science 176: 1416-1417.

LaVail, J.H. and LaVail, M.M. (1974). The retrograde axonal transport of horseradish peroxidase in the chick visual system: a light and electron microscopic study. J. Comp. Neurol. 157: 303-358.

LaVail, M.M. and LaVail, J.H. (1975). Retrograde intraaxonal transport of horseradish peroxidase in retinal ganglion cells of the chick. Brain Res. 85: 273-280.

LaVail, J.H., Winston, K.R. and Tish, A. (1973). A method based on retrograde axonal transport of protein for identification of cell bodies of origin of axons within the CNS. Brain Res. 58: 470-477.

LeVay, S., Hubel, D.H. and Wiesel, T.N. (1975). The pattern of ocular dominance columns in Macaque visual cortex revealed by reduced silver stain. J. Comp. Neurol. 159: 559-576.

Licklider, J.C.R. and Kryter, K.D. (1942) Frequency localization in the auditory cortex of the monkey. Fed. Proc. 1:51.

Locke, S. (1961). The projection of the magnocellular medial geniculate body. J. Comp. Neurol. 116: 179-193.

Lombroso, C.T. and Merlis, J.K. (1957). Suprasylvian auditory responses in the cat. Electroencephalog. and Clin. Neurophysiol. 9: 301-303.

Lorente de No, R. (1933a). Anatomy of the eighth nerve. The central projection of the nerve endings of the internal ear. Layngoscope 43: 1-38.

Lorente de No, R. (1933b). Anatomy of the eighth nerve. III. General plan of structure of the primary cochlear nuclei. Laryngoscope 43: 327-350.

Merzenich, M.M. and Brugge, J.F. (1973). Representation of the cochlear partition on the superior temporal plane of the macaque monkey. Brain Res. 50: 275-296.

Merzenich, M.M., Kaas, J.H. and Roth, G.L. (1976). Auditory cortex in the grey squirrel: tonotopic

organization and architectonic fields. J. Comp. Neurol. 166: 387-402.

Merzenich, M.M., Knight, P.L. and Roth, G.L. (1973). Cochleotopic organization of primary auditory cortex in the cat. Brain Res. 63: 343-346.

Merzenich, M.M., Knight, P.L. and Roth, G.L. (1974). Orderly representation of the cochlea within primary auditory cortex in the cat. J. Acoust. Soc. Amer. 55(Suppl.): 86.

Merzenich, M.M., Knight, P.L. and Roth, G.L. (1975). Representation of cochlea within primary auditory cortex in the cat. J. Neurophysiol. 38: 231-249.

Merzenich, M.M. and Reid, M.D. (1974). Representation of the cochlea within the inferior colliculus of the cat. Brain Res. 77: 397-415.

Merzenich, M.M., Roth, G.L., Andersen, R.A., Knight, P.L. and Colwell, S.A. (1977). Some basic features of organization of the central auditory system. In: E.F. Evans and J.P. Wilson (eds.), Psychophysics and Physiology of Hearing. In Press. London: Academic Press.

Mesulam, M.-M. and Pandya, D.N. (1973). The projection of the medial geniculate complex within the Sylvian fissure of the rhesus monkey. Brain Res. 60: 315-333.

Mettler, F.A. (1932). Connections of the auditory cortex of the cat. J. Comp. Neurol. 55: 139-183.

Mickle, W.A. and Ades, H.W. (1953). Spread of evoked cortical potentials. J. Neurophysiol. 16: 608-633.

Moore, R.Y. and Goldberg, J.M. (1963). Ascending projections of the inferior colliculus in the cat. J. Comp. Neurol. 121: 109-136.

Morest, D.K. (1964). The neuronal architecture of the medial geniculate body of the cat. J. Anat. 98: 611-630.

Morest, D.K. (1965a). The laminar structure of the medial geniculate body of the cat. J. Anat. 99: 143-160.

Morest, D.K. (1965b). The lateral tegmental system of the midbrain and the medial geniculate body of the cat: a study with Golgi and Nauta methods in the cat. J. Anat. 99: 611-634.

Moskowitz, N. and Liu, J. (1972). Central projections of the spiral ganglion of the squirrel monkey. J. Comp. Neurol. 144: 335-344.

Mountcastle, V.B. (1957). Modality and topographic properties of single neurons of cat's somatic sensory cortex. J. Neurophysiol. 20: 408-434.

Munk, H. (1881). On the functions of the cerebral cortex. Translated by G. von Bonin. In: G. von Bonin (ed), The Cerebral Cortex, Springfield, Ill.: Charles C. Thomas, pp. 107-108.

Nauta, H.J.W., Pritz, M.B. and Lasek, R.J. (1974). Afferents to the rat caudoputamen studied with horseradish peroxidase. An evaluation of a retrograde neuroanatomical research method. Brain Res. 67: 219-238.

Neff, W.D. and Diamond, I.T. (1958). The neural basis of auditory discrimination. In: H.F. Harlow and C.N. Woolsey (eds.), Biological and Biochemical Bases of Behavior. Madison: University of Wisconsin Press.

Niimi, K. and Naito, F. (1974). Cortical projections of the medial genicualte body in the cat. Exp. Brain Res. 19: 326-342.

Noda, Y. and Pirsig, W. (1974). Anatomical projection of the cochlea to the cochlear nuclei of the guinea pig. Arch. Oto-rhino-laryng. 208: 107-120.

Oliver, D.L., Merzenich, M.M., Roth, G.L., Hall, W.C. and Kaas, J.H. (1976). Tonotopic organization and connections of primary auditory cortex in the tree shrew, Tupaia glis. Anat. Rec. 184: 491.

Oonishi, S. and Katsuki, Y. (1965). Functional organization and integrative mechanism of the auditory cortex of the cat. Jap. J. Physiol. 15: 342-365.

Osen, K.K. (1969). Cytoarchitecture of the cochlear nuclei in the cat. J. Comp. Neurol. 136: 453-483.

Osen, K.K. (1972) Projection of the cochlear nuclei on the inferior colliculus in the cat. J. Comp. Neurol. 144: 355-372.

Pandya, D.N. and Sanides, F. (1973). Architectonic parcellation of the temporal operculum in rhesus monkey

and its projection pattern. Z. Anat. Entwickl. Gesch. 139: 127-161.

Parker, D.E. (1965). Vertical organization of the auditory cortex of the cat. J. Audit. Res. 2: 99-124.

Paul, R.L., Merzenich, M.M. and Goodman, H. (1972). Representation of slowly and rapidly adapting cutaneous mechanoreceptors of the hand in Brodmann's areas 3 and and 1 of Macaca mulatta. Brain Res. 36: 229-249.

Paula-Barbosa, M.M., Feyo, P.B. and Sousa-Pinto, A. (1975). The association connections of the suprasylvian fringe (SF) and other areas of the cat auditory cortex. Exp. Brain. Res. 23: 535-554.

Paula-Barbosa, M.M. and Sousa-Pinto, A. (1973). Auditory cortical projections to the superior colliculus in the cat. Brain Res. 50: 47-61.

Poliak, S. (1927). An experimental study of the association, callosal and projection fibers of the cerebral cortex of the cat. J. Comp. Neurol. 44: 197-258.

Poliak, S. (1932). The main afferent fiber systems of the cerebral cortex in primates. In: H.M. Evans and I.M. Thompson (eds.), University of California Publications in Anatomy. Berkeley: University of California Press. pp. 81-101.

Pontes, C., Reis, F.F. and Sousa-Pinto, A. (1975). The auditory cortical projections onto the medial geniculate body in the cat. An experimental anatomical study with silver and autoradiographic methods. Brain Res. 91: 43-63.

Powell, T.P.S. and Mountcastle, V.B. (1959). Some aspects of the functional organization of the cortex of the postcentral gyrus of the monkey: a correlation of findings obtained in a single unit analysis with cytoarchitecture. Bull. Johns Hopkins Hosp. 105: 133-162.

Pribram, K.H., Rosner, B.S. and Rosenblith, W.A. (1954). Electrical responses to acoustic clicks in monkey: extent of neocortex activated. J. Neurophysiol. 17: 336-344.

Ralston, H.J. III and Sharp, P.V. (1973). The identification of thalamocortical relay cells in the

adult cat by means of retrograde axonal transport of horseradish peroxidase. Brain Res. 62: 273-278.

Rioch, D. (1929). Studies on the diencephalon of carnivora. I. The nuclear configuration of the thalamus, epithalamus, and hypothalamus of the dog and cat. J. Comp. Neurol. 49: 1-120.

Rockel, A.J. and Jones, E.G. (1973). The neuronal organization of the inferior colliculus of the adult cat. I. The central nucleus. J. Comp. Neurol. 147: 11-60.

Rose, J.E. (1949). The cellular structure of the auditory region of the cat. J. Comp. Neurol. 91: 409-440.

Rose, J.E., Galambos, R. and Hughes, J.R. (1959). Microelectrode studies of the cochlear nuclei of the cat. Bull. Johns Hopkins Hosp. 104: 211-251.

Rose, J.E., Galambos, R. and Hughes, J. (1960). Organization of frequency sensitive neurons in the cochlear nuclear complex of the cat. In: G. Rasmussen and W. Windle (eds.), Neural Mechanisms of the Auditory and Vestibular Systems. Springfield, Ill.: Charles C. Thomas, pp. 116-136.

Rose, J.E., Greenwood, D.D., Goldberg, J.M. and Hind, J.E. (1963). Some discharge characteristics of single neurons in the inferior colliculus of the cat. I. Tonotopic organization, relation of spike counts to tone intensity, and firing patterns of single elements. J. Neurophysiol. 26: 294-320.

Rose, J.E. and Mountcastle, V.B. (1959). Touch and kinesthesis. In: H.W. Magoun and V.E. Hall (eds.), Handbook of Physiology. Section 1, Volume 1, Neurophysiology. Washington: American Physiological Society. pp. 387-429.

Rose, J.E. and Woolsey, C.N. (1949). The relations of thalamic connections, cellular structure and evocable electrical activity in the auditory region of the cat. J. Comp. Neurol. 91: 441-466.

Rose, J.E. and Woolsey, C.N. (1958). Cortical connections and functional organization of the thalamic auditory system of the cat. In: H.F. Harlow and C.N. Woolsey (eds.), Biological and Biochemical Bases of Behavior. Madison: University of Wisconsin Press. pp. 127-150.

Sando, I. (1965). The anatomical interrelationships of the cochlear nerve fibers. Acta otolaryngologica 59: 417-436.

Sanides, F. (1972). Representation in the cerebral cortex and its areal lamination pattern. In: G.H. Bourne (ed.), The Structure and Function of Nervous Tissue, Vol. 5. New York: Academic Press. pp. 329-453.

Sherlock, D.A. and Raisman, G. (1975). A comparison of anterograde and retrograde axonal transport of horseradish peroxidase in the connections of the mammillary nuclei in the rat. Brain Res. 85: 321-324.

Sousa-Pinto, A. (1974). Cortical projections of the medial geniculate body in the cat. Adv. Anat. Embry. Cell Biol. 48: 1-42.

Stotler, W.A. (1953). An experimental study of the cells and connections of the superior olivary complex of the cat. J. Comp. Neurol. 98: 401-432.

Strominger, N.L. (1973). The origins, course and distribution of the dorsal and intermediate acoustic striae in the rhesus monkey. J. Comp. Neurol. 147: 209-234.

Strominger, N.L., Nelson, L.R. and Dougherty, W.J. (1977). Second order auditory pathways in the chimpanzee. J. Comp. Neurol. 172: 349-366.

Strominger, N.L. and Strominger, A.I. (1971). Ascending brainstem projections of the anterior ventral cochlear nucleus in the rhesus monkey. J. Comp. Neurol. 143: 217-241.

Suga, N. (1977). Amplitude spectrum representation in the Doppler-shifted-CF processing area of the auditory cortex of the mustache bat. Science 196: 64-67.

Talbot, S.A. and Marshall, W.H. (1941). Physiological studies of the neural mechanisms of visual localization and discrimination. Am. J. Ophthalmol. 24: 1255-1264.

Tsuchitani, C. (1977). Functional organization of lateral cell groups of cat superior olivary complex. J. Neurophysiol. 40: 296-318.

Tsuchitani, C. and Boudreau, J.C. (1966). Single unit analysis of cat superior olive S segment with tonal stimuli. J. Neurophysiol. 29: 684-697.

Tunturi, A.R. (1945). Further afferent connections of the acoustic cortex of the dog. Amer. J. Physiol. 144: 389-394.

Tunturi, A.R. (1950a). Physiological determination of the boundary of the acoustic area in the cerebral cortex of the dog. Amer. J. Physiol. 160: 395-401.

Tunturi, A.R. (1950b). Physiological determination of the arrangement of the afferent connections to the middle ectosylvian area in the dog. Amer. J. Physiol. 162: 489-502.

Tunturi, A. (1952). A difference in the representation of auditory signals for the left and right ears in the isofrequency contours of the right middle ectosylvian cortex of the dog. Amer. J. Physiol. 168: 712-727.

Trojanowski, J.Q. and Jacobson, S. (1975). A combined horseradish peroxidase-autoradiographic investigation of reciprocal connections between superior temporal gyrus and pulvinar in squirrel monkey. Brain Res. 85: 347-353.

Van Noort, J. (1969). The Structure and Connections of the Inferior Colliculus. Assen: van Gorcan.

Vogt, C. (1900). Etude sur la myelinisation des hemispheres cerebraux. Paris: Steinheil.

Vogt, C. and Vogt, O. (1919). Allgemeinere Ergebnisse unserer Hirnforschung. J. Psychol. Neurol. 25: 279-461.

Vogt, C. and Vogt, O. (1926). Die vergleichend-architektonische und die vergleichend-reizphysiologische Felderung der Grosshirnrinde unter besonderer Beruckichtigung der menschlichen. Die Naturwissenschaften 14: 1190-1194.

Waller, W.H. (1939). Thalamic degeneration induced by temporal lesions in the cat. J. Anat. 74: 528-536.

Walker, A.E. (1937). The projection of the medial geniculate body to the cerebral cortex in the macaque monkey. J. Anat. 71: 319-331.

Walker, A.E. (1938). The Primate Thalamus. Chicago: University of Chicago Press. pp. 200-237.

Walzl, E.M. (1947). Representation of the cochlea in the cerebral cortex. Laryngoscope 57: 778-787.

Walzl, E.M. and Woolsey, C.N. (1943). Cortical auditory areas of the monkey as determined by electrical excitation of nerve fibers in osseous spiral lamina and by click stimulation. Fed. Proc. 2: 52.

Warr, W.B. (1966). Fiber degeneration following lesions in the anterior ventral cochlear nucleus of the cat. Exp. Neurol. 14: 453-474.

Warr, W.B. (1969). Fiber degeneration following lesions in the posterior ventral cochlear nucleus of the cat. Exp. Neurol. 23: 140-155.

Warr, W.B. (1972). Fiber degeneration following lesions in the multipolar and globular cell areas in the ventral cochlear nucleus of the cat. Brain Res. 40: 247-270.

Webster, D.B. (1971). Projection of the cochlea to cochlear nuclei in Merriams's kangaroo rat. J. Comp. Neurol. 143: 323-340.

Welker, W.I. (1973). Principles of organization of the ventrobasal complex in mammals. Brain Behav. Evol. 7: 253-336.

Welker, W.I., Johnson, J.I. Jr., and Pubols, B.H. Jr. (1964). Some morphological and physiological characteristics of the somatic sensory system in raccoons. Amer. Zool. 4: 75-94.

Whitfield, I.C. (1971). Auditory cortex: tonal, temporal, or topical? In: M.B. Sachs (ed.) Physiology of the Auditory System. Baltimore: National Educational Consultants. pp. 289-298.

Wiesel, T.N., Hubel, D.H. and Lam, D. (1974). Autoradiographic demonstration of ocular dominance columns in monkey striate cortex by means of transsynaptic transport. Brain Res. 79: 273-279.

Wilson, M.E. and Cragg, B.G. (1969). Projections from the medial geniculate body to the cerebral cortex of the cat. Brain Res. 13: 462-475.

Winkler, C. and Potter, A. (1914). An Anatomical Guide to Experimental Research on the Cat's Brain. Amsterdam: Versluys.

Wong-Riley, M.T.T. (1976). Endogenous peroxidatic activity in brainstem neurons as demonstrated by their

staining with diaminobenzidine in normal squirrel monkeys. Brain Res. 108: 257-277.

Wollard, H.H. and Harpman, A. (1939). The cortical projection of the medial geniculate body. J. Neurol. Psychiat. 2: 35-44.

Woollard, H.H. and Harpman, J.A. (1940). The connections of the inferior colliculus and of the dorsal nucleus of the lateral lemniscus. J. Anat. 441-458.

Woolsey, C.N. (1960). Organization of cortical auditory system: a review and a synthesis. In: G. Rasmussen and W. Windle (eds.) Neural Mechanisms of the Auditory and Vestibular Systems. Springfield, Ill.: Charles C. Thomas, pp. 165-180.

Woolsey, C.N. (1961). Organization of cortical auditory system. In: W.A. Rosenblith (ed.), Sensory Communication. Cambridge, Mass.: The MIT Press, pp. 235-257.

Woolsey, C.N. (1964). Electrophysiological studies on thalamocortical relations in the auditory system. In: A. Abrams, H.H. Garner and J.E.P. Tamam (eds.), Unfinished Tasks in the Behavioral Sciences. Baltimore, Md.: Williams and Wilkins, pp. 45-57.

Woolsey, C.N. (1971) Tonotopic organization of the auditory cortex. In: M. Sachs (ed.), Physiology of the Auditory System. Baltimore, Md.: National Educational Consultants.

Woolsey, C.N. and Fairman, D. (1946). Contralateral, ipsilateral and bilateral representation of cutaneous receptors in somatic areas I and II of the cerebral cortex of pig, sheep and other mammals. Surgery 19; 684-702.

Woolsey, C.N., Marshall, W.M. and Bard, P. (1942). Representation of cutaneous tactile sensibility in the cerebral cortex of the monkey as indicated by evoked potentials. Bull. Johns Hopkins Hosp. 70: 399-411.

Woolsey, C.N. and Walzl, E.M. (1942). Topical projection of nerve fibers from local regions of the cochlea to the cerebral cortex of the cat. Bull. Johns Hopkins Hosp. 71: 315-344.

Woolsey, C.N. and Walzl, E.M. (1944). Topical projection of the cochlea to the cerebral cortex of the monkey. Amer. J. Med. Sci. 207: 685-686.